Polarons in high-temperature superconductors

A. S. Alexandrov and A. B. Krebs

Moscow Engineering Physics Institute

(Submitted 19 June 1991; resubmitted after revision 27 December 1991)
Usp. Fiz. Nauk **162**, 1–85 (May 1992)

The review deals with the main results of a consistent study of electron-lattice interaction in crystals in the strong-coupling limit. Small polaron and bipolaron formation is shown to provide a number of new physical phenomena both in the normal and superconducting states of the system Two mechanisms of superconductivity are discussed in detail. The first one arises from the Cooper pairing of small polarons in momentum space (polaron superconductivity). The second one is due to polaron pairing in real space leading to on-site or intersite bipolaron formation with superconductivity analogous to the superfluidity of ^{4}He (bipolaron superconductivity). Highly non-adiabatic motion of (bi)polarons in the narrow band results in fundamental differences of their superconducting state properties with respect to the predictions of the BCS theory and its well known strong-coupling generalization. A number of basic properties of high-temperature metallic oxides being analyzed in terms of (bi)polaron theory of superconductivity is shown to reveal a satisfactory agreement of its findings with the available experimental data.

INTRODUCTION

The discovery of high-temperature superconductors (HTSC) (Ref. 1) has become the starting point of the new stage of intensive studies of the physics of superconductivity and has drawn attention to a number of nontraditional approaches to understanding the essence of this phenomenon itself.

The modern theory of superconductivity is based on the Migdal–Eliashberg equations,[2,3] which can, in principle, explain thermodynamic and electromagnetic properties of the normal and superconducting states of metal for the arbitrary strength of the electron-phonon interaction characterized by the effective coupling constant λ.

The small value of the adiabatic parameter

$$\omega/E_F \ll 1$$

and the assumption that the electron and phonon Green's functions are diagonal in the momentum representation make it possible to derive selfconsistent equations for both these functions (E_F is the Fermi energy, ω is the characteristic phonon frequency and $\hbar = 1$). Some properties of the normal and superconducting states, resulting from this approach, are compiled in Table II of Sect. 10. As a whole, the system represents a weakly correlated Fermi-liquid, in which the Cooper pairs of large radius ξ arise if the temperature is below some critical value (T_c):

$$\xi \approx v_F/T_c \gg n_e^{-1/3}.$$

Here n_e is the electron concentration, and v_F is the Fermi velocity.

It has been widely accepted[4] that the Migdal–Eliashberg theory adequately describes the electron-phonon system for sufficiently large values of the effective coupling constant λ. The self-energy Σ appears to be small with respect to E_F for reasonable values of λ:

$$\Sigma \approx \lambda\omega \ll E_F,$$

thus making the Fermi-liquid description applicable at least in the range

$$\lambda \leq E_F/\omega \gg 1.$$

It has been shown,[5] that for larger values of λ vertex corrections and the energy dependence of the electron density of states become important, but the formalism based on the Green's function technique[6] in the momentum representation seemed to remain credible.

On the other hand, some serious doubts have been expressed in a number of papers[7–16] concerning the validity of the traditional theory of strong electron-phonon interaction in metals. In particular it has become clear, that the standard Green's function formalism does not take into account the possibility of a local violation of translational symmetry of the lattice due to the so-called polaron effect.

From a more general viewpoint, an instability of the boson vacuum develops in the system of interacting bosons and electrons at a certain critical value of $\lambda = \lambda_c$. The new boson vacuum corresponds to a lower energy state. The polaron "collapse" takes place at intermediate values of λ:[17]

$$\lambda \geq \lambda_c \approx 1,$$

which makes the use of the standard equations for the case of $\lambda \geqslant \lambda_c$ doubtful.

Here we intend to review in detail some results of studies of the last decade of the polaron effect in many-electron systems with strong electron-phonon interaction.

The single-particle theory of large and small radius polarons, developed over half a century after the classical works of Landau and Pekar,[18,19] is discussed thoroughly in the great number of review papers, monographs and conference proceedings (see e.g. Refs. 18–22). The main results of this theory are presented in Sec. 1. In Sec. 2 we consider the criterion for the existence of the small radius polaron and the transition conditions from the adiabatic wide band electron state to the nonadiabatic narrow band small polaron state. The Cooper pairing of small polarons which is possible in the case of their weak interaction is discussed in Sec. 3, where some physical consequences of the narrow polaron band are analyzed. Sec. 4 deals with the dielectric properties and vi-

 0038-5670/92/050345-39$03.00

brational excitations of the strongly coupled electron-phonon system.

Small bipolarons and their superconducting properties are discussed in Secs. 5–8. The bipolaron superconductivity is shown to be qualitatively different from the BCS one.

Two concluding sections contain an analysis of the electron properties of high-temperature metallic oxides within the framework of the small polaron theory.[12-15,23-28]

The authors are quite aware of the fact that the present state of experiment as well as of theory, does not permit making any final conclusions on the nature of high-temperature superconductivity. That is why we have no intention to convince the reader that there exists full agreement of the presented theory with the experimental data. Moreover, we discuss here only those experiments, that allow a rather simple interpretation on the basis of the polaron theory. There is no doubt that some more work will be necessary to establish the ideas more accurately, this being common to all the theoretical approaches developed at the present time. In this respect the polaron theory is one of the alternatives that is presented here for discussion.

1. POLARONS OF SMALL RADIUS

In a broad widely accepted sense a polaron is a quasiparticle resulting from the dynamic interaction of a charge carrier (customarily an electron) with the crystal lattice. The idea of a possible electron selflocalization in a potential well resulting from the lattice deformation produced by the electron was initially introduced by Landau,[18] who was the first to deal with this problem.

The ordinary Hamiltonian of the electron-lattice system usually includes four terms:

$$H = H_e + H_{ph} + H_{e-ph} + H_{e-e}, \tag{1.1}$$

with H_e being the kinetic energy operator of the electron in the unrenormalized Bloch band, H_{ph}—the free lattice Hamiltonian, H_{e-ph}—the electron-lattice interaction term, and H_{e-e}—the Coulomb interaction of the electrons with themselves. In the single polaron problem (one electron in a deformable lattice) the last term in (1.1) is absent.

In the single-band approximation H_e is given by

$$H_e = \sum_k \varepsilon(\mathbf{k}) c_k^+ c_k, \tag{1.2}$$

where c_k^+ (c_k) is the creation (annihilation) operator for the electron with momentum $\mathbf{k}$ and spin projection s ($k \equiv (\mathbf{k},s)$), and $\varepsilon(\mathbf{k})$ is the bare band dispersion law.

The Hamiltonian of free lattice vibrations is similarly expressed in terms of the phonon creation and annihilation operators d_q^+, d_q ($q \equiv (\mathbf{q},\nu)$, $\mathbf{q}$–denotes the phonon wave vector, ν–is the phonon branch index)

$$H_{ph} = \sum_q \omega(q) d_q^+ d_q; \tag{1.3}$$

Here $\omega(q)$ is the the phonon frequency.

The electron-phonon interaction is described by the Fröhlich Hamiltonian

$$H_{e-ph} = \sum_{k,q} U(q) c_{\mathbf{k}-\mathbf{q}s}^+ c_{\mathbf{k}s} d_q^+ + \text{H.c.} \tag{1.4}$$

with the matrix element $U(q)$ in the following rather general form

$$U(q) = g_0 \omega_0 (1/v^{1/2}) a^{3/2} / (a|\mathbf{q}|)^\gamma. \tag{1.5}$$

In this expression g_0 denotes the dimensionless electron-phonon coupling constant, v is the crystal volume, and a is an arbitrary parameter with dimension of length whose value determines g_0 normalization. The value of $\gamma = 0$ corresponds to the so-called local electron-phonon interaction. Taking $g_0 = i(2\sqrt{2}\pi\alpha/a\sqrt{\omega_0 m})^{1/2}$, $\gamma = 1$ and $\omega(q) = \omega_0$ one obtains the familiar Fröhlich interaction of an electron of mass m with the polarization optical phonons[20] with dimensionless constant α depending on the dielectric properties of the lattice; ω_0 will be assumed to be the maximum value of $\omega(q)$.

The historically first and most widely used approach to the problem was based on two main assumptions, predetermining the polaron state properties.

1. The effective mass approximation for the interaction of an electron with a rigid lattice. According to it the electron dispersion law takes the form $\varepsilon(k) = k^2/2m$ corresponding to an infinite electron band width which thus loses the meaning of the problem parameter.

2. The continuum approximation neglecting the discrete structure of the lattice.

Within the framework of this approach the polaron presents an example of the typical quantum field theory problem of a Fermi-particle interacting with a quantized boson field. It became one of the first applications of the field theory techniques to solid state physics (for a review of the main results see Refs. 21, 22).

The analysis of polaron ground state properties simplifies greatly in the limiting cases of weak and strong electron-phonon interaction. In the weak coupling case one can use the ordinary perturbation theory while the strong coupling limit can be approached with the help of the self-consistent adiabatic method developed by Pekar.[19] The electron induced deformation of the lattice gives rise to an effective potential well with a discrete energy level corresponding to the localized state of the charge carrier. The whole system of electron and the lattice deformation moves through the crystal with the effective mass considerably exceeding the electron mass in a rigid lattice. It was Feynman with his path integral approach[29] who managed to approximate the polaron parameters over a full range of α values. His method is considered now as one of the most reliable and is widely used in polaron physics.

Polaron radius is the important parameter related to the size of the lattice deformation induced by the carrier. For the weak coupling case the uncertainty relations give $r_p \approx 1/\sqrt{m\omega_0}$ as the characteristic size of space fluctuations of an electron due to emission and absorption of virtual phonons. In the opposite limit of strong coupling its value is strongly dependent on the form of the electron-phonon matrix element. For the Pekar–Fröhlich type of coupling ($\gamma = 1, \omega(q) = \omega_0$) and $\alpha \gg 1$ a simple qualitative estimate[20] gives the value of $r_p \approx 1/\alpha\sqrt{m\omega_0}$ decreasing with an increase of α. In the other case of local type of interaction ($\gamma = 0$) the polaron state becomes unstable for large values of the coupling[30-32] and collapses to zero radius if no special cut-off is made which limits the minimal size of lattice distortion. This

cut-off just reflects the discrete structure of the lattice and results in the value of polaron radius of the same order as the lattice constant. Here we come to the limit where the approach based on the continuum and the effective mass approximations is out of the range of validity. Being quite adequate for the problem of large radius polarons it fails to predict accurate results when the size of the region of deformation is comparable with the lattice constant. In this latter case we are faced with the small radius polaron state and its properties will be of main interest for us in the following discussion.

To begin with let us transform the expressions for H_e and H_{e-ph} to the most convenient site representation:

$$H_e = \sum_{\substack{\mathbf{m},\mathbf{m}' \\ s}} T_{\mathbf{m}\mathbf{m}'} c^+_{\mathbf{m}s} c_{\mathbf{m}'s}, \tag{1.6}$$

$$H_{e-ph} = \sum_{\substack{q,\mathbf{m} \\ s}} c^+_{\mathbf{m}s} c_{\mathbf{m}s} (U(q) d_q e^{-i\mathbf{q}\mathbf{m}} + \text{H.c.}); \tag{1.7}$$

Here $c^+_{\mathbf{m}s}$ ($c_{\mathbf{m}s}$) are the creation (annihilation) operators of an electron on the site with the lattice vector $\mathbf{m}$

$$c^+_{\mathbf{m}s} = \frac{1}{N^{1/2}} \sum_{\mathbf{k}} c^+_{\mathbf{k}s} e^{-i\mathbf{k}\mathbf{m}}, \tag{1.8}$$

$T_{\mathbf{m}\mathbf{m}'} = T(\mathbf{m} - \mathbf{m}')(1 - \delta_{\mathbf{m}\mathbf{m}'})$ is the bare tunneling integral describing the electron hopping from one site to another

$$T(\mathbf{m}) = \frac{1}{N} \sum_{\mathbf{k}} \varepsilon(\mathbf{k}) e^{-i\mathbf{k}\mathbf{m}}. \tag{1.9}$$

In the widely explored nearest neighbor approximation with z being the coordination number, $T(\mathbf{m})$ will be considered to be the same (and equal to $-J$) for all the nearest neighbors. J is the so called hopping integral related to the bare electron band width D in the following familiar way

$$J = D/2z. \tag{1.10}$$

For the simple cubic lattice ($z = 6$) the electron dispersion law $\varepsilon(\mathbf{k})$ in this approximation is given by

$$\varepsilon(\mathbf{k}) = -2J[\cos(ak_x) + \cos(ak_y) + \cos(ak_z)], \tag{1.11}$$

where a is the lattice constant assumed to be identical to the dimensional length parameter a in Eq. (1.5). In the range of parabolic behavior of $\varepsilon(\mathbf{k})$ one has for the effective Bloch electron mass the value $m = 1/2Ja^2$.

Let us discuss the role of the condition for a polaron to have a small radius $r_p \leqslant a$. In the weak coupling case with $r_p \approx 1/\sqrt{m\omega_0}$ it means that

$$J \leq \omega_0, \tag{1.12}$$

i.e. the unrenormalized band must be extremely narrow. This limit is of no interest for our discussion of systems with rather large values of the bare bands $D \gg \omega_0$ and strong electron-phonon coupling. In the latter case for the Pekar–Fröhlich type of polarons the smallness of the radius $r_p \approx 1/\alpha\sqrt{m\omega_0} \leqslant a$ is equivalent to the following condition

$$J \leq \alpha^2 \omega_0, \tag{1.13}$$

which can be satisfied for sufficiently large bare bands since $\alpha \gg 1$. The quantity in the right hand side of Eq. (1.13) corresponds up to a certain numerical factor to the energy gain of the system due to electron-phonon interaction. It is the so-called polaron shift E_p, an important energy parameter characterizing the strength of the interaction in question. In terms of E_p and D Eq. (1.13) can be written as

$$E_p/D \geq 1. \tag{1.14}$$

This condition for the existence of the small radius polaron state derived here by simple qualitative arguments is of rather general importance. Its validity for the local type of electron-phonon interaction was demonstrated in Ref. 32. Later on we shall return to it again to clear up its fundamental role in the theory of strong-coupling superconductivity. And now let us start with the discussion of its physical meaning.

In the adiabatic theory of the large radius polaron[19] its size is determined by the condition of the optimal balance of the positive contribution of the electron kinetic energy in the localized state, the positive contribution of the lattice distortion energy and the negative contribution of the electron-phonon interaction energy. All the aforementioned contributions are of the same order of magnitude and the sum of them determines the resulting energy gain of the polaron system with respect to the free electron state in the undistorted lattice. It should be pointed out however that the increase of the electron kinetic energy controls the reduction of polaron radius only as long as the latter remains large compared to the lattice constant, or in other words until the kinetic energy loss due to localization does not exceed its maximum value equal to D. With a subsequent increase of the coupling the polaron size and the electron localization kinetic energy become "frozen" at certain constant values leaving the interaction and distortion terms to be the only varying contributions to the polaron state energy. The sum of these terms decreases with the increase of the coupling thus lowering the polaron energy further, while the polaron radius ($\approx a$) remains constant. The polaron shift in this limit lying outside the range of validity of the continuum approach may become very large in comparison with D. It is obvious that the above mentioned "freezing" takes place in the intermediate region of parameters $E_p \leqslant D$ ($r_p \geqslant a$). It should be added also that the transition of a polaron from the large radius to the small radius state may be discontinuous depending on the type of electron-phonon interaction and the dimensionality of the system. This problem has been repeatedly discussed in the polaron literature (see Sec. 2 and Refs. 21, 22, 29–32).

As follows from the above analysis the polaron state properties are essentially determined by the three parameters D, ω, E_p, with the dimension of energy related to the main three terms of the Hamiltonian of Eq. (1.1). The characteristic phonon frequency ω as well as the polaron shift energy E_p will be defined exactly later. These parameters may be combined in three dimensionless ratios with any two of them being independent of each other. We shall define the first one as

$$E_p/\omega \equiv g^2 \tag{1.15}$$

and use it in the following as the "effective constant of the electron-phonon interaction" not to be confused with the

"effective coupling constant" λ corresponding to the second ratio

$$E_p/D \equiv \lambda. \tag{1.16}$$

The third dimensionless ratio which is also to be used later is the so-called adiabatic parameter ω/D.

The last term in the Hamiltonian Eq. (1.1) describing the direct Coulomb repulsion of electrons is important for the understanding of the cooperative properties of the small polaron system. By introducing the shorthand notations $i \equiv (\mathbf{m},s)$, $j \equiv (\mathbf{n},\tilde{s})$, and the electron density operator

$$n_i = c_i^+ c_i \equiv c_{ms}^+ c_{ms}, \tag{1.17}$$

one easily obtains the site representation form of H_{e-e}

$$H_{e-e} = \sum_{i,j} V_{ij} n_i n_j, \tag{1.18}$$

where V_{ij} is the matrix element of the Coulomb interaction.

We now turn to the limit of $\lambda \gg 1$ (cf. Eq. (1.14)) corresponding to the small radius polaron state. Having assumed initially that $D > \omega$, we are arriving at the inequality $g^2 \gg 1$ confirming that the interaction with the lattice is essentially strong. As a result the electron kinetic energy term H_e may be considered as a small perturbation to be neglected in the zero-order approximation. The residual part of the Hamiltonian (1.1) is then exactly diagonalized over phonon variables by the familiar small polaron canonical transformation:[20]

$$H_p = (\exp S_1) H \exp(-S_1), \tag{1.19}$$

where

$$S_1 = \sum_{i,q} \frac{n_i}{\omega(q)} (U(q) d_q^+ e^{-iqm} - \text{H.c.}). \tag{1.20}$$

Carrying out this procedure one readily finds for the transformed small polaron Hamiltonian

$$H_p = \sum_{i,j} \hat{\sigma}_{ij} c_i^+ c_j + \sum_q \omega(q) d_q^+ d_q - E_p \sum_i n_i + \sum_{i,j} v_{ij} n_i n_j, \tag{1.21}$$

The operators d_q^+, d_q now describe the ion vibrations near the displaced equilibrium positions, and c_i^+, c_i stand for the creation and annihilation operators of the small polaron at the site i. The explicit expression for polaron shift E_p is given by

$$E_p = \sum_q |U(q)|^2 \omega^{-1}(q). \tag{1.22}$$

It is this quantity that defines the electron energy gain due to interaction with the lattice when H_e is neglected and the carrier is localized at one of the sites. It results in additional effective polaron-polaron interaction of the density-density type

$$v_{ij} = V_{ij} - \sum_q (|U(q)|^2 \omega^{-1}(q)) e^{iq(m-n)} \equiv V_{ij} - V_{ij}^{ph}. \tag{1.23}$$

In contrast to the last three terms in Eq. (1.21) the first one which describes polaron hopping now contains matrix elements nondiagonal in the phonon variables

$$\hat{\sigma}_{ij} = \hat{\sigma}_{mn} \delta_{s\tilde{s}} = T_{mn} \delta_{s\tilde{s}} \exp\left\{ \sum_q [U(q) d_q^+ (e^{-iqm} - e^{-iqn}) - \text{H.c.}]/\omega(q) \right\}. \tag{1.24}$$

Band motion of small radius polarons is then viewed as an intersite tunneling without any change in the phonon occupation numbers. It is well described by the operator $\langle \hat{\sigma}_{ij} \rangle$ averaged over the phonon variables corresponding to the effective hopping integral[20]

$$\sigma_{ij} \equiv \langle \hat{\sigma}_{ij} \rangle = \langle \hat{\sigma}_{mn} \rangle \delta_{s\tilde{s}} = T_{mn} \delta_{s\tilde{s}} e^{-g^2} \equiv \sigma_{mn} \delta_{s\tilde{s}}, \tag{1.25}$$

where $g^2 \equiv g^2(\mathbf{m} - \mathbf{n})$ is the effective constant of electron-phonon interaction

$$g^2 = \sum_q (|U(q)|^2 \omega^{-2}(q)) \{1 - \cos[q(m-n)]\} \coth \frac{\omega(q)}{2T}, \tag{1.26}$$

and T is the lattice temperature measured in energy units.

In the case of a simple cubic lattice g^2 does not depend on the tunneling direction and is equal to

$$g^2 = \sum_q (|U(q)|^2 \omega^{-2}(q)) \times \{1 - \frac{1}{3} [\cos(aq_x) + \cos(aq_y) + \cos(aq_z)]\} \coth \frac{\omega(q)}{2T}. \tag{1.27}$$

Given the exact expressions (1.22), (1.26), (1.27) for E_p and g^2 parameters, formula (1.15) should be considered now as an explicit definition of the characteristic phonon frequency ω. Its value is equal to ω_0 in the the case of local type of interaction ($\gamma = 0$) with dispersionless phonons ($\omega(\mathbf{q}) = \omega_0$) at zero temperature and is numerically estimated as $\omega \cong 1.73\omega_0$ for the Fröhlich case. The values of the interaction constant g^2 are respectively given by g_0^2 (see Eq. (1.5)) and $g^2 \cong 0.11 g_0^2$.

According to Eq. (1.25) the width W of the polaron band

$$W = De^{-g^2} \tag{1.28}$$

turns out to be exponentially small with respect to the bare bandwidth. This exponential renormalization of the tunneling probability reflects the smallness of the overlap integrals of the oscillator wave functions describing the deformed state of the lattice when an electron is localized at neighboring sites. Due to this renormalization which takes place at $g^2 \gg 1$ the antiadiabatic inequality $W < \omega$ is fulfilled for the polaron, which is opposite in sign to that for the electron in the bare band. This is the polaron effect which causes exponential contraction of the band and the inversion of adiabatic inequality. Polaron motion from one site to another turns out to be very slow so that the lattice can relax completely within the time of its localization at the site. The local unit comprising a carrier and its concomitant lattice distortion moving together is referred to as a small or antiadiabatic polaron. We note that the narrowing of the band increases with an increase of the temperature. In the low temperature range $T < \omega$ the operator $\hat{\sigma}_{ij}$ in the Hamiltonian (1.21) may

be replaced by its averaged value (1.25), while g^2 may be considered to be temperature independent ($\coth[\omega(q)/2T] \cong 1$).

The effective interaction between small polarons (1.23), which we wish to discuss now, includes the direct Coulomb repulsion as well as the attraction arising from lattice deformation. The value of the latter is determined by the so-called degenerate three-center integrals of the crystal field gradients. For the simple cubic lattice we have

$$U(q) = \frac{e(q)}{(2NM\omega(q))^{1/2}} \sum_{\mathbf{l}} \langle 0|\nabla_{\mathbf{l}} U(\mathbf{r}-\mathbf{l})|0\rangle e^{i\mathbf{q}\mathbf{l}}, \tag{1.29}$$

where $\mathbf{e}(q)$ is a polarization vector of the vibrational mode, and M is the ion mass. The contribution of the $\mathbf{l}=0$ site (occupied by the carrier in a state $|0\rangle$) to the sum in (1.29) vanishes identically due to the parity selection rule. It is then the displacements of the neighboring atoms rather than those of the occupied site that induce the effective electron-lattice interaction. Nondegenerate three-center ($\mathbf{l}\neq\mathbf{m}\neq 0$) integrals

$$\langle 0|\nabla_{\mathbf{l}} U(\mathbf{r}-\mathbf{l})|\mathbf{m}\rangle \tag{1.30}$$

as well as two-center ($\mathbf{m}=\mathbf{l}\neq 0$) integrals may also contribute to this interaction. The role of the former is usually neglected for the reason of small overlap of atomic orbitals. Two-center integrals being taken into account give rise to the phonon emission/absorption processes accompanying electron transfer between neighboring sites. These may contribute to the damping of polaron states.[33] It is worthwhile to mention that for transition metals there is no commonly accepted point of view on the role played by the aforementioned integrals in the electron-phonon interaction. This ambiguity may be related[34] to the strong dependence of the interaction in d-metals on the screening constant which is rather difficult to estimate. If the screening radius is small $1/k \leqslant a$, then the overlap integral smallness of (1.30) may be compensated by the large value of the crystal field for $\mathbf{m}=\mathbf{l}$. Dielectric, semiconducting and intermetallic compounds are characterized by a weaker crystal field screening compared to d-metals. This fact allows one to retain the contribution of degenerate three-center integrals (1.29) as the most important. According to the above discussion it is these integrals that determine the atomic level shift arising from the vibration of the ion surroundings of the site and lead to exponential bandwidth renormalization.

If the resulting interaction of the polarons (1.23) on the same or neighboring sites turns out to be attractive, the ground state of the system will correspond to polarons coupled in local pairs (bipolarons). The properties of these pairs are essentially determined by the specific form of the electron-phonon interaction as well as by the phonon mode type.

In the case of Fröhlich type of coupling with polarization optical phonons the explicit calculation of the attractive part of the interaction (1.23) gives the result[35]

$$\gamma = 1, \quad \omega(q) = \omega_0: \quad V_{ij}^{\mathrm{ph}} \propto (1/R_{ij})\mathrm{Si}(q_{\mathrm{D}} R_{ij}), \tag{1.31}$$

where $q_{\mathrm{D}} \propto 1/a$ is the Debye wavevector, $\mathrm{Si}(x)$ is the integral sine function and $R_{ij} = |\mathbf{m}-\mathbf{n}|$. In a similar way for the interaction via longitudinal acoustic phonons one obtains[35]

$$\gamma = -1/2, \quad \omega(q) \propto |\mathbf{q}|: \quad V_{ij}^{\mathrm{ph}} \propto (1/R_{ij}) j_1(q_{\mathrm{D}} R_{ij}), \tag{1.32}$$

where $j_1(x)$ is the spherical Bessel function of the 1st kind.

According to Eq. (1.31) the exchange of optical phonons leads to the long-range attractive potential decreasing with the distance as $1/R$. In the case of acoustic phonon exchange the potential of Eq. (1.32) is an oscillating function falling off $\propto 1/R^2$ at large R. For a sufficiently strong effective interaction small radius on-site (Anderson) or intersite (Heitler–London) bipolarons may be expected for the both types of coupling.

In compounds with complex molecules polaron pairing may be produced also via the interaction with local intramolecular vibrations. Neglecting the dispersion of the phonon mode yields the result

$$\gamma = 0, \quad \omega(q) = \omega_0: \quad V_{ij}^{\mathrm{ph}} = E_{\mathrm{p}} \delta_{ij} \tag{1.33}$$

implying the attraction to be possible only if the polarons are on the same site.

Having discussed the interaction properties, we come to the conclusion that the "contact" term

$$v_0 = V_{ii} - E_{\mathrm{p}}, \tag{1.34}$$

as well as the intersite one at the adjacent sites

$$v_1 = V_{\langle ij\rangle} - V_{\langle ij\rangle}^{\mathrm{ph}}, \tag{1.35}$$

are of the primary importance for interpolaron attraction ($\langle ij\rangle$ denotes the nearest neighbor sites).

For v_1 being expressed as

$$v_1 = \delta_k V_{ii} - \delta_{\mathrm{ph}} E_p, \tag{1.36}$$

one obtains according to the Hubbard estimate[36] for d-metals $\delta_k \simeq (2/a)\exp(-ka) \simeq 0.1$ (a is in units of the Bohr radius). It means that the intersite Coulomb repulsion is drastically reduced compared to the contact term due to screening and large lattice constant values. Meanwhile the phonon induced intersite attraction may turn out to be of the same order as the on-site one. Summing over only the nearest neighbor ($|\mathbf{l}| = a$) terms in Eq. (1.29) and adopting spherical symmetry for the wave function of the state $|0\rangle$, one arrives at the result

$$\delta_{\mathrm{ph}} = S(a)/S(0), \tag{1.37}$$

where

$$S(\mathbf{m}) = \sum_{\mathbf{q}} \frac{1}{\omega^2(q)} \left| (\mathbf{e}\mathbf{l}) e^{i\mathbf{q}\mathbf{l}} \right|^2 e^{i\mathbf{q}\mathbf{m}} \tag{1.38}$$

The factor δ_{ph} does not contain any parameters since $q \leqslant 1/a$ in the expression (1.38). Direct calculation in the case of a simple one-dimensional chain with $\omega^2(q) \propto [1-\cos(qa)]$ gives

$$\delta_{\mathrm{ph}} = \int_0^{\pi} \frac{\sin^2(x)\cos(x)}{1-\cos(x)} dx \left(\int_0^{\pi} \frac{\sin^2(x)}{1-\cos(x)} dx \right)^{-1} = \frac{1}{2}. \tag{1.39}$$

Hence the intersite attraction may be achieved in a simple lattice even if the contact term is of a repulsive character. For a complex lattice consisting of two diatomic molecules the intersite pairing turns out to be preferable due to the lattice symmetry itself. It may be provided by the interaction with the optical mode of intramolecular vibrations. It should be

noted in addition that in compounds with spatially separated complexes a bound state of two small polarons may be formed on a small group of identical ions within the confines of the cell.

The resulting interpolaron on-site or intersite interaction being attractive, a cooperative instability develops in the small polaron system leading to the bipolaron condensate state. Two qualitatively distinct situations are found to be possible. The first one corresponds to intermediate values of the effective interaction constant g, being strong enough to provide the small polaron formation, and weak enough for bipolaron binding energy Δ not to exceed the polaron bandwidth: $\Delta \leqslant W$. This is a limit of the large radius bipolarons quite similar in nature to the familiar Cooper pairs of electrons. The characteristic time interval ($\approx 1/\Delta$) is sufficient for the polaron to make many hops through the medium and to return back to its partner, thus spreading the paired state over a large number of lattice sites. The traditional methods of superconductivity theory including the Hartree-Fock mean field approach[9,37] reformulated in the site representation are quite adequate for the description of this limit, when the carrier concentration is comparable to the atomic one. The second situation deals with the higher values of the interaction constant when contact or intersite attraction becomes much greater than the polaron bandwidth. In the limit of very large g^2 values the $\Delta \gg W$ condition is guaranteed by the power law increase of the attraction as well as by the exponential contraction of the band. This being the case, one has the system of the local on-site/intersite bipolaronic pairs well separated from each other in space. Their cooperative properties are drastically different from those of the condensate of Cooper pairs.[7,8]

Up to now the existence of small polarons and bipolarons has been demonstrated in a diverse assortment of materials. A few examples of unpaired single polaron states were experimentally observed in some alkali halides KCl, LiF,... (Ref. 20), in rutile TiO_2 (Ref. 38), and in manganese oxide MnO (Ref. 39) as well as in other transition metal oxides ($LaCoO_3$,$SrTiO_3$) (Refs. 20, 40). The possibility of the existence of nonoverlapping local pairs associated with impurity centers in amorphous semiconductors was pointed out by Anderson.[41] In a regular crystal small bipolarons were initially observed and studied in Ti_4O_7 (Ref. 42) in the $(Ti_{1-x}V_x)_4O_7$ system (Ref. 43), and in vanadium bronze $Na_xV_2O_5$ (Ref. 44). Lately the list of bipolaron structures was extended by addition of WO_{3-x} (Ref. 45) PbTe (Tl) (Ref. 46) and possibly of some other compounds. There is also a number of well-known materials whose properties may be interpreted in terms of polaron and bipolaron states. Specifically one should mention intermetallic A-15 compounds such as Nb_3Sn, V_3Ga, V_3Si, Chevrel phases, namely, $PbMo_6S_8$ (Refs. 37, 47, 48), and the thoroughly studied ceramic $BaBi_xPb_{1-x}O_3$ (Refs. 49, 11). It is a well-known fact that the anomalous properties of the latter as well as the ideas of polaron theory for Jahn–Teller compounds became a starting point in Bednorz and Müller experiments[1,50] crowned by the discovery of high-temperature superconductivity in a similar ceramic system $La_{2-x}Ba_xCuO_4$. Therefore it does not seem surprising that it is the polaron theory that is considered by a number of authors[12,23–27] to be the theoretical basis for understanding this new phenomenon.

2. VIOLATION OF THE MIGDAL THEOREM

The effective coupling constant (1.16) being expressed in a form more conventional for superconductivity theory

$$\lambda = N(0)V, \tag{2.1}$$

where $V \equiv E_p$ is the characteristic electron-phonon interaction energy and $N(0) \cong 1/D$ is the electron density of states at the Fermi energy, is identical to the well-known BCS theory constant determining the temperature of the superconducting transition

$$T_c \approx \omega \exp(-1/\lambda) \tag{2.2}$$

for $\lambda \ll 1$. In the opposite case $\lambda > 1$ this formula does not work and one arrives at the strong coupling limit described usually in terms of the Eliashberg equations[3] for the self-energy part of the electron Green's function. Those equations are essentialy based on the results of the Migdal study[2] of the strongly coupled electron-phonon system in a normal metal. It is the small value of the adiabatic parameter

$$\omega/E_F \approx \omega/D \ll 1, \tag{2.3}$$

that leads to some significant simplifications in the equations for the Green's functions, the so called "Migdal theorem" being one of them. According to Migdal one can neglect the interaction vertex corrections which are of the order of $(m/M)^{1/2}$, and in addition use the bare electron Green's function instead of the renormalized one in the important ranges of the momentum integration space in the corresponding integral equations. The renormalized electron mass m^* exceeds the bare electron mass m by the factor $(1+\lambda)$ thus leading to the characteristic electron energy of the order of $E_F/(1+\lambda)$. Therefore sometimes it is concluded (see e.g. Ref. 51) that the Migdal theorem is violated if $E_F/(1+\lambda) < \omega$, or under the condition

$$\lambda > E_F/\omega \gg 1, \tag{2.4}$$

corresponding to the extremely high λ values ($\lambda > 10$–100). However it should be kept in mind that this condition guarantees the internal selfconsistency of the approach that is limited to the continuum as well as to the effective mass approximations. The polaron band narrowing effect which may take place for considerably lower λ values than those specified by condition (2.4) is totally ignored in it. The authors of Ref. 5 have undertaken an attempt to take into account the finite value of the electron bandwidth D by substitution of the Lorentz density of states into the standard equation for the self-energy part of the electron Green's function. They have demonstrated the possibility of a rather strong renormalization of the band up to the values of the order of ω with the corresponding values of λ of the order of D/ω in agreement with (2.4). Obviously this modification of the theory is yet not sufficient to take account of discreteness of the lattice in a consistent way and to reproduce the exponential narrowing of Eq. (1.28). For this to be done one should give up both the continuum and the effective mass approximations. We wish to argue in the following that polaron collapse of the electron band takes place at rather moderate effective coupling values

$$\lambda \approx 1 \tag{2.5}$$

and corresponds to polaron transition from the large radius state to the nonadiabatic small radius state. The Migdal theorem is thus strongly violated under this transition.

Let us consider one of the most studied polaron models referred to as the Holstein or the Molecular Crystal Model.[52] The electron motion in a simple cubic lattice is then described by Eqs. (1.6), (1.9)–(1.11), while the electron interaction (1.7) with the dispersionless phonon mode ($\omega(q) = \omega_0$) is taken to be of local type with γ in (1.5) equal to zero. The vibrational mode in this model is usually interpreted as being related to the intramolecular degree of freedom of the site and is sometimes referred to as a "breathing" mode.

The transformed Hamiltonian (1.21) for the single polaron case can be written as

$$H_p = -Je^{-g^2}\sum_{i,j} c_i^+ c_j e^{g(d_i^+ - d_j^+)} e^{-g(d_i - d_j)} + \omega\sum_j d_j^+ d_j - E_p, \tag{2.6}$$

where d_i^+ (d_i) are the phonon operators in the site representation, describing the creation and annihilation of the single vibrational quantum at the ith site. It would be more correct to use g_0 and ω_0 parameters instead of g and ω in the latter equation but this makes no difference for the case of zero temperature considered in this section. If the first term in Eq. (2.6) is neglected, the ground state of the system corresponds to a polaron localized at the arbitrary site $c_i^+|0\rangle$, $i = 1,...,N$. It is an N-times degenerate state with the energy $E_0 = -g^2\omega$ if the spin variable is not taken into account. The first term in the lowest order of perturbation theory removes this degeneracy of the atomic energy level by transforming it to the polaron band with dispersion emerging as

$$\varepsilon_p(\mathbf{k}) = -2Je^{-g^2}[\cos(ak_x) + \cos(ak_y) + \cos(ak_z)] - E_p, \tag{2.7}$$

and corresponding to the polaron ground state energy at the bottom of the band equal to

$$E_0 = -E_p - \frac{1}{2}De^{-g^2} = -g^2\omega - \frac{1}{2}W. \tag{2.8}$$

The exponential damping of the first correction might seem to confirm the criterion (1.14) or (2.5) for the existence of a small polaron state insofar as the constant g^2 is greater than unity. But this is actually not the case, and the expansion parameter turns out to be of the power rather than exponential form. To make this result evident one has to deal with the second order of perturbation theory with respect to the kinetic energy term of Eq. (2.6). Polaron-phonon interaction in this order comprises the emission and absorption of an arbitrary number of phonons in the polaron hopping processes, thus leading to the second order polaron self-energy represented by the diagrams of the type of Fig. 1. Their sum gives the power law correction to the ground state energy E_0, which becomes equal within the power degree of accuracy to

$$E_0 = -E_p\left[1 + \frac{1}{2}z\left(\frac{J}{E_p}\right)^2\right] = -E_p\left[1 + \frac{1}{2}\left(\frac{D}{2z^{1/2}E_p}\right)^2\right] \tag{2.9}$$

(see also Refs. 53, 54). This result demonstrates that it is $1/\lambda$ that plays the role of the true expansion parameter in the

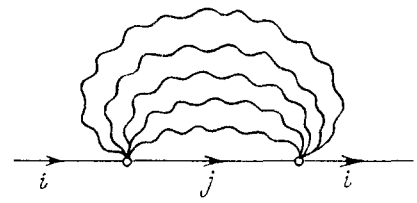

FIG. 1. Polaron self-energy diagram.

strong coupling limit. In accordance with Eq. (2.9) the condition for the existence of the small polaron is given by

$$\lambda = E_p/D \gg 1/2z^{1/2}. \tag{2.10}$$

For $z = 6$, for example, this inequality works well even at $\lambda \simeq 1$.

There have been a number of attempts to calculate the polaron characteristics in order to study the nature of polaron transition from the state with a large radius (a broad band) to the state with a small radius (a narrow band). These attempts have been based largely on variational methods and have shown that the dependence of ground-state energy on λ is nonanalytical and that the renormalization of the polaron mass is discontinuous at the transition point. Emin,[55] for example, predicted the transition to occur at $\lambda = \lambda_c \cong 0.6$ for the three-dimensional variant of the Holstein model with $\omega_0/D = 0.05$. A numerical Monte Carlo simulation method, however, has apparently yielded the most reliable results for the same system.[56,57] In particular, de Raedt and Lagendijk[56] have observed a fairly sharp transition between two states, suggesting a possible nonanalytic behavior near the critical value of the coupling constant. The transition region in this case turned out to be the narrowest for a $3D$ lattice and the widest for a $1D$ lattice. The results reported in Ref. 56 for the case $\omega_0/D = 1/2z$ correspond to the critical values $\lambda_c \cong 0.85$ and $\lambda_c \cong 0.45$ for a $1D$ lattice and $3D$ lattice, respectively.

There is another important result of the Monte Carlo studies of Refs. 56, 57 concerning the critical values of the coupling constant λ_c. Specifically it has been shown that the numerically estimated polaron ground state energy appears to be well approximated by the polaron shift formula

$$E_0 = -g^2\omega_0 = -E_p, \tag{2.11}$$

in the strong coupling region, and by the second order perturbation theory result (with H_{e-ph} in the Hamiltonian (1.1) considered as a small perturbation)

$$E_0 = -zJ - \sum_q |U(q)|^2(\varepsilon(\mathbf{q}) + \omega(\mathbf{q}) - \varepsilon(0))^{-1} \tag{2.12}$$

in the weak coupling region. This fact is itself rather obvious. More surprising is the fact that the numerical values of λ_c coincide, within a small error, with the estimate obtained by equating the expressions (2.11) and (2.12). This circumstance supporting the idea of a sharp transition provides us with a simple procedure for determining λ_c for any chosen value of the adiabatic parameter ω_0/D. The results of the calculations for a local interaction ($\gamma = 0$) and for the Fröh-

lich interaction ($\gamma = 1$) of an electron with a dispersionless phonon mode in a simple cubic lattice are shown in Fig. 2. The small polaron mass renormalization factor at the transition point

$$m_c^*/m = \exp g_c^2, \tag{2.13}$$

is also presented in this figure, where g_c^2 is the critical value of the electron-phonon interaction coupling constant. In particular, it follows from Fig. 2 that at $D/\omega_0 \geqslant 5$ the values of $\lambda \geqslant 1$ correspond to the small polaron state and the Migdal theorem is inapplicable. In the case of a wider bare band, where $D/\omega_0 \geqslant 20$, its range of validity is limited to even smaller values of $\lambda \leqslant 0.7$.

3. POLARON SUPERCONDUCTORS. SOME PHYSICAL CONSEQUENCES OF THE NARROW BAND

Let us turn to a discussion of superconducting correlations in the small polaron system when the resultant interaction between them is weak in comparison with the polaron bandwidth.[9] The relevant part of the polaron Hamiltonian (1.21) after averaging (1.25) takes the form of the extended Hubbard Hamiltonian:

$$H = \sum_{i,j}(\sigma_{ij}c_i^+c_j + v_{ij}n_in_j) - \varepsilon_F\sum_i n_i, \tag{3.1}$$

with the Fermi energy ε_F being measured from the middle of the polaron band shifted with respect to the initial zero energy level by the value of E_p.

In the second term in parentheses we shall retain only the contact $v_{ii} \equiv v_0$ and the nearest neighbor intersite $v_{\langle ij\rangle} \equiv v_1$ interaction terms. In addition we shall restrict ourselves to the case of singlet pairing.

In the weak coupling limit polarons constituting a pair (bipolaron) make numerous hopping transitions during the characteristic time interval, thus spreading the bound state over a large number of sites. As a result, a bipolaron does not differ qualitatively from a Cooper pair, and standard Hartree–Fock approximation may be applied to the Hamiltonian (3.1). By introducing two order parameters

$$\Delta_0 = -v_0\langle c_{m\uparrow}c_{m\downarrow}\rangle, \quad \Delta_1 = -zv_1\langle c_{n\uparrow}c_{m\downarrow}\rangle \tag{3.2}$$

and transforming to the **k**-representation one arrives at the usual BCS Hamiltonian

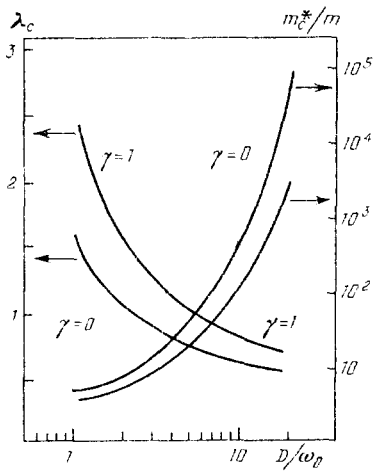

FIG. 2. Critical values of the effective coupling constant and of electron mass renormalization as functions of the adiabatic parameter.

$$H = \sum_{\mathbf{k},s}\xi_{\mathbf{k}}c_{\mathbf{k}s}^+c_{\mathbf{k}s} + \sum_{\mathbf{k}}[\Delta(\mathbf{k})c_{\mathbf{k}\uparrow}^+c_{-\mathbf{k}\downarrow}^+ + \text{H.c.}], \tag{3.3}$$

where

$$\xi_{\mathbf{k}} = -\sigma\sum_{|\mathbf{n}|=a} e^{i\mathbf{k}\mathbf{n}} - \varepsilon_F \tag{3.4}$$

is the energy of the polaron with momentum **k** in the nearest neighbor approximation measured from the Fermi level ($\varepsilon_F = 0$ for the half-filled band), and

$$\sigma = \sigma_{\langle mn\rangle} = J\exp(-g^2) = W/2z \tag{3.5}$$

is the polaron hopping integral for the neighboring sites.

In contrast to the BCS theory taking account of the intersite interaction term results in spatial dispersion of the order parameter which has the form

$$\Delta(\mathbf{k}) = \Delta_0 - \Delta_1[2(\xi_{\mathbf{k}} + \varepsilon_F)/W], \tag{3.6}$$

corresponding to s-wave pairing. More generally d-wave singlet as well as p-wave triplet types of pairing are possible for the Hamiltonian (3.1) (see the review article of Ref. 58 and references therein).

Applying the standard diagonalization procedure to the Hamiltonian (3.3), one obtains for the order parameter

$$\langle c_{\mathbf{k}\uparrow}c_{-\mathbf{k}\downarrow}\rangle = \frac{\Delta(\mathbf{k})}{2(\xi_{\mathbf{k}}^2 + |\Delta(\mathbf{k})|^2)^{1/2}}\text{th}\frac{(\xi_{\mathbf{k}}^2 + |\Delta(\mathbf{k})|^2)^{1/2}}{2T}. \tag{3.7}$$

With Eq. (3.2) in mind one is easily able to find the equations for Δ_0 and Δ_1

$$\Delta_0 = -\frac{v_0}{N}\sum_{\mathbf{k}}\frac{\Delta(\mathbf{k})}{2(\xi_{\mathbf{k}}^2 + |\Delta(\mathbf{k})|^2)^{1/2}}\text{th}\frac{(\xi_{\mathbf{k}}^2 + |\Delta(\mathbf{k})|^2)^{1/2}}{2T}, \tag{3.8}$$

$$\Delta_1 = -\frac{v_1}{z\sigma N}\sum_{\mathbf{k}}\frac{(\xi_{\mathbf{k}} + \varepsilon_F)\Delta(\mathbf{k})}{2(\xi_{\mathbf{k}}^2 + |\Delta(\mathbf{k})|^2)^{1/2}}\text{th}\frac{(\xi_{\mathbf{k}}^2 + |\Delta(\mathbf{k})|^2)^{1/2}}{2T}, \tag{3.9}$$

which may be rewritten as a single equation of BCS-type, but with the potential depending on energy

$$\Delta(\xi) = \bar{\lambda}\int_{-(W/2)-\varepsilon_F}^{(W/2)-\varepsilon_F} d\xi' N_p(\xi')\left[\mu + \frac{(\xi + \varepsilon_F)(\xi' + \varepsilon_F)}{(W/2)^2}\right] \times \frac{\Delta(\xi')}{2[(\xi')^2 + |\Delta(\xi')|^2]^{1/2}}\text{th}\frac{[(\xi')^2 + |\Delta(\xi')|^2]^{1/2}}{2T}, \tag{3.10}$$

where $\bar{\lambda} = z|v_1|/W$ has the meaning of the effective coupling,

$$N_p(\xi) = \frac{W}{N}\sum_{\mathbf{k}}\delta(\xi - \xi_{\mathbf{k}}) \tag{3.11}$$

is the dimensionless density of polaron states, and $\mu = v_0/zv_1$ is the contact to intersite interaction ratio. The value of $\mu < 0$ is possible if the contact Coulomb repulsion is sufficiently strong.

The quantity that plays the role of interaction in the BCS-like equation (3.10) for the order parameter is

$$\bar{\lambda}\left[\mu+\frac{(\xi+\varepsilon_F)(\xi'+\varepsilon_F)}{(W/2)^2}\right]. \tag{3.12}$$

We note that all the parameters $(\bar{\lambda},\mu,W)$ may be explicitly expressed in terms of the atomic wave function matrix elements of the corresponding potentials and the phonon spectrum. Insofar as $N_p(\xi)$ describes the narrow polaron band with integration limits being determined by the bandwidth value, the explicit form of the $N_p(\xi)$ function as well as the Fermi level position in the polaron band may greatly influence the magnitude of Δ and T_c.

The critical temperature is determined by Eq. (3.10) in the limit $\Delta\to 0$:

$$\Delta(\xi)=\bar{\lambda}\int_{-(W/2)-\varepsilon_F}^{(W/2)-\varepsilon_F} d\xi' N_p(\xi')\left[\mu+\frac{(\xi+\varepsilon_F)(\xi'+\varepsilon_F)}{(W/2)^2}\right]\times\frac{\Delta(\xi')}{2|\xi'|}\operatorname{th}\frac{|\xi'|}{2T_c}. \tag{3.13}$$

If one takes for simplicity the energy independent density of states $N_p(\xi)=1$ from the solvability condition of Eq. (3.13) with respect to Δ_0 and Δ_1 one obtains in the limit $T_c \ll [(W/2)^2-\varepsilon_F^2]^{1/2}$ (Refs. 9 and 37)

$$T_c=1{,}14\frac{W}{2}\left(1-\frac{4\varepsilon_F^2}{W^2}\right)^{1/2}\times\exp\left\{-\frac{1+\frac{\bar{\lambda}}{2}\left[\frac{3\varepsilon_F^2}{(W/2)^2}-1\right]-\bar{\lambda}^2\mu\frac{4\varepsilon_F^2}{W^2}}{\bar{\lambda}\left(\frac{4\varepsilon_F^2}{W^2}+\mu\left[1-\frac{\bar{\lambda}}{2}\left(1+\frac{4\varepsilon_F^2}{W^2}\right)\right]\right)}\right\}. \tag{3.14}$$

This expression represents the analytically derived equivalent of the well-known MacMillan formula for the case of weak and intermediate coupling of polarons. In the small polaron regime under the condition $W<\omega$ (antiadiabatic limit) the polaron bandwidth plays the role of the Debye temperature and retardation is absent. In the limit of $\bar{\lambda}\ll 1$ a simplified formula for T_c emerges as

$$T_c\approx 1{,}14\frac{W}{2}\left(1-\frac{4\varepsilon_F^2}{W^2}\right)^{1/2}\exp\left\{-\left[\bar{\lambda}\left(\frac{4\varepsilon_F^2}{W^2}+\mu\right)\right]^{-1}\right\}. \tag{3.15}$$

It is seen that T_c is governed by both the contact and nearest neighbor intersite interaction terms, with the latter depending on the Fermi level position in the band. For the half-filled band ($\varepsilon_F=0$) the nearest neighbor contributions are compensating each other and superconductivity survives only if contact attraction is present ($\mu>0$). Because of the exponential dependence of the polaron bandwidth W on g^2 a considerable change in the value of T_c may be produced even by a small change in the phonon frequencies. A softening of the phonon spectrum results in an increase of g^2 and decreases the polaron bandwidth thus leading to $\bar{\lambda}$ growth. A similar strong dependence of T_c on the Fermi level position in the band exists which provides the T_c correlation with the number n_e of electrons per atom in the partially filled band. Since

$$\varepsilon_F\approx(W/2)(n_e-1), \tag{3.16}$$

in the model with $N_p(\xi)=\text{const}$ (2D-lattice), Eq. (3.15) leads to $T_c(n_e)$ dependence of the following type:

$$T_c\approx 1{,}14\frac{W}{2}[n_e(2-n_e)]^{1/2}\exp\left\{-\frac{1}{\bar{\lambda}[\mu+(n_e-1)^2]}\right\}. \tag{3.17}$$

For negative or small positive μ values Eq. (3.17) as a function of n_e has two maxima separated by a deep minimum at $n_e=1$. The T_c decrease in $n_e\to 0$ and $n_e\to 2$ limits with Fermi level approaching the boundaries of the band is interpreted as a result of a reduction of the number of states contributing to pairing. The minimum at $n_e=1$ is provided by the above mentioned compensation of the nearest neighbor contributions to the interaction constant.

Let us now discuss some of the consequences of the polaron band narrowing for the normal phase.

3.1. Polaron heat capacity

In the normal phase for sufficiently high temperature the correlations due to interaction are unimportant and in first approximation the polaron contribution to the heat capacity as well as to the magnetic susceptibility can be evaluated without taking v_{ij} into account. In the temperature range of $T<\omega/2$ with the polaron band being almost independent of T this contribution is described by the expression for the heat capacity of a Fermi-gas:

$$C_P=-2T\int_{-(W/2)-\varepsilon_F}^{(W/2)-\varepsilon_F} d\xi N_p(\xi)\frac{\partial f}{\partial\xi}\left[\left(\frac{\xi}{T}\right)^2-\frac{\xi}{T}\frac{\partial\varepsilon_F}{\partial T}\right], \tag{3.18}$$

where f stands for the Fermi distribution function.

Eq. (3.18) provides a linear temperature dependence of C_P in the low temperature limit $T\ll W$ and a power law decrease $\propto T^{-2}$ for $T\gg W$. If $N_p(\xi)=1$, one has

$$C_P=\frac{\pi^2}{3}\frac{NT}{W},\qquad T\ll W, \tag{3.19}$$
$$C_P=\frac{(W/2)^2 n_p}{3T^2}\left(1-\frac{n_e}{2}\right),\qquad T\gg W,$$

where n_e denotes as previously the number of electrons per atom in the partially filled band, and $n_p=Nn_e$ is the polaron number in the normalization volume. The numerical calculation which is required in the intermediate region reveals negligible changes of the position of the maximum C_P with variation of band filling (n_e):

$$T_{max}\approx 0{,}2W, \tag{3.20}$$

and a gradual increase of maximum value with n_e from the value of $C_P\cong 0.2N$ at $n_e=0.2$ to the value of $C_P\cong 0.6N$ at $n_e=1$.

On the whole the temperature dependence of the heat capacity is similar to the Shottky anomaly except for the low temperature range with the linear T-dependence of C_P instead of the exponential growth typical of two-level systems. The polaron heat capacity in the considered region ($T<\omega/2$) is formally the same as the electron one in the well-known phenomenological model of Clogston and Jaccarino,[59] where all the Brillouin zone states are contributing

to the formation of the density of states peak (narrow energy band).

As a consequence of the nonlinear behavior of the polaron heat capacity the coefficient $\gamma(T) = C_P/T$ turns out to be a function of temperature varying from the value

$$C_P/T = (2\pi^2/3)k_B^2 N_p(0) \quad \text{at} \quad T = 0 \tag{3.21}$$

to zero at $T \gg W$. In the last equation $N_p(0)$ is the dimensional density of polaron states at the Fermi surface, the temperature is expressed in the usual units (K), and k_B is the Boltzmann constant. The most appreciable change of $\gamma(T)$ is predicted in the temperature range $T \leqslant T_{max}$.

3.2. Spin susceptibility

In the model considered the narrow peak in the density of states arises due to the polaron band which comprises all the states of the Brillouin zone rather than a small part of them as in the Labbe–Friedel models. This fact provides us with the possibility to get absolute values of spin susceptibility considerably higher than those for the ordinary wide-band metals.

Taking in analogy with the previous treatment $N_p(\xi) = 1$ we can write for the polaron paramagnetic susceptibility

$$\chi_p = 2\frac{N}{W}\mu_B^2 \int_{-(W/2)-\varepsilon_F}^{(W/2)-\varepsilon_F} d\xi \left(-\frac{\partial f}{\partial \xi}\right). \tag{3.22}$$

The Fermi energy is fixed by the polaron concentration relation

$$n_p = 2\frac{N}{W} \int_{-(W/2)-\varepsilon_F}^{(W/2)-\varepsilon_F} d\xi f(\xi, T). \tag{3.23}$$

As a result we have

$$\frac{\varepsilon_F}{T} = \ln \frac{\exp(n_e W/2T) - 1}{\exp(W/2T) - \exp[(n_e - 1)W/2T]}, \tag{3.24}$$

and

$$\chi_p = 2\frac{N}{W}\mu_B^2 \left(\exp\frac{n_e W}{2T} - 1\right) \frac{\exp[(2 - n_e)W/2T] - 1}{\exp(W/T) - 1}. \tag{3.25}$$

For $T \gg W$ Eq. (3.25) reduces to the Curie law

$$\chi_p \approx n_p \mu_B^2 [1 - (n_e/2)]/T. \tag{3.26}$$

For $T \leqslant W$ the χ_p saturates and approaches the limit

$$\chi_p(0) = 2N\mu_B^2/W. \tag{3.27}$$

We wish to note that for temperatures $T < W$ Eq. (3.25) should be considered only as an estimate because the polaron band structure or equivalently the energy dependence of the density of states $N_p(\xi)$ become important in this region.

To conclude the discussion of the polaron theory results for the normal phase we refer to the more detailed review of Ref. 48 where these and some other consequences were utilized to analyze the physical properties of superconducting materials such as A-15 and C-15 compounds, ternary chalcogenides and some others. It was concluded in particular that the unusual properties of most of these materials, namely, the large and strongly temperature-dependent values of the magnetic susceptibility $\chi(T)$ and the C/T ratio, the anomalous temperature behavior of resistivity, the phonon spectrum softening as the temperature decreases, are due to the strong interaction of d-electrons with phonons resulting in small polaron formation and polaron band-narrowing effect.

4. NORMAL STATE OF STRONGLY COUPLED ELECTRON-PHONON SYSTEM: DIELECTRIC PROPERTIES AND VIBRATIONAL EXCITATIONS

It will be our primary aim in this section to discuss the dielectric response of a many-polaron system and the effect of polaron-polaron interaction on the phonon frequencies. The rigorous expression for the Hamiltonian is developed on the basis of the small polaron canonical transformation. It contains the main part of the electron-phonon interaction in the diagonal form leaving the rest in the form of the polaron-polaron interaction and of the residual small polaron-phonon interaction. The last two contributions are taken into account by the ordinary random phase approximation (RPA) and perturbation theory in the reciprocal coupling constant $1/\lambda$, respectively. The polaron Green's function is obtained. The study of the static and dynamic response shows that due to the exponentially large mass renormalization the Debye radius and the plasma frequency appear to be much smaller than they are for a weakly coupled electron-phonon system and depend on temperature for $T > W$. Small polarons screen effectively the on-site Coulomb interaction, reducing it to the value of the order of W. At the same time the on-site attraction, if it is present, is enhanced by many-body effects. We generalize our expression for the phonon self-energy by taking into account the polaron-polaron interaction. The polarization loop with small polaron lines is analyzed in the site representation and the vibration excitation spectrum is obtained. One of the most interesting results is the existence of a new type of vibrational excitations emerging from the coupling of phonons with low frequency polaron plasmons. We refer to these excitations as "plasphons".

4.1. Polaron-polaron and polaron-phonon interactions, and the polaron Green's function

The interaction of carriers in a doped dielectric parent compound with a dielectric matrix as well as with each other will be described as previously in terms of the Hamiltonian (1.1)–(1.4), where the H_{e-e} contribution (1.18) will be taken in the form

$$H_{e-e} = \sum_{k,k'} V(q) c^+_{k+q,s} c^+_{k'-q,s'} c_{k',s'} c_{k,s} + H'_{e-e}, \tag{4.1}$$

In Eq. (4.1) $V(\mathbf{q}) = 4\pi e^2/vq^2$ is the Coulomb repulsion matrix element (the Fourier transform of V_{ij} in (1.18). H'_{e-e} corresponds to the carrier interaction with the dielectric matrix, accompanied by the polarization of the electron shells of the ions that cannot be included in the crystal field. This polarization is described below by the dielectric response function $\varepsilon_d(\mathbf{q},\omega)$ assumed to be constant in the frequency and momentum region under consideration. Thus one can

omit the H'_{e-e} term while replacing the bare Coulomb interaction by the renormalized one:

$$\tilde{V} = V/\varepsilon_d. \tag{4.2}$$

In this way the theoretical formalism becomes well defined to describe both the electron-phonon and electron-electron correlations of the carriers.

It is worthwhile to note that parametrizing the electron-phonon and the Coulomb interactions by the matrix elements being dependent only on the momentum transfer, we neglect the contributions proportional to the overlap integrals of atomic orbitals at the different sites. This approximation is good for sufficiently narrow bare bands with the width not exceeding the crystal field value. The site-nondiagonal ("hopping") terms are responsible for the polaron bandwidth and may reduce the small polaron mass through the electron-phonon interaction. In simple metals with the wide bare bands the hopping terms are dominating in the electron-phonon interaction and may destroy selflocalized polaronic state. In lead, for example, with $\lambda > 1$ there is no evidence of small polaron behavior.

Strictly speaking, the subdivision of electrons into "carriers" and "inner" electrons is being consistent for semiconductors only, when the parent dielectric compound does really exist. For metals our Hamiltonian may be considered generally as the bare one with the matrix elements of no direct physical meaning. Nevertheless we believe, that it can be used in metals also, provided that strong electron-phonon interaction including the possible polaron collapse of the band is treated in a proper way.

The canonical transformation (1.19) of the initial Hamiltonian (1.1) gives rise to the explicit polaron Hamiltonian H_p (1.21) which for the purposes of this section is expedient to express as the sum of three terms

$$H_p = H_0 + H_{p-p} + H_{p-ph}, \tag{4.3}$$

Here the main part of the electron-phonon interaction is included in the Hamiltonian of "zero order" approximation diagonal with respect to the phonon variables

$$H_0 = \sum_{i,j} \sigma_{ij} c_i^+ c_j + \sum_q \omega(q) d_q^+ d_q, \tag{4.4}$$

and two other contributions describing the residual polaron-polaron and phonon-polaron interactions are respectively written as

$$H_{p-p} = \sum_{i,j} v_{ij} n_i n_j, \tag{4.5}$$

$$H_{p-ph} = \sum_{i,j} (\hat{\sigma}_{ij} - \sigma_{ij}) c_i^+ c_j . \tag{4.6}$$

In accordance with the preceeding sections the matrix element σ_{ij} diagonal over phonon variables and describing the polaron band motion is obtained as the temperature average of the operator $\hat{\sigma}_{ij}$ carried out with the phonon density matrix. It is further assumed that the element v_{ij} in Eq. (4.5) now contains the renormalized Coulomb interaction $\tilde{V}_{ij}$ rather than V_{ij} and the polaron shift term E_p is excluded by the equivalent shift of the energy reference level.

In contrast to the ordinary Fröhlich interaction the polaron-phonon term H_{p-ph} gives rise to multiphonon vertices, which play the dominant role. Following the analysis of Sec. 2 this term at $\lambda > 1$ will be treated as a perturbation for both the polaron and phonon Green's functions.

According to the previous discussion the polaron-polaron interaction in the site representation (see Eqs. (1.21), (1.23)) is governed by the matrix elements v_{ij} of the form

$$v_{ij} = (V_{ij}/\varepsilon_d) - V_{ij}^{ph} = (e^2/|m-n|\varepsilon_d) - V_{ij}^{ph}, \tag{4.7}$$

where in the case of polarized optical phonons one has[20,35]

$$V_{ij}^{ph} = \frac{e^2(\varepsilon_0 - \varepsilon_d)}{2\pi\varepsilon_0\varepsilon_d} \frac{\mathrm{Si}(q_D|m\,n|)}{|m-n|} \tag{4.8}$$

(ε_0 is the static permittivity of the crystal). This result obtained from Eq. (1.5) for the case of $\gamma = 1$ and $g_0 = i[2\pi e^2(\varepsilon_d^{-1} - \varepsilon_0^{-1})/a\omega_0]^{1/2}$ is valid in the long wavelength region only. In contrast to the long-range interaction via the optical phonons, for the interaction via the acoustic modes or the intramolecular vibrations the corresponding term is of short-range type (see Eqs. (1.32), (1.33)). Thus at large distances the polaron-polaron interaction takes the form of the effective Coulomb repulsion

$$v_{ij} = e^2/|m-n|\varepsilon_0 \tag{4.9}$$

or

$$v_{ij} = e^2/|m-n|\varepsilon_d \tag{4.10}$$

depending on the type of phonons strongly coupled with electrons. This fact makes it possible to treat v_{ij} on the ground of the usual RPA for the long-wave excitations. At short distances the polaron-polaron interaction may be attractive, thus leading to the instability with respect to small bipolaron formation at a low enough temperature.[7]

Later on in this section we consider the polaron-polaron and the polaron-phonon correlations in the normal state assuming only that the temperature of the system is above the small bipolaron pair formation temperature, which, in turn, is higher than the critical temperature of the superconducting (superfluid) transition.

Let us write the zero order Hamiltonian in the momentum representation

$$H_0 = \sum_{\mathbf{k},s} \xi_{\mathbf{k}} c_{\mathbf{k}s}^+ c_{\mathbf{k}s} + \sum_{\mathbf{q}} \omega(\mathbf{q}) d_{\mathbf{q}}^+ d_{\mathbf{q}}, \tag{4.11}$$

where

$$\xi_{\mathbf{k}} = \sum_{\mathbf{n}} \sigma_{\mathbf{m}\mathbf{n}} \exp[i\mathbf{k}(\mathbf{m}-\mathbf{n})] \tag{4.12}$$

is the small polaron energy dispersion in a narrow band.

Thus the free polaron Green's function is given by

$$G_{\mathbf{k}}(\omega_n) = (i\omega_n - \xi_{\mathbf{k}} + \varepsilon_F)^{-1} \tag{4.13}$$

with $\omega_n = \pi T(2n+1)$. In the site representation it corresponds to

$$G_{ij}(\omega_n) = \frac{1}{N}\sum_{\mathbf{k}} \exp[-i\mathbf{k}(\mathbf{m}-\mathbf{n})](i\omega_n - \xi_{\mathbf{k}} + \varepsilon_F)^{-1}. \tag{4.14}$$

Taking into account the exponential smallness of the polaron bandwidth one can obtain for the polaron Green's function in the "total localization approximation" (TLA):

$$G_{ij}(\omega_n) = \delta_{ij}(i\omega_n + \varepsilon_F)^{-1}, \tag{4.15}$$

which turns out to be useful in the temperature range $T \gg W$. In this approximation one has

$$\varepsilon_F = T \ln \frac{n_e}{2 - n_e}, \tag{4.16}$$

and for the small polaron distribution function:

$$n_k = \left(\exp\frac{\xi_k - \varepsilon_F}{T} + 1\right)^{-1} \approx \frac{1}{2}n_e\left[1 - \frac{\xi_k(2 - n_e)}{2T}\right]. \tag{4.17}$$

Taking into account the finite polaron bandwidth $\xi_k \approx W$ one gets corrections of the order of $\lambda^{-1}\exp(-g^2)$. They are exponentially small compared to the main power-law corrections of the residual polaron-phonon interaction, which are proportional to λ^{-2}. We shall ignore them since λ^{-1} is small.

4.2. Response function of small polarons

In the RPA the effect of the polaron-polaron interaction may be characterized by the dielectric "constant" $\varepsilon(\omega,\mathbf{q})$, which describes the response of small polarons to the longitudinal electric field with the wave vector $\mathbf{q}$ and the frequency ω. In this way the screening behavior of the system and the plasmon frequency may be calculated:

$$\varepsilon(\omega, q) = 1 - 2v(q)\sum_k (n_{k+q} - n_k)(\omega - \xi_k + \xi_{k+q})^{-1}, \tag{4.18}$$

where $v(\mathbf{q})$ is the Fourier component of the polaron-polaron interaction matrix element.

Let us start with the static permittivity. For $T = 0$ in the long wavelength limit $q \to 0$ one arrives at the usual Debye screening:

$$\varepsilon(0, q) = 1 + (qr_D)^{-2}, \quad r_D = \left(\frac{\varepsilon}{4\pi e^2 N_p(0)}\right)^{1/2}, \tag{4.19}$$

where $N_p(0) = N_e(0)\exp(g^2)$ is the density of states in the polaron band on the Fermi level, which is exponentially enhanced with respect to the electron density of states $N_e(0)$, ε equals ε_0 or ε_d depending on the type of phonons taking part in the interaction. One can see from Eq. (4.19) that the Debye radius of small polarons r_D is much smaller than that of electrons due to the strong enhancement of the effective mass. In the short wave-length limit $q \gg k_F$, with k_F being the Fermi wave-vector, one obtains

$$\varepsilon(0, q) = 1 + \{v(q)Nzn_e/W[1 - \cos(qa)]\}, \tag{4.20}$$

where a is the lattice constant, the $\mathbf{q}$-vector is directed along the x axis, the concentration is small $n_e \ll 1$ and ξ_k for simplicity is taken in the nearest neighbor approximation

$$\xi_k = -2(W/z)[\cos(ak_x) + \cos(ak_y) + \cos(ak_z)]. \tag{4.21}$$

The short wavelength behavior of the dielectric response function is completely different from that of free electrons (wide band). In the latter case the polarization loop goes to zero like $1/q^2$ for $q \gg k_F$. On the other hand, small polarons screen effectively the short-range interaction due to the finite bandwidth. For the case of contact interaction

$$v(q) = U_c/N \tag{4.22}$$

with $U_c \gg W/zn_e$ the screened potential $\tilde{U}_c$ is given by:

$$\tilde{U}_c = \frac{U_c}{1 + \{U_c zn_e/W[1 - \cos(qa)]\}}, \tag{4.23}$$

$$\tilde{U}_c < \frac{2W}{zn_e}. \tag{4.24}$$

We therefore conclude that the correlation effect resulting from modification of electron trajectories by two-particle collisions reduces the intra-site interaction (the Coulomb self-energy) to a value of the order of the bandwidth when the self-energy is much larger than the bandwidth. Kanamori[60] was the first to prove this result for electrons in transition metals.

Let us turn to the temperature behavior of the small polaron response and show that the correlation effect enhances the short-range attraction and on the contrary reduces the short-range repulsion.

For the temperatures $T \gg W$ one can use TLA, Eq. (4.17), with the following result

$$\varepsilon(0, q) = 1 + [v(q)Nn_e(2 - n_e)/2T]. \tag{4.25}$$

The screened short-range interaction is given by

$$\tilde{U}_c = U_c T/(T \pm T_b), \tag{4.26}$$

where

$$T_b = |U_c|(2 - n_e)n_e/2 \tag{4.27}$$

is the characteristic temperature and the upper (lower) sign in Eq. (4.26) corresponds to repulsion (attraction) of the carriers. It follows from Eq. (4.26) and Fig. 3a, that in the temperature range $T < T_b$ the short-range Coulomb repulsion is substantially suppressed by the screening. In the case of attraction according to Eq. (4.26) there is a singularity in the two particle correlator at $T = T_b$. Thus T_b appears to be the critical temperature for the small bipolaron formation. The short-range attraction is enhanced near T_b (see Fig. 3b).

The small polaron response becomes dynamic at rather low frequency values $\omega > W$:

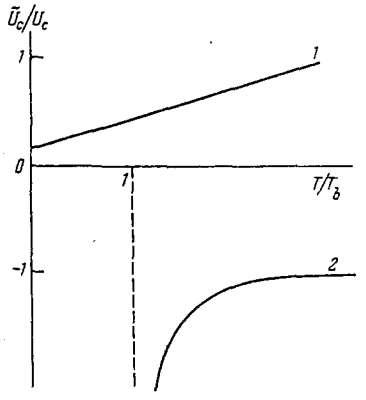

FIG. 3. Screened short-range interaction between small bipolarons as a function of temperature; *1*—repulsion, *2*—attraction.

$$\varepsilon(\omega, \mathbf{q}) = 1 - (\omega_p^2/\omega^2) \tag{4.28}$$

with the temperature-dependent plasma frequency

$$\omega_p^2(\mathbf{q}) = 2v(\mathbf{q})\sum_{\mathbf{k}} n_{\mathbf{k}}(\xi_{\mathbf{k}+\mathbf{q}} - \xi_{\mathbf{k}}), \tag{4.29}$$

being proportional to $1/T$ in the $T \gg W$ region. At low temperatures $T < W$ and concentrations the long-wave plasmon has the frequency

$$\omega_p^2 = 4\pi N e^2 n_e/m^*\varepsilon, \tag{4.30}$$

which is much smaller than the common values of this quantity due to the exponential mass renormalization $m^*/m = \exp(g^2)$.

Thus we come to the conclusion that in the simple RPA the small polaron response is of a rather unusual character with a small temperature-dependent Debye radius and plasma frequency. For the case of repulsion the polaron plasmon has a well defined dispersion with zero damping in the entire region of wave-vector space. If $v(\mathbf{q}) < 0$ for some values of $\mathbf{q}$, the plasmon disappears in this region of $\mathbf{q}$-space.

4.3. Phonon self-energy

The phonon self-energy Σ_{ph} is given to the second order in polaron-phonon interaction by the sum of diagrams of Fig. 4, which can be expressed in terms of the multiphonon correlator:[61]

$$\Phi_{ij}^{i'j'}(\tau) = \langle T_\tau \hat{\sigma}_{ij}(\tau)\hat{\sigma}_{i'j'}(0)\rangle, \tag{4.31}$$

where

$$\hat{\sigma}_{ij}(\tau) = \exp(H_0\tau)\hat{\sigma}_{ij}\exp(-H_0\tau), \tag{4.32}$$

and $-1/T < \tau < 1/T$. The first order diagrams as well as the second order terms containing two polarization loops are exponentially reduced by a factor $\exp(-g^2)$.[61]

For imaginary values of τ the correlator of Eq. (4.31) was calculated by Lang and Firsov.[62] To get $\Phi(\tau)$ for real τ-values one has to make a substitution $t \to -i|\tau|$ in Eq. (A1.7) of Ref. 62 thus arriving at the result

$$\Phi_{ij}^{i'j'}(\tau) = \sigma_{mn}\sigma_{m'n'}\exp\left\{\frac{1}{N}\sum_{\mathbf{q}} \frac{\mathcal{S}^2(\mathbf{q})}{\mathrm{sh}(\omega(\mathbf{q})/2T)} f_{\mathbf{q}}\,\mathrm{ch}\left[\omega\left(\mathbf{q}\right)\left(|\tau| - \frac{1}{2T}\right)\right]\right\}, \tag{4.33}$$

where

$$\mathcal{S}(\mathbf{q}) = (2N)^{1/2}U(\mathbf{q})/\omega(\mathbf{q}) \tag{4.34}$$

is a dimensionless electron-phonon interaction matrix element,

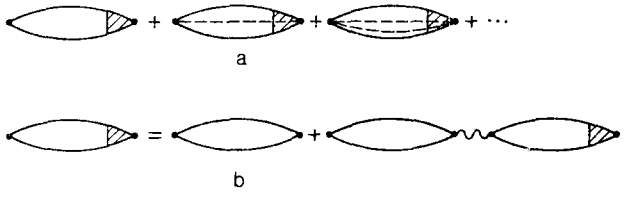

FIG. 4. Phonon self-energy diagram (a); polaron polarization loop (b).

$$f_{\mathbf{q}} = \frac{1}{2}\{\cos(\mathbf{q}[\mathbf{c} - \mathbf{a}]) + \cos(\mathbf{q}[\mathbf{c} + \mathbf{b}]) - \cos(\mathbf{q}\mathbf{c}) - \cos(\mathbf{q}[\mathbf{c} - \mathbf{a} + \mathbf{b}])\}, \tag{4.35}$$

and $\mathbf{a} = \mathbf{m} - \mathbf{n}$, $\mathbf{b} = \mathbf{m}' - \mathbf{n}'$, $\mathbf{c} = \mathbf{n}' - \mathbf{n}$. The sum of diagrams of Fig. 4a gives

$$\Sigma_{ph}(\mathbf{q}, \omega_n) = -T\sum_{\omega_{n'}} \sum_{\substack{i,j \\ i',j'}} (u_i^* - u_j^*)(u_{i'} - u_{j'})\Phi_{ij}^{i'j'}(\omega_{n'}) \times \Pi_{iji'j'}(\omega_{n'} - \omega_n), \tag{4.36}$$

where

$$u_i \equiv u_i(q) = \frac{1}{(2N)^{1/2}}\mathcal{S}(\mathbf{q})e^{i\mathbf{q}\mathbf{m}}, \tag{4.37}$$

$$\Phi_{ij}^{i'j'}(\omega_n) = \frac{1}{2}\int d\tau\,[\Phi_{ij}^{i'j'}(\tau)\exp(i\omega_n\tau)],$$
$$\omega_n = 2\pi nT,\ \omega_{n'} = 2\pi n'T, \tag{4.38}$$

and $\omega_n = 2\pi nT$, $\omega_{n'} = 2\pi n'T$.

Taking the simple loop $\Pi^{(0)}$ for the polarization operator Π, one arrives at the result of Ref. 61. Taking further into account polaron-polaron correlations we obtain in RPA (Fig. 4b)

$$\Pi_{iji'j'} = \Pi_{iji'j'}^{(0)} + \sum_{l,p} \Pi_{ijll}^{(0)} v(\mathbf{l} - \mathbf{p})\Pi_{ppi'j'} \tag{4.39}$$

To get the solution of Eq. (4.39) we use the Fourier transform of the function Π:

$$\Pi_{iji'j'} = \frac{1}{N^3}\sum_{k,g,k'} \Pi(\mathbf{k}, \mathbf{k}', \mathbf{g}) \times \exp[-i\mathbf{k}(\mathbf{m}' - \mathbf{n}) + i\mathbf{k}'(\mathbf{n}' - \mathbf{m}) + i\mathbf{g}(\mathbf{m}' - \mathbf{n}')]. \tag{4.40}$$

The Fourier-component of the polarization operator has to satisfy the following equation:

$$\Pi(\mathbf{k}, \mathbf{k}', \mathbf{g}) = \Pi^{(0)}(\mathbf{k}, \mathbf{k}')[N\delta_{g,0} + v(\mathbf{k} - \mathbf{k}')\sum_{g'} \Pi(\mathbf{k} + \mathbf{g}' - \mathbf{g}, \mathbf{k}' + \mathbf{g}' - \mathbf{g}, \mathbf{g}')], \tag{4.41}$$

where

$$\Pi^{(0)}(\mathbf{k}, \mathbf{k}') = 2(n_k - n_{k'})/(i\omega_n + \xi_k - \xi_{k'}). \tag{4.42}$$

One can replace $\mathbf{k},\mathbf{k}'$ in Eq. (4.41) by $\mathbf{k} + \mathbf{g}$ and $\mathbf{k}' + \mathbf{g}$, respectively, to obtain

$$\Pi(\mathbf{k} + \mathbf{g}, \mathbf{k}' + \mathbf{g}, \mathbf{g}) = \Pi^{(0)}(\mathbf{k} + \mathbf{g}, \mathbf{k}' + \mathbf{g})[N\delta_{g,0} + v(\mathbf{k} - \mathbf{k}')A(\mathbf{k}, \mathbf{k}')], \tag{4.43}$$

with

$$A(\mathbf{k}, \mathbf{k}') = \sum_{g'} \Pi(\mathbf{k} + \mathbf{g}', \mathbf{k}' + \mathbf{g}', \mathbf{g}'). \tag{4.44}$$

Taking the sum in Eq. (4.43) over $\mathbf{g}$ we find

$$A(\mathbf{k}, \mathbf{k}') = N\Pi^{(0)}(\mathbf{k}, \mathbf{k}')\varepsilon^{-1}(i\omega_n, \mathbf{k} - \mathbf{k}'). \tag{4.45}$$

The substitution of Eq. (4.45) into Eq. (4.41) leads to the result

$$\Pi(\mathbf{k}, \mathbf{k}', \mathbf{g}) = N\Pi^{(0)}(\mathbf{k}, \mathbf{k}') \times [\delta_{g,0} + v(\mathbf{k} - \mathbf{k}')\Pi^{(0)}(\mathbf{k} - \mathbf{g}, \mathbf{k}' - \mathbf{g})\varepsilon^{-1}(i\omega_n, \mathbf{k} - \mathbf{k}')]. \tag{4.46}$$

To carry out the summation in Eq. (4.36) one can express $\Phi(\tau)$ in the form

$$\Phi(\tau) = \sigma_{\mathbf{mn}}\sigma_{\mathbf{m}'\mathbf{n}'} + \tilde{\Phi}(\tau). \tag{4.47}$$

The function $\tilde{\Phi}(\tau)$, defined by this equation behaves like

$$\tilde{\Phi}(\tau) \propto \exp(2g^2e^{-\omega|\tau|}) - 1, \tag{4.48}$$

varying rapidly within the characteristic time interval $\tau < E_p^{-1}$. Thus its Fourier component $\tilde{\Phi}(\omega_n)$ appears to be frequency-independent for the entire ω_n range under consideration. Substituting Eq. (4.47) into Eq. (4.36) one gets

$$\Sigma_{ph}(\mathbf{q}, \omega_n) = \Sigma_{ph}^{res}(\mathbf{q}, \omega_n) - \Delta(\mathbf{q}), \tag{4.49}$$

where

$$\Sigma_{ph}^{res}(\mathbf{q}, \omega_n) = -\sum_{\substack{i,i',\\ j,j'}} (u_i^* - u_j^*)(u_{i'} - u_{j'})\sigma_{\mathbf{mn}}\sigma_{\mathbf{m}'\mathbf{n}'}\Pi_{iji'j'}(-\omega_n) \tag{4.50}$$

is the frequency-dependent resonance contribution, and

$$\Delta(\mathbf{q}) = T\sum_{\substack{ii',\\ jj'}} (u_i^* - u_j^*)(u_{i'} - u_{j'})\tilde{\Phi}_{ij}^{i'j'}(\omega_n = 0)\sum_{\omega_{n'}} \Pi_{iji'j'}(\omega_{n'}) \tag{4.51}$$

is the frequency-independent softening. The Fourier transformation in Eqs. (4.50), (4.51) gives

$$\Sigma_{ph}^{res}(\mathbf{q}, \omega_n) = \frac{\mathcal{G}^2(\mathbf{q})}{2N^2}\sum_{\mathbf{k},\mathbf{g}} (\xi_{\mathbf{k}}\xi_{\mathbf{k}-\mathbf{q}-\mathbf{g}} + \xi_{\mathbf{k}-\mathbf{q}}\xi_{\mathbf{k}-\mathbf{g}} - \xi_{\mathbf{k}-\mathbf{g}}\xi_{\mathbf{k}-\mathbf{q}-\mathbf{g}} - \xi_{\mathbf{k}}\xi_{\mathbf{k}-\mathbf{g}}) \times \Pi(\mathbf{k}, \mathbf{k} - \mathbf{q}, \mathbf{g}; \omega_n), \tag{4.52}$$

$$\Delta(\mathbf{q}) = \frac{\mathcal{G}^2(\mathbf{q})}{2N^2} \times \sum_{\substack{\mathbf{k},\mathbf{k}',\\ \mathbf{g}}} \sum_{\omega_{n'}} \tilde{\Phi}(\mathbf{k}, \mathbf{k}' + \mathbf{q}, -\mathbf{g})[\Pi(\mathbf{k}, \mathbf{k}', -\mathbf{g} - \mathbf{q}; \omega_{n'}) - \Pi(\mathbf{k}, \mathbf{k}', -\mathbf{g}; \omega_{n'})] + \tilde{\Phi}(\mathbf{k} - \mathbf{q}, \mathbf{k}', -\mathbf{g})[\Pi(\mathbf{k}, \mathbf{k}', -\mathbf{g} + \mathbf{q}; \omega_{n'}) - \Pi(\mathbf{k}, \mathbf{k}', -\mathbf{g}; \omega_{n'})], \tag{4.53}$$

where

$$\tilde{\Phi}_{ij}^{i'j'}(\omega_n = 0) = \frac{1}{N^3}\sum_{\substack{\mathbf{k},\mathbf{k}',\\ \mathbf{g}}} \tilde{\Phi}(\mathbf{k}, \mathbf{k}', \mathbf{g})\exp[-i\mathbf{k}(\mathbf{m}' - \mathbf{n}) + i\mathbf{k}'(\mathbf{n}' - \mathbf{m}) + i\mathbf{g}(\mathbf{m}' - \mathbf{n}')]. \tag{4.54}$$

To calculate the frequency-dependent contribution Σ_{ph}^{res} one can expand the simple polarization loop in a power series with W/ω as a small parameter:

$$\Pi^{(0)}(\mathbf{k}, \mathbf{k}') = 2\left[\frac{n_{\mathbf{k}} - n_{\mathbf{k}'}}{i\omega_n} - \frac{(n_{\mathbf{k}'} - n_{\mathbf{k}})(\xi_{\mathbf{k}} - \xi_{\mathbf{k}'})}{\omega_n^2} + \ldots\right]. \tag{4.55}$$

Substitution of Eq. (4.55) into Eqs. (4.46), (4.52) leads to

$$\Sigma_{ph}^{res}(\mathbf{q}, \omega_n) = -\beta(\mathbf{q})\omega_p^4(\mathbf{q})/[\omega(\mathbf{q})(\omega_n^2 + \omega_p^2(\mathbf{q}))], \tag{4.56}$$

where

$$\beta(\mathbf{q}) = \omega(\mathbf{q})\mathcal{G}^2(\mathbf{q})/v(\mathbf{q}) \tag{4.57}$$

is the dimensionless plasmon-phonon coupling constant.

To extract the main contribution to $\Delta(\mathbf{q})$ one can use the TLA thus obtaining

$$\Pi(\mathbf{k}, \mathbf{k}', \mathbf{g}; \omega_n) \approx -N\delta_{\omega_n,0}\frac{(2 - n_e)n_e}{2T}\left[\delta_{g,0} - \frac{v(\mathbf{k} - \mathbf{k}')(2 - n_e)n_e}{2T\varepsilon(0, \mathbf{k} - \mathbf{k}')}\right]. \tag{4.58}$$

The second term in the figure brackets of the last expression is independent of $\mathbf{g}$. Therefore the direct polaron-polaron interaction does not contribute to the phonon softening:

$$\Delta(\mathbf{q}) = \frac{1}{2}\mathcal{G}^2(\mathbf{q})(2 - n_e)n_e\sum_{\mathbf{a}} \tilde{\Phi}_{\mathbf{a}}(0)[1 - \cos(\mathbf{qa})], \tag{4.59}$$

where

$$\tilde{\Phi}_{\mathbf{a}}(0) = \tilde{\Phi}_{ij}^{ii}(\omega_n = 0). \tag{4.60}$$

By expanding the exponential in Eq. (4.33) in a power series, in accordance with Eqs. (4.38), (4.47) and (4.60) for the case of dispersionless phonons $\omega(\mathbf{q}) = \omega_0$ we obtain

$$\tilde{\Phi}_{\mathbf{a}}(0) = \frac{2\sigma_{\mathbf{mn}}^2}{\omega_0}\sum_{k=1}^{\infty}\sum_{p=0}^{k}\binom{k}{p}\frac{\sinh[(k - 2p)\omega_0/2T]}{2^k k!(k - 2p)\sinh^k(\omega_0/2T)} \times \left\{\frac{1}{N}\sum_{\mathbf{q}'}\mathcal{G}^2(\mathbf{q}')[1 - \cos(\mathbf{q}'\mathbf{a})]\right\}^k. \tag{4.61}$$

The terms with $p = 0$ and $p = k$ are dominant in the $T \ll \omega_0$ temperature range. In this case

$$\tilde{\Phi}_{\mathbf{a}}(0) = T^2(\mathbf{a})/\omega_0 g^2(\mathbf{a}). \tag{4.62}$$

In the multiphonon diagram technique in contrast to the ordinary one there is an additional possibility to connect

both external phonon lines to the same vertex of the loop and not only to different vertices. As a result one arrives at the compensation of the greater part of the softening calculated in Refs. 61, 63. Taking this fact into account the final expression for the softening can be written as

$$\Delta(\mathbf{q}) = \frac{g^2(\mathbf{q})(2-n_e)n_e}{2\omega_0}\sum_{\mathbf{a}}\frac{T^2(\mathbf{a})[1-\cos(\mathbf{qa})]}{g^6(\mathbf{a})}. \quad (4.63)$$

4.4. New type of vibrational excitations

The strong electron-phonon interaction, $\lambda > \lambda_c$, results in a rather small value of the plasma frequency, comparable to the frequency of phonons, as well as in the coupling of bare phonons with polaron plasmons, Eq. (4.57). Therefore the real vibrational excitation appears to be a superposition of a phonon and a plasmon, referred to as a "plasphon." To find out the plasphon dispersion law an analytic continuation is required of $\Sigma_{ph}^{res}(\mathbf{q},\omega_n)$ into the region of real values of frequency Ω. Keeping in mind that Σ_{ph}^{res} has only simple poles $\omega_n = \pm i\omega_p$, Eq. (4.56), this continuation may be carried out by the trivial substitution $i\omega_n \to \Omega$ in Eq. (4.56), thus leading to the following equation for the plasphon frequency:

$$\Omega = \omega(\mathbf{q}) + \Sigma_{ph}(\mathbf{q},\Omega), \quad (4.64)$$

or

$$\Omega - \omega(\mathbf{q}) + \Delta(\mathbf{q}) - \frac{\beta(\mathbf{q})\omega_p^4(\mathbf{q})}{\omega(\mathbf{q})(\Omega^2-\omega_p^2(\mathbf{q}))} = 0. \quad (4.65)$$

Eq. (4.65) has three different solutions:

$$\Omega_1 = \frac{\tilde{\omega}}{3} + \frac{2}{3}\cos\frac{\alpha}{3}\cdot(\tilde{\omega}^2+\omega_p^2)^{1/2}, \quad (4.66)$$

$$\Omega_2 = \frac{\tilde{\omega}}{3} - \frac{2}{3}\cos\left(\frac{\alpha}{3}+\frac{\pi}{3}\right)\cdot(\tilde{\omega}^2+\omega_p^2)^{1/2}, \quad (4.67)$$

$$\Omega_3 = \frac{\tilde{\omega}}{3} - \frac{2}{3}\cos\left(\frac{\alpha}{3}-\frac{\pi}{3}\right)\cdot(\tilde{\omega}^2+\omega_p^2)^{1/2}, \quad (4.68)$$

where

$$\cos\alpha = \frac{\tilde{\omega}^3 - 9\tilde{\omega}\omega_p^2 + (27\beta\omega_p^4/2\omega)}{(\tilde{\omega}^2+3\omega_p^2)^{3/2}} \quad (4.69)$$

and $\tilde{\omega} = \omega - \Delta$. All parameters in Eqs. (4.66)–(4.69) are assumed to be $\mathbf{q}$-dependent.

Only two solutions Ω_1 and Ω_2 appear to be real and positive, while the last one, Ω_3 (or Ω_2 depending on the choice of α) is negative and has no physical meaning.

We thus conclude that the vibrational spectrum of the lattice strongly coupled to the carriers contains two branches of excitations corresponding to the propagation of the mixed phonon and plasmon states instead of the bare phonon branch. In the weak plasmon-phonon coupling case, $\beta \ll 1$, the plasphon dispersion law takes the form:

$$\Omega_{1,2} = \frac{1}{2}\{\tilde{\omega}+\omega_p \pm [(\tilde{\omega}-\omega_p)^2 + (2\beta\omega_p^3/\omega)]^{1/2}\}. \quad (4.70)$$

In the $\beta \to 0$ limit $\Omega_1(+)$ and $\Omega_2(-)$ describe phonons with the renormalized frequency $\tilde{\omega}$ and the plasmons, respectively. The ratio of the two plasphon contributions to the phonon Green's function

$$D(\mathbf{q},\Omega) = \sum_{i=1}^{3}\frac{P_i(\mathbf{q})}{\Omega-\Omega_i(\mathbf{q})} \quad (4.71)$$

is equal to

$$\frac{P_2}{P_1} = \frac{(\Omega_2^2-\omega_p^2)(\Omega_3-\Omega_1)}{(\Omega_1^2-\omega_p^2)(\Omega_3-\Omega_2)}. \quad (4.72)$$

Even in the weak coupling case it may be of the order of unity:

$$P_2/P_1 \approx (\Delta-\Delta_0)/(\Delta+\Delta_0), \quad (4.73)$$

if the plasmon and phonon frequencies have sufficiently close values. Here $\Delta_0 = \tilde{\omega} - \omega_p$ stands for the bare and

$$\Delta = [(\tilde{\omega}-\omega_p)^2 + (2\beta\omega_p^3/\omega)]^{1/2} \quad (4.74)$$

—for the renormalized gap between the two branches of excitations.

5. BIPOLARON OF SMALL RADIUS. BIPOLARON BAND

As has been pointed out already, for a sufficiently strong electron-phonon interaction the contact or the intersite attraction of small polarons may greatly exceed the polaron bandwidth thus leading to localization of the polaron pair on the same site (or nearest neighbor sites). These small bipolarons being spatially separated prove to be qualitatively different in their cooperative properties from the condensate of Cooper pairs. In this section we wish to formulate the small bipolaron theory by presenting it in the universal form independent of the number of sites involved in the localized single bipolaron formation. With Δ denoting the bipolaron binding energy (i.e. the difference between the energies of the bipolaron state and the uncoupled two-polaron state) the small parameter $W/\Delta \ll 1$ arises providing us with a consistent treatment of the strong polaron attraction on one site or inside the lattice cell. The initial Hamiltonian (1.21) is thus reduced to the bipolaron one which describes the interaction and the tunneling of the spatially separated electron pairs—small bipolarons. As a result of the fact that pair correlations inside the lattice cell are large compared to the contributions from intercell hopping it is convenient to subdivide the total Hamiltonian H_p into the part (H_0) describing the motion and the interaction of the polarons inside the cell and the residual part of interaction (H_1) to be treated as a perturbation. The Hamiltonian H_0 may have eigenstates of different type corresponding either to the on-site singlet Anderson bipolaron or to the two-site singlet (triplet) Heitler–London bipolaron,[7] which depends on the explicit form of the v_{ij} matrix elements and the structure of the lattice. The localized bipolaron levels are split into bands due to the interaction term H_1 which tends to destroy the bipolarons in the first order and delocalizes them in the second order. The hopping motion of bipolarons is caused by virtual transitions to the unpaired polaron states, while the interaction includes besides the ordinary Coulomb and phonon-exchange terms

the additional virtual polaron-exchange part.[7]

We shall for the sake of simplicity restrict our further discussion to the on-site bipolaron case. Then shifting the origin of the energy by the value of E_p we arrive at the following representation for the Hamiltonian (1.21) in terms of H_0 and H_1 portions

$$H_p = H_0 + H_1,$$
$$H_0 = v_0 \sum_{\mathbf{m}} c^+_{\mathbf{m}\uparrow} c_{\mathbf{m}\uparrow} c^+_{\mathbf{m}\downarrow} c_{\mathbf{m}\downarrow} + \sum_{\substack{i,j \\ (m\neq n)}} v_{ij} n_i n_j + \sum_q \omega(q) d^+_q d_q,$$
$$H_1 = \sum_{\substack{i,j \\ (m\neq n)}} \hat{\sigma}_{ij} c^+_i c_j, \tag{5.1}$$

where $-v_0 = \Delta$ is the bipolaron binding energy. Under the condition $\Delta \gg W$ which leads to the absence of real polarons at zero temperature the bipolaron motion may be described by a new canonical transformation S_2, which is similar to the electron-polaron transformation S_1. It is fixed by the requirement to eliminate from H_p those terms that destroy the bipolaron state:

$$H_b = (\exp S_2) H \exp(-S_2), \tag{5.2}$$

where

$$(S_2)_{fv} = \sum_{i,j} [\langle f|\hat{\sigma}_{ij} c^+_i c_j|v\rangle/(E_f - E_v)], \tag{5.3}$$

E_f, E_v are the energy levels corresponding to the eigenstates $\langle f|$, $|v\rangle$ of the Hamiltonian H_0.

Neglecting the terms of higher order than $(W/\Delta)^2$ gives

$$H_b \approx H_p + [S_2, H_p]_- + \tfrac{1}{2}(S_2^2 H_0 + H_0 S_2^2) - S_2 H_0 S_2, \tag{5.4}$$

or in explicit form

$$(H_b)_{ff'} = (H_0)_{ff'} - \frac{1}{2}\sum_v (E_f + E_{f'} - 2E_v) \times \sum_{\substack{i,i', \\ m\neq m'}} \sum_{\substack{j,j', \\ n\neq n'}} \frac{\langle f|\hat{\sigma}_{ii'} c^+_i c_{i'}|v\rangle\langle v|\hat{\sigma}_{jj'} c^+_j c_{j'}|f\rangle}{(E_f - E_v)(E_v - E_{f'})}. \tag{5.5}$$

The nonzero matrix elements of S_2 act between a localized bipolaron state and a state of two polarons in different cells. Eq. (5.5) defines matrix elements of H_b in the subspace containing no real polarons. Hence $|f\rangle$ and $|f'\rangle$ represent the set of H_0 eigenstates describing the bipolarons localized in different cells. Intermediate states $|v\rangle$ on the other hand refer to configurations involving two unpaired polarons, so that

$$E_f - E_v = -\Delta + \sum_q \omega(q)(n^{ph}_f(q) - n^{ph}_v(q)), \tag{5.6}$$

where $n^{ph}_f(q)$ and $n^{ph}_v(q)$ denote the phonon occupation numbers.

It is clear that the lowest eigenstates of the Hamiltonian H_b are in the subspace, which involves only those cells that are either occupied by a bipolaron ($c^+_{m\uparrow} c^+_{m\downarrow}|0\rangle_m$) or are empty ($|0\rangle_m$). The bipolaron band motion takes place via a transition to the virtual unpaired state implying a single polaron tunneling to the adjacent site and a change of the phonon state of the lattice. The subsequent tunneling of the second polaron restores the initial energy state of the lattice and creates a bipolaron on the neighboring site. When the characteristic bipolaronic kinetic energy is small

$$W^2/\Delta \ll \omega, \tag{5.7}$$

the bipolaron tunneling processes accompanied by emission or absorption of real phonons have small matrix elements and may be neglected. In this case one can average Eq. (5.5) using the phonon density matrix

$$\rho = \exp(-H_{ph}/T)\mathrm{Tr}\exp(-H_{ph}/T) \tag{5.8}$$

and obtain the effective fermion Hamiltonian in the form

$$H_b = -\Delta \sum_{\mathbf{m}} c^+_{\mathbf{m}\uparrow} c_{\mathbf{m}\uparrow} c^+_{\mathbf{m}\downarrow} c_{\mathbf{m}\downarrow} + \sum_{\substack{i,j \\ (m\neq n)}} v_{ij} n_i n_j - \sum_{\substack{i,i' \\ (m\neq m')}} \sum_{\substack{j,j \\ (n\neq n')}} c^+_i c_{i'} c^+_j c_{j'}(i) \int_0^\infty d\tau \langle \hat{\sigma}_{ii'}(\tau)\hat{\sigma}_{jj'}(0)\rangle \exp[(-i\Delta + \delta)\tau], \tag{5.9}$$

where $\langle ... \rangle$ denotes the phonon average, $\delta \to +0$, and

$$\hat{\sigma}(\tau) = \exp(iH_{ph}\tau)\hat{\sigma}\exp(-iH_{ph}\tau). \tag{5.10}$$

At low enough temperature

$$T \ll \Delta, \tag{5.11}$$

where the real polarons are absent it is convenient in the Hamiltonian (5.9) to replace polaron operators by bipolaron operators defined as

$$b^+_{\mathbf{m}} = c^+_{\mathbf{m}\uparrow} c^+_{\mathbf{m}\downarrow}, \quad b_{\mathbf{m}} = c_{\mathbf{m}\downarrow} c_{\mathbf{m}\uparrow}, \tag{5.12}$$

and obeying the mixed commutation rules

$$[b_{\mathbf{m}}, b^+_{\mathbf{m}}]_+ = 1, \quad [b_{\mathbf{m}}, b^+_{\mathbf{m}'}]_- = 0 \quad (\mathbf{m} \neq \mathbf{m}'). \tag{5.13}$$

The Hamiltonian (5.9) is then expressed in the form

$$H_b = -\sum_{\mathbf{m}} (\Delta + \varepsilon^{(2)}) b^+_{\mathbf{m}} b_{\mathbf{m}} + \sum_{\mathbf{m}\neq\mathbf{m}'} (\bar{v}_{\mathbf{mm}'} b^+_{\mathbf{m}} b_{\mathbf{m}} b^+_{\mathbf{m}'} b_{\mathbf{m}'} - t_{\mathbf{mm}'} b^+_{\mathbf{m}} b_{\mathbf{m}'}); \tag{5.14}$$

where $t_{\mathbf{mm}'}$ is the bipolaron intersite hopping integral

$$t_{\mathbf{mm}'} = 2i \int_0^\infty d\tau \langle \hat{\sigma}_{\mathbf{mm}'}(\tau)\hat{\sigma}_{\mathbf{mm}'}(0)\rangle \exp[(-i\Delta + \delta)\tau], \tag{5.15}$$

$\bar{v}_{\mathbf{mm}'}$ is the matrix element of the interbipolaron interaction on neighboring sites

$$\bar{v}_{\mathbf{mm}'} = 4v_{\mathbf{mm}'} + v^{(2)}_{\mathbf{mm}'} \equiv 4v_{\mathbf{mm}'} + 2i \int_0^\infty d\tau \langle \hat{\sigma}_{\mathbf{mm}'}(\tau)\hat{\sigma}_{\mathbf{m}'\mathbf{m}}(0)\rangle \exp[(-i\Delta + \delta)\tau], \tag{5.16}$$

and

$$\varepsilon^{(2)} = \sum_{\mathbf{m}'} v^{(2)}_{\mathbf{mm}'}$$

is the bipolaron self-energy renormalization.

In the following we shall omit the first term of Eq. (5.14) thus shifting the origin of the energy to the level of the bipolaron state localized on the site. The second term in Eq. (5.16) describes the effective repulsion of bipolarons. The reason for this repulsion is quite clear: a virtual hop of one of the polarons making up a bipolaron to the neighboring site is forbidden when it is occupied by another bipolaron.

The temperature average over the phonon variables in (5.15) and (5.16) is carried out in a standard way[20] thus leading to

$$\langle \hat{\sigma}_{mm'}(\tau)\hat{\sigma}_{mm'}(0)\rangle = T^2_{mm'}\exp(-2g^2) \times \exp\left[-2\sum_q \frac{|U(q)|^2}{\omega^2(q)}\{1-\cos(q|m-m'|)\} \times \frac{\cos\{\omega(q)[\tau+(i/2T)]\}}{\sinh(\omega(q)/2T)}\right], \quad (5.17)$$

where g^2 is T-dependent effective constant of the electron-phonon interaction (1.26). The only difference in the analogous temperature average of the matrix element $\bar{v}_{mm'}$ is the opposite sign of the argument in the second exponential of Eq. (5.17).

At temperature $T=0$ for the case of electron interaction with the single dispersionless phonon mode of frequency ω the matrix elements $t_{mm'}$ and $v^{(2)}_{mm'}$ may be written in a more simple form:[10]

$$t_{mm'} = \frac{2T^2_{mm'}}{\Delta}e^{-2g^2}\sum_{n=0}^{\infty}\frac{(-2g^2)^n}{n!}\frac{1}{1+(n\omega/\Delta)}, \quad (5.18)$$

$$v^{(2)}_{mm'} = \frac{2T^2_{mm'}}{\Delta}e^{-2g^2}\sum_{n=0}^{\infty}\frac{(+2g^2)^n}{n!}\frac{1}{1+(n\omega/\Delta)}. \quad (5.19)$$

Eq. (5.18) makes it possible to get an estimate of the effective bipolaron mass m^{**} by relating it to the effective mass of an electron in its initial bare band m and the hopping integral ratio

$$m/m^{**} = |t_{mm'}/T_{mm'}|. \quad (5.20)$$

In the limit of $\Delta \ll \omega$ the sum in Eq. (5.18) may be well approximated by the first term which gives the result

$$m/m^{**} \approx (1/z)(D/\Delta)e^{-2g^2} \quad (\Delta \ll \omega), \quad (5.21)$$

where $D = 2z|T_{mm'}|$ is the electron bandwidth. In this case the bipolaron motion from site to site proceeds via incoherent hopping of each of the two polarons which constitute the bipolaron with no emission or absorption of virtual phonons in the intermediate state. It implies the obvious relation between the bipolaron hopping matrix element and the polaron bandwidth $W = D\exp(-g^2)$

$$t_{mm'} \approx W^2/\Delta. \quad (5.22)$$

The effective bipolaron repulsion (5.19) may be expressed in a similar way in the parameter range under consideration as

$$v^{(2)}_{mm'}/T_{mm'} \approx (1/z)(D/\Delta)e^{-2g^2} \quad (\Delta \ll \omega). \quad (5.23)$$

In the opposite limit of $\Delta \gg \omega$ the possibility of virtual phonon emission in the unpaired intermediate state gives rise to a much heavier bipolaron mass

$$m/m^{**} \approx (1/z)(D/\Delta)e^{-4g^2} \quad (\Delta \gg \omega). \quad (5.24)$$

The effective bipolaron repulsion on the neighboring sites is also greatly enhanced in this limit

$$v^{(2)}_{mm'}/T_{mm'} \approx (1/z)D/\Delta \quad (\Delta \gg \omega). \quad (5.25)$$

It is quite clear that the approximate relations (5.21) and (5.22) obtained previously in Ref. 7 correspond to replacement in Eqs. (5.15), (5.16) of the temperature average of the product of two operators by the product of the temperature averages of both of them. This procedure is equivalent to taking the initial average with the phonon density matrix of Hamiltonian Eq. (5.1) thus reducing it to the Hubbard Hamiltonian with attraction ($U_{Hub} < 0$) and a narrow temperature-dependent band W. Therefore the phenomenological negative-U Hubbard Hamiltonian appears to be applicable to a polaron system only in the limit of $\omega \gg |U_{Hub}| = \Delta$. In the opposite limit of $\omega \ll \Delta$ the bipolaron Hamiltonian can not be parametrized in the form of an attractive Hubbard Hamiltonian with strong coupling.

Summing up the analysis of the preceeding sections let us discuss the qualitative picture of the major changes in the electron spectrum taking place as the effective coupling constant λ increases.

The electron which occupies a site, (Fig. 5a), gives rise at $\lambda \geqslant 1$ to a static lattice deformation of a size of the order of the lattice constant. The ground state ceases being the vacuum for the unrenormalized phonons, and the middle of the electron band (atomic level) is shifted down by the value of E_p. As a result an electron is moving in a narrow polaron band carrying the local lattice deformation with itself, (Fig. 5b). This deformation is also responsible for the small polaron pairing on one site, or on two neighboring sites, (Fig. 5c), depending on the value of the Coulomb repulsion. If the polaron-polaron binding energy Δ is low enough, ($\Delta \leqslant W$), the ground state becomes a condensate of the polaron Cooper pairs. If $\Delta > W$, on the other hand, the ground state is a condensate of charged bosons—bipolarons, moving in a narrow bipolaron band (Fig. 5d).

6. BIPOLARON SUPERCONDUCTORS. EXCITATION SPECTRUM AND THERMODYNAMICS

6.1. Ground state

According to the previous section the low-lying eigenstates of a narrow band crystal may be described in terms of a

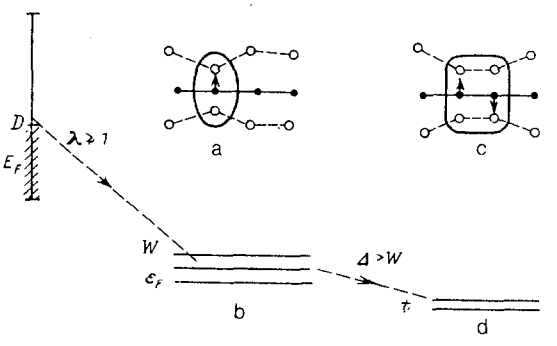

FIG. 5. Schematic picture of polaron and bipolaron band formation.

bipolaron Hamiltonian. With the energy origin chosen at the level of the bipolaron state localized on the site it is given by

$$H_b = -\mu \sum_{\mathbf{m}} b_{\mathbf{m}}^+ b_{\mathbf{m}} + \sum_{\mathbf{m}\neq\mathbf{m}'} (\bar{v}_{\mathbf{mm}'} b_{\mathbf{m}}^+ b_{\mathbf{m}} b_{\mathbf{m}'}^+ b_{\mathbf{m}'} - t_{\mathbf{mm}'} b_{\mathbf{m}}^+ b_{\mathbf{m}'}), \tag{6.1}$$

where μ is the chemical potential of the system containing no unpaired polarons. To study this Hamiltonian just as in the BCS theory it is convenient to use the well-known pseudospin analogy, as the bipolaron operators are fully equivalent to the set of Pauli spin matrices

$$b_{\mathbf{m}}^+ = S_{\mathbf{m}}^x - iS_{\mathbf{m}}^y, \quad b_{\mathbf{m}} = S_{\mathbf{m}}^x + iS_{\mathbf{m}}^y, \quad b_{\mathbf{m}}^+ b_{\mathbf{m}} = (1/2) - S_{\mathbf{m}}^z, \tag{6.2}$$

$$S^x = \frac{1}{2}\begin{pmatrix} 0 & 1 \\ 1 & 0 \end{pmatrix}, \quad S^y = \frac{1}{2}\begin{pmatrix} 0 & -i \\ i & 0 \end{pmatrix}, \quad S^z = \frac{1}{2}\begin{pmatrix} 1 & 0 \\ 0 & -1 \end{pmatrix}. \tag{6.3}$$

In this pseudospin language a half-unity spin is associated with each lattice site. Its z-projection is assumed equal to $-1/2$ for a site occupied by a bipolaron and to $+1/2$ for an empty site. The corresponding pseudospin operators preserve the boson character of bipolarons if they are localized on different sites. On the other hand they obey the Pauli principle which prohibits the presence of two bipolarons on the same site.

Replacement of bipolaron operators by pseudospin ones in Eq. (6.1) transforms it into an anisotropic Heisenberg Hamiltonian

$$H_b = \mu \sum_{\mathbf{m}} S_{\mathbf{m}}^z + \sum_{\mathbf{m}\neq\mathbf{m}'} [\bar{v}_{\mathbf{mm}'} S_{\mathbf{m}}^z S_{\mathbf{m}'}^z - t_{\mathbf{mm}'} (S_{\mathbf{m}}^x S_{\mathbf{m}'}^x + S_{\mathbf{m}}^y S_{\mathbf{m}'}^y)], \tag{6.4}$$

where the bipolaron chemical potential μ plays the role of the external magnetic pseudofield and is determined by the number of electrons per unit cell n_e

$$\frac{1}{N}\sum_{\mathbf{m}} \langle S_{\mathbf{m}}^z \rangle = \frac{1 - n_e}{2}. \tag{6.5}$$

It will be usually assumed that $n_e < 1$. For $1 < n_e < 2$ holes should be used, all the results being the same.

The anisotropic Heisenberg Hamiltonian (6.4) has been investigated in detail in the theory of magnetic materials. It was used also in the studies of quantum solids[64] (the model of boson lattice liquid for ^{4}He). In this latter case the operator $b_{\mathbf{m}}$ describes a helium atom on site $\mathbf{m}$ with the Pauli statistics being equivalent to the large on-site repulsion. However, while in those cases the magnetic field and pressure respectively are independent thermodynamic variables, for a bipolaron crystal the electrical neutrality condition (6.5) fixes the total "magnetization". Moreover, the interaction between bipolarons is assumed to be repulsive while the long range interaction in quantum solids is of an attractive nature (^{4}He). We show in the following that these two facts lead to the existence, in addition to homogeneous (superconducting and normal) phases, also of charge-ordered inhomogeneous phases with a bipolaron condensate in one of them.

To find the ground state of the pseudospin Hamiltonian (6.4) we use the "semiclassical" method of the theory of magnetism. The pseudomagnetic field $\mathbf{H}_{\mathbf{m}}$ on the site $\mathbf{m}$ is defined by

$$\mathbf{H}_{\mathbf{m}} = -(\mu + 2\bar{v}S_{\mathbf{m}'}^z)\mathbf{e}_z + 2t\mathbf{S}_{\mathbf{m}'}^{\perp}, \tag{6.6}$$

where $\bar{v} = z\bar{v}_{\mathbf{mm}'}$, $t = zt_{\mathbf{mm}'}$, $\mathbf{m}'$ is the index of the nearest neighbor sites to the site $\mathbf{m}$, $\mathbf{e}_z$ is the unit vector in the z direction, and $\mathbf{S}_{\mathbf{m}}^{\perp}$, is the component of the pseudospin vector of the site $\mathbf{m}'$ which is orthogonal to the z axis.

Taking without loss of generality $S_{\mathbf{m}}^y = 0$, we have at $T = 0$:

$$S_{\mathbf{m}0}^z = \frac{1}{2}\cos\theta, \quad S_{\mathbf{m}0}^x = \frac{1}{2}\sin\theta, \tag{6.7}$$

with θ being the angle between $\mathbf{S}_{\mathbf{m}}$ and the z axis which is fixed by the minimum energy condition $\mathbf{S}_{\mathbf{m}} \| \mathbf{H}_{\mathbf{m}}$. Taking account of Eq. (6.5) we arrive at the following set of equations for θ and the chemical potential μ:

$$\begin{aligned} \sin\theta &= \frac{t\sin\theta'}{[(\mu + \bar{v}\cos\theta')^2 + t^2\sin^2\theta']^{1/2}}, \\ \cos\theta &= \frac{-(\mu + \bar{v}\cos\theta')}{[(\mu + \bar{v}\cos\theta')^2 + t^2\sin^2\theta']^{1/2}}, \\ \cos\theta &+ \cos\theta' = 2(1 - n_e). \end{aligned} \tag{6.8}$$

Here θ' is the angle for the nearest neighbors.

The combination of the first two equations of (6.8) allows us to solve for the chemical potential μ:

$$\mu = -(\bar{v}\cos\theta + t\sin\theta\cdot\cot\theta'), \tag{6.9}$$

and to obtain the following equation for θ and θ'

$$\begin{aligned} 0 = &(\cos\theta - \cos\theta') \\ &\times [1 + \cos\theta\cdot\cos\theta' - (\bar{v}/t)\sin\theta\cdot\sin\theta']. \end{aligned} \tag{6.10}$$

Together with the last equation of the set (6.8) it provides the solution for θ and θ'.

As a matter of fact two solutions are possible.

The first one is a homogeneous ("ferromagnetic") solution with full equivalence of all the sites:

$$\begin{aligned} &\cos\theta = \cos\theta' = 1 - n_e, \\ &\mu = -(\bar{v} + t)(1 - n_e). \end{aligned} \tag{6.11}$$

In this case the bipolarons are distributed uniformly over the crystal lattice:

$$n_b = n_e/2,$$

and

$$n_b = \langle b_{\mathbf{m}}^+ b_{\mathbf{m}} \rangle = (1 - \cos\theta)/2. \tag{6.12}$$

The second solution is the "antiferromagnetic" one, where $\cos\theta \neq \cos\theta'$ and two sublattices occur which have different densities of bipolarons, $n_b \neq n_b'$:

$$\begin{aligned} n_b &= \frac{1}{2}(1 - \cos\theta) \\ &= \frac{1}{2}\{n_e + [1 + (1 - n_e)^2 + 2\bar{v}(1 - n_e)(\mu')^{-1}]^{1/2}\} \end{aligned} \tag{6.13}$$

$$\begin{aligned} n_b' &= \frac{1}{2}(1 - \cos\theta') \\ &= \frac{1}{2}\{n_e - [1 + (1 - n_e)^2 + 2\bar{v}(1 - n_e)(\mu')^{-1}]^{1/2}\}, \end{aligned} \tag{6.14}$$

$$\mu' = -(\bar{v}^2 - t^2)^{1/2}. \quad (6.15)$$

It is clear from these equations that the "antiferromagnetic" solution exists only in the range of sufficiently high electron concentration:

$$n_e \geq n_c = 1 - [(\bar{v} - t)/(\bar{v} + t)]^{1/2}. \quad (6.16)$$

Therefore, at $n_e \geqslant n_c$ the repulsion between bipolarons results in formation of a charge-density wave (CDW) state.

Figure 6 illustrates the bipolaron distribution over the cells in the ferromagnetic and antiferromagnetic states as a function of the electron concentration n_e. The energy of the system is

$$E = \frac{1}{4}N[2\mu(1 - n_e) + \bar{v}\cos\theta\cdot\cos\theta') - t\sin\theta\cdot\sin\theta']. \quad 6.17)$$

Substituting Eqs. (6.11) and (6.13)–(6.15) into Eq. (6.17) we get the energies of the ferromagnetic and antiferromagnetic phases (E and E' respectively):

$$E = -\frac{1}{4}N[t + (t + \bar{v})(1 - n_e)^2], \qquad E' = -\frac{1}{4}N\bar{v}. \quad (6.18)$$

From Eqs. (6.18) it follows that for $n_e \geqslant n_c$ the antiferromagnetic (CDW) state is the ground state of the bipolaron system. Both phases exhibit off-diagonal long-range order:

$$\langle b_m \rangle = \langle S_m^x \rangle = \frac{1}{2}\sin\theta \neq 0. \quad (6.19)$$

The only exception is $n_e = 1$, where $\sin\theta' = 0$. Ferro- and antiferro-ordering of pseudospins means "locking" the phase of the multielectron wave function. The ground state of the bipolaron crystal represents therefore either a homogeneous bipolaron condensate phase (BS-phase) at $n_e < n_c$ or a charge-density wave coexisting with condensate (M-phase) at $n_e > n_c$. It will be shown by further analysis of the excitation spectrum that both these phases may be superconducting.

6.2. Phase (T–n)-diagram of a bipolaron crystal

An increase of temperature leads to evaporation and at some point to disappearence of a condensate phase. The (T–n) phase diagram as it was initially pointed out in Ref. 9 has to contain four phases: two low-temperature phases with off-diagonal long-range order (BS, M), and two high-temperature phases, namely, the normal one (N) and the charge-ordered (CO) or, equivalently, charge-density wave (CDW) phase. The qualitative features of this diagram may be analyzed with the aid of finite temperature mean-field approximation (MFA) being applied to the anisotropic Heisenberg Hamiltonian (6.4). Taking

$$\mathbf{H_m} = -(\mu + 2\sum_{m'} \bar{v}_{mm'}\langle S_{m'}^z\rangle)\mathbf{e}_z + 2\sum_{m'} t_{mm'}\langle S_{m'}^x\rangle\mathbf{e}_x, \quad (6.20)$$

we obtain for the mean value of pseudospin at the site $\mathbf{m}$:

$$\langle \mathbf{S_m} \rangle = (\mathbf{H_m}/2|\mathbf{H_m}|)\mathrm{th}(|\mathbf{H_m}|/2T). \quad (6.21)$$

Let us consider the homogeneous phases, where

$$\langle \mathbf{S_m} \rangle = \mathbf{S}_0, \quad S_0^z = (1 - n_e)/2. \quad (6.22)$$

We find from Eq. (6.21)

$$\mu = -2(\bar{v}_0 + t_0)S_0^z, \quad (6.23)$$

where

$$\bar{v}_k = \sum_m \bar{v}_{m0}e^{i\mathbf{km}}, \quad t_k = \sum_m t_{m0}e^{i\mathbf{km}} \quad (6.24)$$

are the Fourier-components of the interaction and the effective hopping integral respectively ($\bar{v}_0 = \bar{v}, t_0 = t$).

To the linear approximation in $S_0^x \neq 0$, Eq. (6.21) provides the critical temperature for transition from the condensate (BS) phase to the normal (N) phase:

$$T_c = t(1 - n_e)/\ln[(2 - n_e)/n_e]. \quad (6.25)$$

According to Eq. (6.25) T_c becomes equal to zero for $n_e = 0$ and approaches a maximum value of $T_c^{\max} = t$ at $n_e = 1$.

In extension of the studies of Refs. 7 and 8 the phase diagram of the bipolaron system described by the pseudospin Hamiltonian (6.4) and the condition (6.5) has been calculated numerically by Kubo and Takada[65] by means of the MFA of Eq. (6.20) with allowance for a CDW. For a certain value of the interaction with the second coordination sphere which was taken into account, these authors claimed the possibility of two new phases corresponding to the incommensurate CDW-phase and incommensurate M-phase.

The complete ($T - n$) phase diagram of the Hamiltonian (6.4) together with the condition (6.5), was derived by Robaszkiewicz *et al.*[66] It is shown in Fig. 7 for $\bar{v}/t = 2$.

We note that the transition into a charge-ordered state at $n_e = 1$ was considered earlier by Ionov *et al.*[67,68] within the framework of the phenomenological Hubbard model with strong contact attraction. The homogeneous conden-

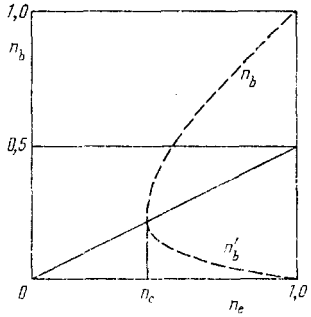

FIG. 6. Average bipolaron occupation of a site as a function of electron concentration in the ferromagnetic phase (inclined solid line) and in the antiferromagnetic phase (dashed line).

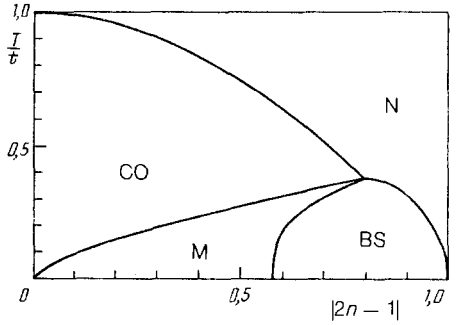

FIG. 7. MFA (T–n) phase diagram of a bipolaron crystal for $(\bar{v}/t) = 2$ (Ref. 66).

sate state was analyzed by Kulik and Pedan.[69] Using a MFA they obtained for T_c the result of Eq. (6.25). Since t is suppressed by the exponential factor $\exp(-2g^2)$ for a bipolaron crystal one has the condition $t \ll \bar{v}$. Therefore a homogeneous condensate phase exists only in the narrow range of concentrations

$$n_e \leq n_c \approx t/\bar{v}. \tag{6.26}$$

However, it was shown in Ref. 8 that for the spin Hamiltonian of Eq. (6.4) the pseudomagnonlike fluctuations become essential in this range and $T_c(n_e)$ dependence differs from Eq. (6.25).

In the range of $n_e \approx 1$ MFA turns out to be also inapplicable because of the important role of dynamical correlation between the pairs which arises from their interaction $\bar{v}$. This fact was established in Ref. 70 in the analysis of the charge-ordered state in the Hubbard model. In particular taking into account the dynamical correlations results in a decrease in T_c at $n_e \approx 1$ and limits from below ($n_e \geqslant 1/z$, Ref. 70) the range of concentration where a CDW does exist. We thus conclude that expression (6.25) for T_c as well as the whole phase diagram obtained within the framework of the MFA are only of qualitative importance.

6.3. Excitation spectrum of the low-temperature coherent phases

The excitation spectrum of the Hamiltonian (6.4) was found for zero temperature in Refs. 7 and 8 and for a nonzero one in Refs. 65 and 66. It is magnonlike with a linear dispersion in the long-wavelength limit both for the BS and for the M (mixed) phase. In the latter case, MFA–RPA (Refs. 65 and 66) gives a linear behavior for the entire temperature range for the M phase, except at $T = 0$.[7] However, it turns out that if one takes into account quantum zero-point fluctuations, one obtains a linear dispersion for the excitation spectrum of the mixed phase for $T = 0$ also.[65]

The application of MFA to obtain the excitation spectrum with the classical pseudofield $\mathbf{H}_m$, Eq. (6.20), leads to a gap in the spectrum proportional to t (Ref. 69), which corresponds to local spin flips. This is an artifact of the MFA which leads to exponential temperature dependence of the specific heat. The true excitations of the spectrum are pseudomagnons with a gapless dispersion.

We shall now generalize the MFA results concerning the excitation spectrum by taking into account quantum fluctuations, and determine the thermodynamics of the superconducting phase within this scheme. It turns out that this leads to qualitative changes in the phase diagram as compared to MFA (see Fig. 7).

Using the RPA equations of motion for double-time retarded Green's functions, one arrives at the following temperature-dependent excitation spectrum of the BS phase:[11]

$$\omega_k = R[(t - t_k\cos^2\theta + \bar{v}_k\sin^2\theta)(t - t_k)]^{1/2}, \tag{6.27}$$

where R is the occupation probability which obeys the following equation:

$$R^{-1} = \frac{1}{N}\sum_k \frac{A_k}{\omega_k}\coth\frac{\omega_k}{2T}, \tag{6.28}$$

where

$$A_k = R[t - t_k\cos^2\theta - (1/2)(t_k - \bar{v}_k)\sin^2\theta], \tag{6.29}$$

and

$$\cos\theta = (2n_b - 1)/R \tag{6.30}$$

determines the angle between $\mathbf{S}_m$ and $\mathbf{H}_m$. The superconducting order parameter is given by

$$S^x = \langle S_m^x\rangle, \quad S^x = (1/2)R\sin\theta = (1/2)[R^2 - (2n_b - 1)^2]^{1/2}. \tag{6.31}$$

The quantity R is defined in such a way that it includes quantum as well as thermal fluctuations. We note that MFA gives $R = 1$ at $T = 0$.

In the nearest-neighbor approximation one easily obtains from Eq. (6.27)

$$\omega_k^2 = (Rt)^2[1 - \gamma_k(t\cos^2\theta - \bar{v}\sin^2\theta)t^{-1}](1 - \gamma_k), \tag{6.32}$$

with

$$\gamma_k = t_k/t = \frac{1}{z}\sum_{|m|=a} e^{ikm}, \tag{6.33}$$

so that

$$\omega_k \approx sk + 0(k^2) \text{ при } k \to 0. \tag{6.34}$$

The "sound" velocity is temperature-dependent:

$$s(T) = R\sin\theta\delta[t(\bar{v} + t)]^{1/2},$$
$$\delta^2 = \frac{1}{6z}\sum_{|m|=a}[(km)/k]^2. \tag{6.35}$$

The boundary line between the BS and the normal phase determining $T_c(n_b)$ is given by the condition

$$s(T_c) = 0, \tag{6.36}$$

which is the same as $S^x = 0$. The boundary of the BS phase with the mixed phase M is determined by the condition of the instability of the spectrum, Eq. (6.32), against doubling of the lattice periodicity, i.e.,

$$\omega_Q = 0, \tag{6.37}$$

where $2\mathbf{Q}$ is the smallest reciprocal-lattice vector.

Together with Eq. (6.32), Eq. (6.37) reduces to

$$\frac{R^2 + (2n_b^c - 1)^2}{R^2 - (2n_b^c - 1)^2} = \frac{\bar{v}}{t}, \tag{6.38}$$

where $R(T,n,\bar{v}/t)$ has to be determined from Eqs. (6.28)–(6.30). We should mention that s becomes imaginary for $\bar{v} < -t$, which indicates that the system becomes unstable with respect to a transition into a phase of bipolaron "droplets".

Let us derive the critical concentration n_b^c as a function of $\bar{v}/t$ at $T = 0$. Substituting

$$R(0) = (1 + 2\psi_0)^{-1} \tag{6.39}$$

into Eq. (6.28) we obtain together with Eq. (6.30), the self-consistent equation for the zero-point fluctuation contribution ψ_0

$$2\psi_0 + 1 = \frac{1}{N}\sum_{\mathbf{k}} \frac{1 - \{1 + [(2n_b - 1)^2(1 + 2\psi_0)^2(1 + \bar{v}t^{-1}) - \bar{v}t^{-1}]\gamma_{\mathbf{k}}\}/2}{[\{1 - \gamma_{\mathbf{k}}[(2n_b - 1)^2(1 + 2\psi_0)^2(1 + \bar{v}t^{-1}) - \bar{v}t^{-1}]\}(1 - \gamma_{\mathbf{k}})]^{1/2}}. \quad (6.40)$$

The numerical solution of Eqs. (6.38)–(6.40) for a simple cubic lattice is shown in Fig. 8. One can notice the qualitative difference of the behavior of n_b^c determined in this way as compared to the MFA results (Refs. 7 and 66). The quantum fluctuations extend the region of stability of the homogeneous superconducting BS phase. Thus, the BS phase exists even in the limit $\bar{v}/t \to \infty$ provided

$$2n_b < 0{,}156, \quad (6.41)$$

for a simple cubic lattice, contrary to the MFA result which gives $n_b^c = 0$ in this limit. The behavior of the order parameter S^x as a function of $\bar{v}/t$, determined numerically from Eqs. (6.31), (6.39), and (6.40) is shown in Fig. 9. One can see that the bipolaron interaction suppresses the order parameter, contrary to MFA results in which the order parameter is independent of $\bar{v}$.

From Eq. (6.28) one obtains the following temperature expansion for $R(T)$:

$$R(T) = [4(S^x(0))^2 + (2n_b - 1)^2]^{1/2} - (T^2/6^{5/2})(1 + \bar{v}t^{-1})^{1/2}t^2(S^x(0))^2 + O(T^4). \quad (6.42)$$

Let us now consider the low-temperature behavior for the internal energy and the specific heat C_s. Using the RPA the internal energy is determined at low temperatures by

$$E \approx E_0 + \sum_{\mathbf{k}} \omega_{\mathbf{k}}[\exp(\omega_{\mathbf{k}}/T) - 1]^{-1}, \quad (6.43)$$

where E_0 is the ground-state energy. For a simple cubic lattice direct calculation yields

$$E - E_0 \approx \pi^2 T^4 \frac{1 + 18T^2[S^x(0)t(t + \bar{v})]^{-1}}{240\delta^{3/2}S^x(0)[t(t + \bar{v})]^{3/2}}. \quad (6.44)$$

In the derivation of this result we used the expansion of R in Eq. (6.42). In this way we arrive at the power-law temperature behavior of the specific heat:

$$C_s = \pi^2[S^x(0)t(t + \bar{v})]^{-3/2}(60\delta^{3/2})^{-1} \times \{T^3 + [27T^5/S^x(0)t(t + \bar{v})]\}. \quad (6.45)$$

We should mention that the temperature range of validity of Eq. (6.45) diminishes as $n_b \to 0$. At fixed n_b and a sufficiently high temperature the quadratic term in Eq. (6.34) will be dominant and will give rise to

$$C_s \propto T^{3/2}. \quad (6.46)$$

In concluding this subsection, we shall derive the expression for T_c. Substituting $S^x = 0$ into Eqs. (6.28)–(6.30), we obtain

$$\frac{1}{2n_b - 1} = \frac{1}{N}\sum_{\mathbf{k}} \coth\left[\frac{2n_b - 1}{2T_c}(t - t_k)\right]. \quad (6.47)$$

The numerical solution of Eq. (6.47) for a simple cubic lattice gives rise to the concentration dependence of the critical temperature for a bipolaron superconductor which is plotted in Fig. 10.

For a dilute system ($n_b \ll 1$), we obtain from Eq. (6.47) the following analytic expansion:

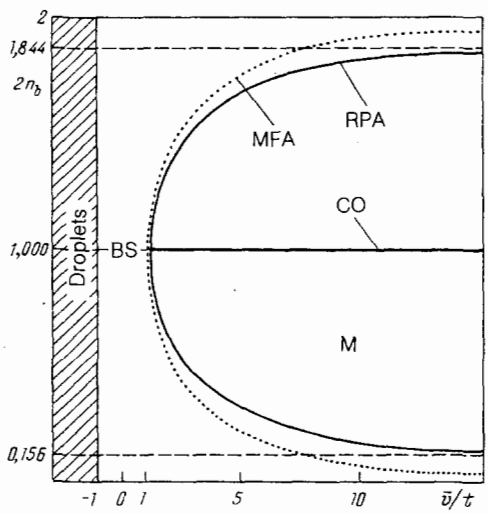

FIG. 8. Ground-state phase diagram ($T = 0$). RPA (solid line), MFA (dotted line).

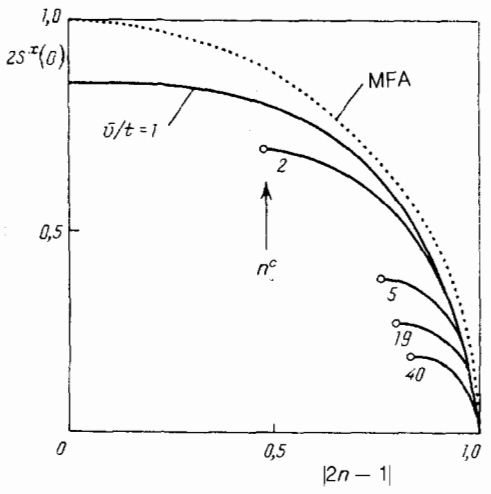

FIG. 9. Concentration dependence of the order parameter of a superconducting phase at $T = 0$. For $n_b > n_b^c$, a mixed phase with two order parameters exists.

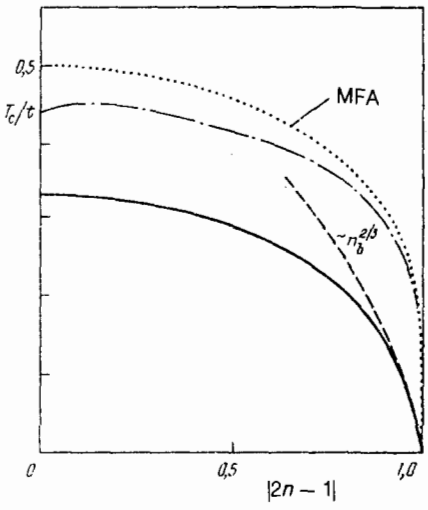

FIG. 10. Critical temperature of a bipolaron superconductor as a function of concentration. RPA result—solid line, MFA result—dotted line, cluster approximation result for $\bar{v}/t = 1$—dashed-dotted line. The T_c for the ideal Bose gas is indicated by the dashed line.

$$T_c \approx \frac{3{,}31(n_b a^{-3})^{3/2}}{m^{**}}(1 - 0{,}54 n_b^{2/3}), \tag{6.48}$$

where $m^{**} = 3/ta^2$ is the bipolaron effective mass (for the case of a simple cubic lattice). In the opposite limit of high density, $|2n_b - 1| \ll 1$, Eq. (6.47) gives

$$T_c \approx \frac{t}{2}\left[c^{-1} - \frac{(2n_b - 1)^2}{3}\right], \tag{6.49}$$

where $c = 1.5164$, 1.393, and 1.345 for simple cubic, base centered cubic, and face centered cubic lattices, respectively. One can see from Fig. 10 that the region $2n_b \leqslant 0.2T_c$ is practically the same as for the ideal Bose gas. In contrast, the MFA result, Eq. (6.25), as well as the cluster approximation,[70] gives a qualitatively different concentration dependence of the critical temperature $T_c \propto [\ln(1/n_b)]^{-1}$ for low densities and overestimates T_c (by a factor of about 1.5) for $2n_b = 1$. Moreover, in the cluster approximation the $T_c(n_b)$ curve intersects the n_b axis not at $n_b = 0$, but at $n_b = \exp(-z)$.

We would like to stress that the RPA has proven to be very fruitful in problems of magnetism (Refs. 71–74). In particular, it predicts the absence of long-range order in one and two dimensions for a short-range interaction at finite temperatures, in agreement with exact theorems.

6.4. Normal-state properties of a bipolaron system

One of the most striking features of a bipolaron system is that above T_c the normal phase is characterized by an ensemble of Bose particles on a lattice, forming a very narrow bipolaron band. This is quite different from ordinary BCS superconductors which above T_c go into a metallic state characterized by an ensemble of electrons on a lattice, forming a fairly broad electron band.

We shall in the following consider some of the thermodynamic normal-state properties of a bipolaron system. This can be done easily if the concentration of bipolarons is small. In this case, neither the hard core nor the effective interaction between bipolarons on different sites is important. Our initial Hamiltonian of Eq. (6.1) thus reduces to

$$H_b = -\sum_{\mathbf{m}\neq\mathbf{m}'} t_{\mathbf{m}\mathbf{m}'} b_{\mathbf{m}}^{+} b_{\mathbf{m}'}, \tag{6.50}$$

where the b operators are of the boson type. This is due to the fact that within the physically relevant subspace of either singly occupied or empty sites, they satisfy the commutation relations

$$[b_{\mathbf{m}}, b_{\mathbf{m}}^{+}]_- = 1 - 2n_b, \tag{6.51}$$

which reduce to the relations of Bose-statistics for small bipolaron concentration ($n_b \ll 1$). It will be shown in the following that as far as the temperature dependence of the specific heat is concerned, such bosonlike bipolarons behave in practically the same way as fermions (electrons) with a relatively narrow band. We shall include in the present discussion electrons ($s = 1/2$), singlet bipolarons ($s = 0$), and triplet bipolarons ($s = 1$) (s denoting the spin).

The corresponding expressions for the specific heat and the chemical potential which have to be evaluated are the following:

$$\begin{aligned} C_{b,e} &= -2(s+1)\int d\varepsilon N(\varepsilon)\partial f_{b,e}(\varepsilon)/\partial T \\ &= -2(s+1)T\int_{-t-\mu}^{t-\mu} d\xi N(\xi+\mu)\partial f_{b,e}(\xi)/\partial\xi\left[(\xi/T)^2 + (\xi/T)\frac{\partial\mu}{\partial T}\right], \end{aligned} \tag{6.52}$$

$$\begin{aligned} n &= 2(s+1)\int d\varepsilon N(\varepsilon) f_{b,e}(\varepsilon) \\ &= 2(s+1)\int_{-t-\mu}^{t-\mu} d\xi N(\xi+\mu) f_{b,e}(\xi), \end{aligned} \tag{6.53}$$

where $f_{b,e}(\varepsilon)$ denote, respectively, the Bose and the Fermi distribution function $f_{b,e}(\varepsilon) = 1/\{\exp[(\varepsilon-\mu)/T] \mp 1\}$, μ denotes the chemical potential, and $N(\varepsilon)$ is the energy density of states.

We are interested in the temperature dependence of the thermodynamic quantities on a temperature scale of the order of the bandwidth (a few or about ten meV). Moreover, we restrict ourselves to a discussion of the normal-state properties, well above T_c—the transition temperature to the superfluid phase. Under these conditions the fine structure of the $N(\varepsilon)$ function for the low-lying energy states is of no importance. Hence, we choose a constant density of states

$$N(\xi) = 1/2t, \tag{6.54}$$

for which $T_c = 0$ and which permits us to treat the normal phase in a consistent fashion. In such a way we can compare self-consistently the thermodynamic behavior of electrons and bosons in the normal phase down to zero temperature.

Introducing the dimensionless parameters $\beta = t/T$ and $\mu^* = \mu/T$, we obtain for bosons using Eqs. (6.52)–(6.54)

$$C_b = \frac{2s+1}{8\beta}\int_{-\beta-\mu^*}^{\beta-\mu^*} dx\left[x^2 + x\left(\mu^* - \beta\frac{\partial\mu^*}{\partial\beta}\right)\right]\mathrm{sh}^{-2}\frac{x}{2}, \tag{6.55}$$

$$\mu^* = \ln\frac{1-\exp(-2n^*\beta)}{\exp\beta - \exp[(-2n^*+1)\beta]}, \quad n^* = \frac{n_b}{2s+1}. \tag{6.56}$$

In the high-temperature limit ($\beta \ll 1$), we find from Eq. (6.56)

$$\mu^* \approx \ln[n^*/(n^*+1)] - \beta^2[(1+2n^*)/6]. \tag{6.57}$$

Substituting Eq. (6.57) into Eq. (6.55), we obtain

$$C_b \approx n_b[1 + n_b(2s+1)^{-1}]\beta^2/3, \quad \beta \leq 1. \tag{6.58}$$

The coefficient in the $1/T^2$ term of the last expression is physically quite obvious. Specific heat is related to the probability of absorption of thermal energy, which is proportional to the number of occupied initial states (n^*) times a factor (n^*+1) coming from the number of final states and reflecting the two contributions characteristic for Bose systems, i.e., processes connected with spontaneous and induced emission.

Let us next consider the low-temperature behavior of the specific heat. For $\beta n, \beta \gg 1$ we obtain from Eq. (6.57)

$$\mu^* \approx -\beta - \exp(-2n^*\beta). \tag{6.59}$$

which shows that the chemical potential at low temperature is localized near the bottom of the band ($\mu \approx -t$) and is practically temperature independent. Substituting Eq. (6.59) into Eq. (6.55), we get for the specific heat

$$C_b = (2s+1)\pi^2/6\beta \quad (\beta n, \beta \gg 1). \tag{6.60}$$

This result shows that bosons in narrow band at low temperature have a temperature-independent specific-heat coefficient $\gamma = C/T$, just as for electrons. The linear temperature dependence in fermion as well as boson systems is related to the existence of a quasilocked chemical potential. For comparison we quote here the results for the electron specific heat in the same limiting cases. Based on the constant density of states as before, one arrives at

$$\begin{aligned} C_e &\approx n[1-(n/2)]\beta^2/3 \quad (\beta \leq 1), \\ C_e &\approx \pi^2/3\beta \quad (\beta n, \beta > 1). \end{aligned} \tag{6.61}$$

If $n \ll 1$, an intermediate temperature region exists for $1/n \gg \beta \gg 1$ in which the boson and fermion specific heat shows logarithmic behavior,

$$C_{b,e} \approx -2n\ln(n\beta). \tag{6.62}$$

Thus bosons and electrons in narrow-band systems have similar temperature dependences of their specific heat in the normal phase (see Figs. 11(a) and 11(b)) with the following ratio of γ at low temperature $\gamma_b/\gamma_e = s + 1/2$. It is necessary to point out that the temperature region in which we expect linear behavior of the specific heat can be very small if $n \ll 1$. In this case, we find for γ a fairly sharp rise as one approaches $T = 0$ which will abruptly turn over into a constant for extremely small temperature ($T \leqslant nt$). For real systems which show a transition to a superconducting phase, the region for the linear temperature behavior of the specific heat can practically disappear if the critical temperature is high enough. In particular, for ideal bosons we have $T_c \propto n^{2/3}t$ (Ref. 8). In this case, the low-temperature behavior will be given by Eq. (6.62) down to T_c.

The $1/T^2$ law for the specific heat at high temperature, common to both fermions and bosons originates from the finite width of the band, which is a direct consequence of the discreteness of the lattice. The classical behavior for the specific heat is only obtained for continuous media which have infinite bandwidth.

Let us now briefly discuss the magnetic susceptibility for bipolarons in the normal phase. For singlet bipolarons evidently the spin susceptibility is zero due to the fairly large binding energy of those bipolarons (typically, $\Delta \approx 0.1 - 1$ eV). For triplet bipolarons, however, the magnetic field couples to the spin of those bosons and the magnetic susceptibility is determined by the linear term of the induced magnetization

$$M(H) = 2\mu_B \int d\varepsilon N(\varepsilon)[f_b(\varepsilon - \mu_B H) - f_b(\varepsilon + \mu_B H)], \tag{6.63}$$

where H denotes the magnetic field and μ_B, the Bohr magneton. We thus obtain

$$\begin{aligned} \chi_t &= -\frac{4\mu_B^2}{t}\int_{-t-\mu}^{t-\mu} d\xi \partial f_b(\xi)/\partial\xi \\ &= -(4\mu_B^2/t)[f_b(t-\mu) - f_b(-t-\mu)], \end{aligned} \tag{6.64}$$

which, together with the corresponding expression for the chemical potential of triplet bipolarons, Eq. (6.56), finally gives us

$$\chi_t = \frac{4\mu_B^2}{t}\frac{(e^{2n\beta/3}-1)(e^{2\beta}-e^{-2n\beta/3})}{e^{2\beta}-1}. \tag{6.65}$$

At high temperatures ($\beta n, \beta \leqslant 1$) we obtain from Eq. (6.65) a Curie behavior (just as for narrow-band electrons[47] given below for comparison):

$$\begin{aligned} \chi_t &\approx (8\mu_B^2/3T)n[1 + (n/3)], \\ \chi_e &\approx (\mu_B^2/T)n[1 - (n/2)]. \end{aligned} \tag{6.66}$$

At low temperatures ($\beta n, \beta \gg 1$) the behavior of the susceptibility of triplet bosons differs significantly from that of electrons (see Fig. 12):

$$\begin{aligned} \chi_t &= (4\mu_B^2/t)\exp(2n\beta/3) \propto \exp(2nt/3T), \\ \chi_e &= \mu_B^2/t \propto \text{const}. \end{aligned} \tag{6.67}$$

Thus, we have shown that while the specific heat for narrow-band systems is the same for bosons and fermions this is not true as far as the susceptibility is concerned. It is well illustrated in Figs. 11 and 12.

7. ELECTRODYNAMICS OF BIPOLARON SUPERCONDUCTORS

In this section we deal with the electrodynamic equations for bipolaron superconductors.[11,13]

In analogy with the procedure used in exciton theory[75] we start with the transformation of the bipolaron Hamiltonian to a representation containing Bose operators instead of the Pauli bipolaron operators:

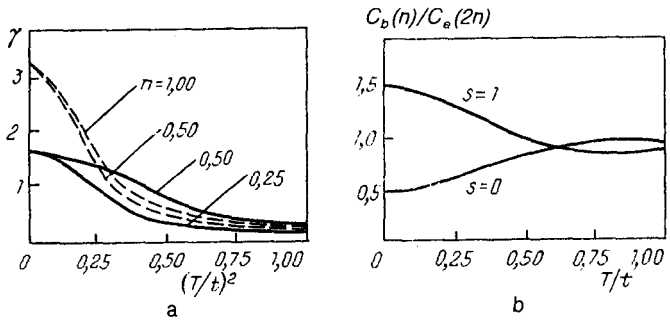

FIG. 11. (a) Temperature dependence of $\gamma = C\beta$ for electrons (dashed line) and for singlet bosons (solid line). (b) Ratio of the triplet ($s = 1$) and singlet ($s = 0$) boson specific heat to the electron specific heat ($n = 0.25$).

$$b_{\mathbf{m}} = \sum_{\nu=0}^{\infty} \beta_\nu (a_{\mathbf{m}}^+)^\nu (a_{\mathbf{m}})^{\nu+1},$$
$$b_{\mathbf{m}}^+ = \sum_{\nu=0}^{\infty} \beta_\nu (a_{\mathbf{m}}^+)^{\nu+1} (a_{\mathbf{m}})^\nu, \tag{7.1}$$

where $a_{\mathbf{m}}$ and $a_{\mathbf{m}}^+$ are operators obeying Bose-statistics: $[a_m, a_{m'}^+ = \delta_{mm'}]$. The first few coefficients β_ν determined by the substitution of Eq. (7.1) into Eq. (5.13) are:

$$\beta_0 = 1, \quad \beta_1 = -1, \quad \beta_2 = (1/2)[1 + (\sqrt{3}/3)], \ldots \tag{7.2}$$

We transform further to field bipolaron and boson operators defining them by the relations:

$$\hat{\varphi}(\mathbf{r}) = \frac{1}{N^{1/2}} \sum_{\mathbf{m}} \delta(\mathbf{r} - \mathbf{m}) b_{\mathbf{m}}, \quad \hat{\varphi}^+(\mathbf{r}) = \frac{1}{N^{1/2}} \sum_{\mathbf{m}} \delta(\mathbf{r} - \mathbf{m}) b_{\mathbf{m}}^+,$$
$$\hat{\psi}(\mathbf{r}) = \frac{1}{N^{1/2}} \sum_{\mathbf{m}} \delta(\mathbf{r} - \mathbf{m}) a_{\mathbf{m}}, \quad \hat{\psi}^+(\mathbf{r}) = \frac{1}{N^{1/2}} \sum_{\mathbf{m}} \delta(\mathbf{r} - \mathbf{m}) a_{\mathbf{m}}^+. \tag{7.3}$$

Here N is the total number of unit cells, and $\delta(\mathbf{r} - \mathbf{m})$ is the eigenfunction of the $\hat{\mathbf{r}}$-operator in the coordinate representation.

The transformation (7.1) for the field operators takes the form

$$\hat{\varphi}(\mathbf{r}) = \hat{\psi}(\mathbf{r}) - \frac{1}{N}\hat{\psi}^+(\mathbf{r})\hat{\psi}(\mathbf{r})\hat{\psi}(\mathbf{r}) + \frac{1}{2}\left(1 + \frac{1}{\sqrt{3}}\right)\frac{1}{N^2}\hat{\psi}^+(\mathbf{r})\hat{\psi}^+(\mathbf{r})\hat{\psi}(\mathbf{r})\hat{\psi}(\mathbf{r})\hat{\psi}(\mathbf{r}) + \ldots . \tag{7.4}$$

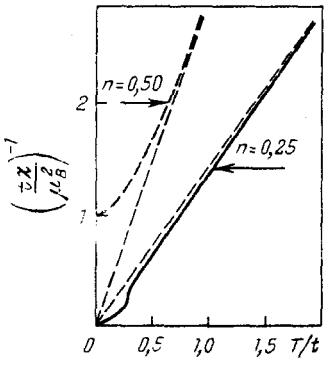

FIG. 12. Temperature dependence of the inverse magnetic susceptibility for electrons (dashed line) and for triplet bosons (solid line).

Substituting the operators $b_{\mathbf{m}}$ and $b_{\mathbf{m}}^+$ expressed with the aid of Eqs. (7.3), (7.4) in terms of $\hat{\psi}(\mathbf{r})$ and $\hat{\psi}^+(\mathbf{r})$, we obtain the Hamiltonian of the interacting boson field

$$\hat{H} = \int d^2r d^3r' \psi^+(\mathbf{r}) t(\mathbf{r} - \mathbf{r}') \hat{\psi}(\mathbf{r}') + \frac{1}{2}\int d^3r d^3r' \{\bar{v}(\mathbf{r} - \mathbf{r}')\hat{\psi}^+(\mathbf{r})\hat{\psi}^+(\mathbf{r}')\hat{\psi}(\mathbf{r})\hat{\psi}(\mathbf{r}') - \frac{2}{N}[\hat{\psi}^+(\mathbf{r}) t(\mathbf{r} - \mathbf{r}')\hat{\psi}^+(\mathbf{r}')\hat{\psi}(\mathbf{r}')\hat{\psi}(\mathbf{r}') + \hat{\psi}^+(\mathbf{r})\hat{\psi}^+(\mathbf{r})\hat{\psi}(\mathbf{r}) t(\mathbf{r} - \mathbf{r}')\hat{\psi}(\mathbf{r}')]\} + \hat{H}_{UP}, \tag{7.5}$$

where

$$t(\mathbf{r} - \mathbf{r}') = -\frac{1}{N}\sum_{m \neq m'} t(\mathbf{m} - \mathbf{m}')\delta(\mathbf{r} - \mathbf{m})\delta(\mathbf{r}' - \mathbf{m}'),$$
$$\bar{v}(\mathbf{r} - \mathbf{r}') = \frac{2}{N^2}\sum_{m \neq m'} \bar{v}(\mathbf{m} - \mathbf{m}')\delta(\mathbf{r} - \mathbf{m})\delta(\mathbf{r}' - \mathbf{m}'), \tag{7.6}$$

and $\hat{H}_{UP}$ includes the terms with powers of $\hat{\psi}$ higher than the fourth (nonpair interaction). In the momentum representation

$$t(\mathbf{r} - \mathbf{r}') = -\sum_{\mathbf{k}} t_{\mathbf{k}} \exp[i\mathbf{k}(\mathbf{r} - \mathbf{r}')],$$
$$\bar{v}(\mathbf{r} - \mathbf{r}') = \frac{2}{N}\sum_{\mathbf{k}} \bar{v}_{\mathbf{k}} \exp[i\mathbf{k}(\mathbf{r} - \mathbf{r}')], \tag{7.7}$$

where

$$t_{\mathbf{k}} = \sum_{m \neq 0} t(\mathbf{m}) \exp(-i\mathbf{k}\mathbf{m}),$$
$$\bar{v}_{\mathbf{k}} = \sum_{m \neq 0} \bar{v}(\mathbf{m}) \exp(-i\mathbf{k}\mathbf{m}). \tag{7.8}$$

We thus obtain a Bose gas with a complicated nonpair interaction of the particles, consisting of dynamic, $\bar{v}(\mathbf{r} - \mathbf{r}')$, and kinetic, $t(\mathbf{r} - \mathbf{r}')$, contributions. Since t contains an exponential reduction factor $\exp(-2g^2)$, one has the following condition to be met in systems with strong electron-phonon coupling: $\bar{v} \gg t$. This allows us to take account only of the dynamic part of the interaction.

A quasi-classical approximation for the magnetic field is sufficient here, since real fields are weak compared with characteristic atomic fields: $eHa^2 \ll 1$ (a is the lattice constant).

If the variation of the vector potential is rather slow, the bipolaron hopping integral is renormalized as follows:

$$\tilde{t}(\mathbf{m}, \mathbf{m}') = t(\mathbf{m} - \mathbf{m}') \exp[-2ie\mathbf{A}(\mathbf{m})(\mathbf{m} - \mathbf{m}')]. \tag{7.9}$$

The dynamic interaction $\bar{v}(\mathbf{m}-\mathbf{m}')$ in a magnetic field remains unchanged, while for $\tilde{t}(\mathbf{r}-\mathbf{r}')$ with allowance for renormalization (7.9) we obtain:

$$\tilde{t}(\mathbf{r}-\mathbf{r}') = -\frac{1}{N}\sum_{\mathbf{k}} t_{k+2eA}\exp[i\mathbf{k}(\mathbf{r}-\mathbf{r}')]. \tag{7.10}$$

Using the weak coordinate dependence of $\mathbf{A}$ and expanding t_{k+2eA} in the vicinity of $\mathbf{k}=0$, we have

$$\tilde{t}(\mathbf{r}-\mathbf{r}') = -\left[t_0 + \frac{(\nabla - 2ie\mathbf{A}(\mathbf{r}))^2}{2m^{**}}\right]\delta(\mathbf{r}-\mathbf{r}'), \tag{7.11}$$

where

$$\frac{1}{m^{**}} = -\frac{\partial^2 t_{\mathbf{k}}}{\partial \mathbf{k}^2}\Big|_{\mathbf{k}=0}. \tag{7.12}$$

According to the analysis of the preceeding section the spatially homogeneous state of the bipolaron Hamiltonian is realized only in the limit of low atomic concentration of the particles:

$$n_b < t/\bar{v}. \tag{7.13}$$

In the opposite case a bipolaron charge-density wave appears. In the following we confine ourselves to the analysis of the magnetic properties of the spatially homogeneous superconducting phase.

To present the results in analytic form, we consider the region of small values of the gas parameter:

$$\eta = n^{1/3}l \ll 1, \tag{7.14}$$

where

$$l = \frac{m^{**}}{4\pi}\int d^3r\bar{v}(\mathbf{r}) \tag{7.15}$$

is the scattering length in the Born approximation and $n = n_b/a^3$ is the particle density. As a result the Hamiltonian of a strongly coupled ($\lambda > 1$) electron-phonon system on a lattice reduces to that of a charged dilute Bose gas:

$$\hat{H} = -\mu\int d^3r\hat{\psi}^+(\mathbf{r})\hat{\psi}(\mathbf{r}) - \frac{1}{2m^{**}}\int d^3r\hat{\psi}^+(\mathbf{r})[\nabla - 2ie\mathbf{A}(\mathbf{r})]^2\hat{\psi}(\mathbf{r}) + \frac{1}{2}\int d^3r d^3r'\bar{v}(\mathbf{r}-\mathbf{r}')\psi^+(\mathbf{r}-\mathbf{r}')\hat{\psi}^+(\mathbf{r})\hat{\psi}^+(\mathbf{r}')\hat{\psi}(\mathbf{r})\hat{\psi}(\mathbf{r}'), \tag{7.16}$$

where μ is the chemical potential.

In the following we consider the case of a short-range interaction.

7.1. Lower critical field

The evolution equation of the Heisenberg field operator $\hat{\psi}(\mathbf{r},t)$ for the Hamiltonian (7.16) may be written as

$$i\frac{\partial\hat{\psi}(\mathbf{r},\tau)}{\partial\tau} = -\left[\mu + \frac{(\nabla - 2ie\mathbf{A}(\mathbf{r}))^2}{2m^{**}}\right]\hat{\psi}(\mathbf{r},\tau) + \int d^3r'\hat{\psi}^+(\mathbf{r}',\tau)\bar{v}(\mathbf{r}-\mathbf{r}')\hat{\psi}(\mathbf{r}',\tau)\hat{\psi}(\mathbf{r},\tau). \tag{7.17}$$

We represent the field operator in the form $\hat{\psi} = \psi_0 + \tilde{\psi}$, where ψ_0 is a c-number having the meaning of a macroscopic wave function normalized to the particle density in the condensate. It is defined as that part of the $\hat{\psi}$-operator which decreases the number of particles in the condensate by unity, leaving the rest part of the system unchanged:

$$\psi_0(\mathbf{r},\tau) = \langle m, N|\hat{\psi}|m, N+1\rangle \quad \text{for } N\to\infty,\ N/V = \text{const}, \tag{7.18}$$

where N is the total particle number, V is the system volume and the $\tilde{\psi}(\mathbf{r},\tau)$-operator describes the overcondensate part.

The set of equations for ψ_0 and $\tilde{\psi}$ is

$$i\frac{\partial\psi_0}{\partial\tau} = -\left[\mu + \frac{(\nabla - 2ie\mathbf{A}(\mathbf{r}))^2}{2m^{**}}\right]\psi_0(\mathbf{r},\tau) + \int d^3r'\bar{v}(\mathbf{r}-\mathbf{r}')(|\psi_0(\mathbf{r}',\tau)|^2\psi_0(\mathbf{r},\tau) + \langle\tilde{\psi}^+(\mathbf{r}',\tau)\tilde{\psi}(\mathbf{r}',\tau)\rangle\psi_0(\mathbf{r},\tau) + \langle\tilde{\psi}^+(\mathbf{r}',\tau)\tilde{\psi}(\mathbf{r},\tau)\rangle\psi_0(\mathbf{r}',\tau)). \tag{7.19}$$

$$i\frac{\partial\tilde{\psi}}{\partial\tau} = -\left[\mu + \frac{(\nabla - 2ie\mathbf{A}(\mathbf{r}))^2}{2m^{**}}\right]\tilde{\psi}(\mathbf{r},\tau) + \int d^3r'\bar{v}(\mathbf{r}-\mathbf{r}')[|\psi_0(\mathbf{r}',\tau)|^2\tilde{\psi}(\mathbf{r},\tau) + \tilde{\psi}^+(\mathbf{r}',\tau)\tilde{\psi}(\mathbf{r}',\tau)\tilde{\psi}(\mathbf{r},\tau) + \psi_0^*(\mathbf{r}',\tau)\psi_0(\mathbf{r},\tau)\tilde{\psi}(\mathbf{r}',\tau) + \psi_0(\mathbf{r}',\tau)\psi_0(\mathbf{r},\tau)\tilde{\psi}^+(\mathbf{r}',\tau)]. \tag{7.20}$$

This set should be supplemented by the Maxwell equation

$$\text{curl curl } A(r) = 4\pi\mathbf{J}_s, \tag{7.21}$$

where $\mathbf{J}_s$ is the density of the superconducting current. The latter is determined by the order parameter $\psi_s = \sqrt{n_s}\exp(i\varphi)$ normalized to the density of the superfluid (superconducting) component $n_s = \rho_s/m^{**}$. However in the dilute gas approximation (7.14) one can assume ψ_s be equal to ψ_0 and express $\mathbf{J}_s$ in terms of the macroscopic wave function ψ_0. Then with allowance for gauge invariance one has

$$\mathbf{J}_s = -\frac{ie}{m^{**}}[\psi_0^*\nabla\psi_0 - \psi_0\nabla\psi_0^*] - \frac{4e^2}{m^{**}}|\psi_0|^2\mathbf{A}. \tag{7.22}$$

Consider now Eq. (7.19) for ψ_0. In the steady-state case ψ_0 is independent of time: $\partial\psi_0/\partial\tau = 0$. Taking the short-range potential in the form $\bar{v}(r-r') = v_0\delta(r-r')$, we rewrite the equation for ψ_0 as follows:

$$\left[\mu + \frac{(\nabla - 2ie\mathbf{A}(\mathbf{r}))^2}{2m^{**}}\right]\psi_0(\mathbf{r}) - v_0|\psi_0(\mathbf{r})|^2\psi_0(\mathbf{r}) = 0. \tag{7.23}$$

The condition (7.14) was also used here allowing us to neglect the overcondensate particle density with respect to $|\psi_0|^2$.

At low temperatures a dilute Bose gas becomes superfluid. In the present case of a charged Bose gas we can thus determine the critical magnetic fields that destroy superconductivity (superfluidity) of this system. First we point out the analogy between the set of Eqs. (7.21)–(7.23) and the equations of the Ginzburg–Landau phenomenological theory.

Recognizing that the chemical potential of the homoge-

neous dilute Bose gas is $\mu \approx n v_0$ (Ref. 76), one has for the characteristic length parameters

$$\lambda_H = (m^{**}/16\pi e^2 n)^{1/2}, \quad \xi = (2m^{**} n v_0)^{-1/2}, \tag{7.24}$$

which are respectively the field penetration depth and the characteristic scale of ψ_0 variation. The Ginzburg-Landau parameter is $\varkappa = m^{**}(v_0/16\pi e^2)^{1/2}$. The large value of the bipolaron mass gives rise to the assumption that the condition for type-II superconductivity is met:

$$\varkappa \gg 1. \tag{7.25}$$

Using Eqs. (7.21)–(7.23), we can calculate the lower critical field H_{c1} in which a normal vortex appears in a superconducting Bose gas. At large $\varkappa$ in analogy with the standard superconductivity theory

$$H_{c1}(T \approx 0) \approx (\Phi_0/4\pi\lambda_H^2)\ln(\lambda_H/\xi), \tag{7.26}$$

where $\Phi_0 = \pi/|e|$ is the magnetic field flux quantum. Substituting expressions (7.24) for λ_H and ξ into (7.26) we obtain

$$H_{c1}(0) \approx \frac{4\pi e n}{m^{**}} \ln\left[m^{**}\left(\frac{v_0}{8\pi e^2}\right)^{1/2}\right]. \tag{7.27}$$

We now calculate the thermodynamic critical field H_c meaning the field in which the homogeneous superconducting and normal phases are in thermodynamic equilibrium.

Let us assume that the energy of the ground state $E(0)$ is determined by the particle interaction energy. Neglect of the kinetic energy of the superconducting phase representing a homogeneous condensate means the neglect of the overcondensate contribution which is small in terms of the gas parameter (7.14). The normal phase is a homogeneous state in which the particles occupy a lower Landau level that is degenerate over the positions of the particle-orbit centers. Allowance for only the interaction energy in this state is equivalent to neglect of the susceptibility.

We thus obtain for the superconducting (S) phase

$$E_s(0) \approx n^2 v_0 V/2. \tag{7.28}$$

For the normal (N) state

$$E_N(0) \approx v_0 \sum_{i,k} n_i n_k \int d^3r |\varphi_i(\mathbf{r})|^2 |\varphi_k(\mathbf{r})|^2, \tag{7.29}$$

where n_i is the particle density in the ith state. By virtue of homogeneity we have

$$\sum_i n_i |\varphi_i(\mathbf{r})|^2 = n, \tag{7.30}$$

and

$$E_N(0) \approx n^2 v_0 V. \tag{7.31}$$

The double value of the energy compared to that of the superconducting state is due to the additional exchange interaction of the particles on the lower level. As a result we obtain:

$$H_c(0)^2/8\pi = F_N(0) - F_s(0) \approx n^2 v_0 V/2, \tag{7.32}$$

and we arrive at the critical field value

$$H_c(0) \approx (4\pi v_0)^{1/2} n. \tag{7.33}$$

The thermodynamic critical field of a charged Bose gas has already been calculated by Schafroth.[77] He considered an ideal charged Bose gas as a model of a superconductor and obtained for the thermodynamic critical field the value $H_0 = 4\pi n \mu_0$, where $\mu_0 = e/2m^{**}$. Comparing Eq. (7.33) with the Schafroth result

$$H_c/H_0 \approx \varkappa, \tag{7.34}$$

we see that under the condition (7.25) the thermodynamic critical field is determined exclusively by the interaction while the contribution due to the charged Bose gas diamagnetism is negligibly small.

7.2. Upper critical field. "Dirty" limit

It is known[77] that the ideal charged Bose gas does not condense in a homogeneous magnetic field. We wish to demonstrate now that the interparticle interaction results in the finite magnetic field value of condensation and to determine the critical curve $H_{c2}(T)$.[11]

First of all we shall calculate the upper critical field H_{c2} of a charged Bose gas taking into account scattering by impurities. The coherence length will be shown to be significantly different from both the interparticle and the interatomic distances.

As usual H_{c2} is defined to be the field value corresponding to the first nonzero solution of Eq. (7.23) for ψ_0. Approximating Eq. (7.23) to the lowest order in ψ_0 we get

$$\tilde{\mu}\psi_0(\mathbf{r}) = \left\{-\frac{[\nabla - 2ie\mathbf{A}(\mathbf{r})]^2}{2m^{**}} + U_{\text{imp}}(\mathbf{r})\right\}\psi_0(r), \tag{7.35}$$

where $\tilde{\mu} = \mu - \bar{v}n$. In deriving Eq. (7.35) we have confined ourselves to the short-range interparticle interaction

$$\bar{v}(\mathbf{r} - \mathbf{r}') = v_0 \delta(\mathbf{r} - \mathbf{r}') \tag{7.36}$$

and have utilized the effective mass approximation.

Consider the random impurity potential $U_{\text{imp}}(\mathbf{r})$ describing the scattering of bosons. The effective mass approximation [$\varepsilon(\mathbf{k}) = -t + k^2/2m^{**}$] remains valid provided that H_{c2} is weaker then the intra-atomic fields. Hence only low-energy states of the band ($\varepsilon \ll \omega^*$) are relevant:

$$\omega^* = 2eH_{c2}/m^* \ll t. \tag{7.37}$$

The chemical potential $\tilde{\mu}$ to the lowest order in ψ_0 is determined by the equation

$$\int d\varepsilon \frac{N(\varepsilon, H_{c2})}{\exp[(\varepsilon - \tilde{\mu})/T] - 1} = n, \tag{7.38}$$

where $N(\varepsilon, H_{c2})$ is the field-dependent single-particle density of states. It is however more convenient to express $\tilde{\mu}$ explicitly from Eq. (7.35) and to put it into Eq. (7.38). In this manner we obtain for $H = H_{c2}$

$$\tilde{\mu} = \varepsilon_0(H_{c2}), \tag{7.39}$$

where $\varepsilon_0(H_{c2})$ is the lowest eigenvalue of the Schrödinger equation (7.35).

Let us begin with the ideal charged Bose gas without scattering, $U_{\text{imp}} \equiv 0$. Then

$$N(\varepsilon, H) = \frac{\sqrt{2}}{4\pi^2}\omega^*(m^{**})^{3/2}\sum_{N=0}^{\infty}\left[\varepsilon - \omega^*\left(N + \frac{1}{2}\right)\right]^{-1/2}, \quad (7.40)$$

and

$$\tilde{\mu} = \omega^*/2. \quad (7.41)$$

Substituting Eqs. (7.40), (7.41) into Eq. (7.38) we get

$$\omega^* = \left[\frac{\sqrt{2}(m^{**})^{3/2}T}{4\pi^2 n}\int_0^{\infty} d\varepsilon\varepsilon^{-3/2}\right]^{-1} = 0, \quad (7.42)$$

so that the upper critical field of the ideal charged Bose gas is

$$H_{c2} = 0. \quad (7.43)$$

This result has been known for a long time and was initially obtained by Schafroth who was the first to prove that the charged Bose gas in analogy with the one-dimensional neutral one does not condense in a homogeneous magnetic field.

In order to obtain a nonzero H_{c2} value one has to take into account boson scattering due to interparticle as well as particle-impurity interaction. Both interactions destroy the one-dimensional character of the low-energy excitations in a magnetic field and smear out the one-dimensional singularities of the ideal density of states, Eq. (7.40). For sufficiently "dirty" and dilute Bose systems one can neglect interparticle scattering compared to particle-impurity scattering. Moreover, if the mean free path l is large enough,

$$l \gg n^{-1/3}, \quad (7.44)$$

as is usually the case for BCS superconductors, $N(\varepsilon,H)$ may be determined by means of the analytical ladder approximation which has been developed for semiconductors in a magnetic field.[78,79] For low energies it gives[79]

$$N(\tilde{\varepsilon}, H) = \frac{\sqrt{6}\omega^*(m^{**})^{3/2}}{8\pi^2\Gamma_0^{3/2}} \times\left\{\left[\frac{\tilde{\varepsilon}^3}{27} + \frac{\Gamma_0^3}{2} + \left(\frac{\Gamma_0^6}{4} + \frac{\tilde{\varepsilon}^3\Gamma_0^3}{27}\right)^{1/2}\right]^{1/3} - \left[\frac{\tilde{\varepsilon}^3}{27} + \frac{\Gamma_0^3}{2} - \left(\frac{\Gamma_0^6}{4} + \frac{\tilde{\varepsilon}^3\Gamma_0^3}{27}\right)^{1/2}\right]^{1/3}\right\}, \quad (7.45)$$

where

$$\tilde{\varepsilon} = \varepsilon - (\omega^*/2), \quad \Gamma_0 = (8\pi n_{\text{imp}} f^2 eH)^{2/3}/2m^{**}, \quad (7.46)$$

n_{imp} is the impurity concentration, f is the scattering amplitude, and

$$\mu = \varepsilon_0 = [\omega^* - (3\Gamma_0/\sqrt{2})]/2. \quad (7.47)$$

Let us consider the rather wide temperature range: $\omega^* \ll T \leqslant T_c$. In this case two contributions to the integral Eq. (7.38) are important. The first one arises from the low-energy regime $\varepsilon \leqslant \omega^*$ within which one has to use the expression (7.45), while the second one corresponds to the high-energy regime, $\omega^* < \varepsilon \leqslant T$, and is described by the classical density of states:

$$N_{\text{cl}}(\varepsilon) = (\varepsilon/2)^{1/2}(m^{**})^{3/2}/\pi^2. \quad (7.48)$$

Subdividing the integration interval in Eq. (7.38) into a low-energy part with the density of states in the form of Eq. (7.45) and a high-energy part with the density of states in the form of Eq. (7.48) we finally obtain

$$H_{c2} = \Phi_0/2\pi\xi^2(T), \quad (7.49)$$

where

$$\xi(T) = K\left(\frac{l}{n}\right)^{1/4}\left\{\frac{T_c}{T}\left[1 - \left(\frac{T}{T_c}\right)^{3/2}\right]\right\}^{-3/4} \quad (7.50)$$

is the coherence length,

$$K^{4/3} = \frac{3{,}31\sqrt{3}}{2^{8/3}\pi^2}\int_0^{\infty}\frac{dx}{x}\left[[x^3 + 2 + 2(1 + x^3)^{1/2}]^{1/3} - [x^2 + 2 - 2(1 + x^3)^{1/2}]^{1/3}\right]^{1/2}, \quad (7.51)$$

$$K \approx 0{,}8, \quad l^{-1} = 4\pi n_{\text{imp}} f^2, \quad T_c = 3{,}31 n^{2/3}/m^{**}.$$

From Eq. (7.50) it follows that $\xi(T)$ is much larger than the interatomic distance, its temperature dependence being different from that expected from the BCS theory. In particular $H_{c2}(T)$ of a charged Bose gas appears to have a positive second derivative

$$d^2H_{c2}/dT^2 > 0 \quad (7.52)$$

and a nonlinear behavior near T_c (see Fig. 14). It is interesting to note that the interatomic distance ($\approx n^{-1/3}$) of the charged Bose gas is a direct analog of the coherence length ξ_0 in the BCS theory:

$$\xi_0 = v_c/T_c \approx n^{-1/3}, \quad (7.53)$$

if one takes $v_c = 2(T_c/m^{**})^{1/2}$ instead of the Fermi velocity. In the considered case of weak scattering the physical coherence length ξ, Eq. (7.50), is greater than ξ_0 from Eq. (7.53):

$$\xi \approx (\xi_0^3 l)^{1/4} \gg \xi_0. \quad (7.54)$$

The Meissner effect for bipolaron superconductors was considered in Ref. 8 and the penetration depth was obtained

$$\lambda\hat{H} = (m^{**}/16\pi ne^2)^{1/2}, \quad (7.55)$$

which considerably (by a factor of $\sqrt{m^{**}/m}$) exceeds the London penetration depth λ_L.

We are now in a position to estimate the Ginzburg-Landau parameter $\varkappa$ for a charged Bose gas in the "dirty" limit:

$$\varkappa \approx \frac{1}{4\sqrt{\pi}}\frac{1}{(n^{1/3}l)^{1/4}}\left(\frac{m^{**}}{e^2 n^{1/3}}\right)^{1/2} \quad (7.56)$$

It turns out to be much greater than unity for all reasonable values of n and l.

We thus come to the conclusion that a charged Bose gas is a type-II superconductor. For $T \to 0$ Eq. (7.49) gives formally $H_{c2} = \infty$. However, for very low temperatures $T\tau \leqslant 1$

(τ denoting the scattering time) localization of bosons in a random potential must be taken into account thus reducing H_{c2} to a finite value. The ladder approximation giving rise to Eq. (7.45) is not relevant in this region.

7.3. Upper critical field. "Clean" limit

Let us treat the interaction between the particles in terms of temperature Green's functions.

We choose the unperturbed wave functions to be Landau solutions of the Schrödinger equation in a uniform magnetic field

$$\varphi(r) = \varphi_\nu(r), \quad \nu = (k, p_x, p_y) \quad (k = 0, 1, ...),$$
$$\varepsilon_\nu^0 = \frac{p_z^2}{2m^{**}} + \omega\left(k + \frac{1}{2}\right), \quad \omega = \frac{2eH}{m^{**}}. \tag{7.57}$$

If the interparticle interaction is ignored the temperature Green's function in a magnetic field is equal to

$$G_\nu^0(\omega_j) = [i\omega_j - (\varepsilon_\nu^0 - \mu)]^{-1}, \tag{7.58}$$

where $\omega_j = 2\pi jT, j = 0, \pm 1, \pm 2, \ldots$. The total number of particles in the system is given by

$$N = T \lim_{\tau \to 0-} \sum_\nu \sum_{\omega_j} G_\nu(\omega_j)\exp(-i\omega_j\tau). \tag{7.59}$$

After substitution of the Green's function, Eq. (7.58), into Eq. (7.59) one can see that the divergence of the integral over p_z leads to the absence of Bose-condensation for all temperatures. This fact reflects the quasi-one-dimensional character of motion in a magnetic field. Let us write down the Dyson equation

$$\hat{G}^{-1} = \hat{G}_0^{-1} - \hat{\Sigma}. \tag{7.60}$$

To calculate the self-energy part we confine ourselves to the loop approximation (Fig. 13). The neglected diagrams are small in terms of the parameter Σ/ω which in turn is small because the interaction is weak. In the wave function representation given by Eq. (7.57) one can rewrite Eq. (7.60) as

$$G_{\nu\nu'}^{-1} = (G_\nu^0)^{-1}\delta_{\nu\nu'} - \Sigma_{\nu\nu'}. \tag{7.61}$$

The smallness of the interaction (7.14) allows us to use the diagonal approximation. It is convenient to express the Dyson equation (7.60) in the coordinate representation

$$G(x, x') = G^0(x, x') + \int dz dz' G^0(x, z)D(z - z')G(z, z')G(z', x'), \tag{7.62}$$

where $x = (\mathbf{x}, \tau)$, τ is the "imaginary time",

$$G(x, x') = T \sum_{\nu,\omega_j} G_\nu(\omega_j)\psi_\nu^*(\mathbf{x})\psi_\nu(\mathbf{x}')\exp[i\omega_j(\tau - \tau')], \tag{7.63}$$

$$D(z - z') = T \sum_{q,\omega_j} D(\mathbf{q}, \omega_j)\exp[i\omega_j(\tau - \tau')]\exp[i\mathbf{q}(\mathbf{z} - \mathbf{z}')], \tag{7.64}$$

$$D(\mathbf{q}, \omega_j) = \frac{v_0}{1 + v_0\Pi(\mathbf{q}, \omega_j)}. \tag{7.65}$$

Substituting Eqs. (7.63) and (7.64) into Eq. (7.62) we obtain for the self-energy part the equation

$$\Sigma_\nu(\omega_j) = T \sum_{\nu',\mathbf{k}} \sum_{\omega_j} D(\mathbf{k}, \omega_j)G_{\nu'}(\omega_j - \omega_j')|I_\nu^{\nu'}|^2, \tag{7.66}$$

where $I_\nu^{\nu'} = \langle\nu|\exp(i\mathbf{kr})|\nu'\rangle$. It will be sufficient to consider the interaction induced renormalization of the spectrum associated with the lowest Landau level which makes a singular contribution to (7.59) at $\omega_j = 0$. The Bose-condensation point is fixed by the condition

$$\mu = \Sigma_0(0) + (\omega/2), \tag{7.67}$$

with $\Sigma_0(0)$ being the value of Σ_ν at $k = p_z = 0$.

The static component of the self-energy part $\Sigma_0(0)$ depends on the renormalized interaction $D(\mathbf{k},0)$. The latter is determined by the polarization operator

$$\Pi(\mathbf{k}) = T \sum_{\nu,\nu'} \sum_{\omega,j'} G_\nu(\omega_{j'})G(-\omega_{j'})|I_\nu^{\nu'}(\mathbf{k})|^2. \tag{7.68}$$

We shall look for the lowest-level energy in the form

$$\varepsilon(p_z) = \varepsilon_0(p_z) - \mu = (p_z^2/2m^{**}) + J|p_z|^\sigma \tag{7.69}$$

and limit our treatment to the temperature range of $T \gg \omega$. We introduce the dimensionless momentum and energy variables instead of p_z and ε

$$p_z = (2m^{**}J)^{1/(2-\sigma)}p,$$
$$\varepsilon(p_z) = [(2m^{**})^\sigma J^2]^{1/(2-\sigma)}\varepsilon(p). \tag{7.70}$$

To the lowest order in η Eq. (7.66) for $\varepsilon(p)$ is reduced to one singular nonlinear integral equation

$$\varepsilon(p) = p^2 + \frac{v_0(m^{**}\omega)^2T^2}{16\pi^4J^{6/(2-\sigma)}}(2m^{**})^{(2-4\sigma)/(2-\sigma)} \times \int_{-\infty}^{\infty} \frac{dk}{\varepsilon(k)} \int_{-\infty}^{\infty} \frac{dq}{\varepsilon(q)}\left(\frac{1}{\varepsilon(q + k + p)} - \frac{1}{\varepsilon(q + k)}\right). \tag{7.71}$$

Substituting $\varepsilon(p_z)$, from Eq. (7.69), and neglecting the p_z^2 term we find $\sigma = 1/2$ and

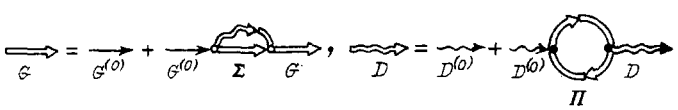

FIG. 13. Green's function diagrams in the loop approximation for an interacting charged Bose gas.

$$J^4 = (v_0/4\pi^3)(m^{**}\omega)^2T^2. \tag{7.72}$$

Summation of (7.59) over all levels except the lowest one may be carried out with no allowance for quantization, since $T \gg \omega$. For the lowest level one should use the spectrum of Eq. (7.69). In this way we obtain for the upper critical field H_{c2}

$$n(1 - t^{3/2}) = \frac{m^{**}\omega}{2\pi^2}T\int_{-\infty}^{\infty}\frac{dp_z}{\varepsilon(p_z)}, \quad \omega = \frac{2eH_{c2}}{m^{**}}. \tag{7.73}$$

Evaluation of the integral yields

$$H_{c2}(T) = 0{,}18\psi_0 m^{**}T_c\eta^{1/2}(1 - t^{3/2})^{3/2}/t, \tag{7.74}$$

where $t = T/T_c$.

Expression (7.74) differs from H_{c2} of the ordinary superconductors in the second derivative sign (it is positive here) and in the nonlinear growth near T_c (Fig. 14).

The expression for J is obtained by direct substitution of Eq. (7.74) into Eq. (7.72):

$$J = 1{,}09[\eta^3(1 - t^{3/2})^3T_c^3/m^{**}]^{1/4}. \tag{7.75}$$

We see that the temperature range of validity of Eq. (7.74) ($\Sigma \ll \omega$) is bounded from above: $(1 - t)/\eta \gg 0.03$. For $t \to 0$ Eq. (7.74) is formally divergent. It should be noted, however, that in this limit the use of an expansion in powers of η to derive (7.71) is erroneous in view of a possible boson localization in the self-consistent interaction potential. This localization is similar to localization in the random potential of impurities.

8. TRANSITION FROM BCS TO POLARON AND BIPOLARON SUPERCONDUCTIVITY

As has been pointed out for the first time in Refs. 9, 12, and 15, a sharp polaron narrowing of the electron band leads to a considerable enhancement of T_c due to an increase in the density of states. The transition from the standard superconductivity of BCS-type to polaron superconductivity (PS) with an increase in λ may be continuous or discontinuous, depending on the value of g^2 and the type of electron-phonon interaction.

If the electron-phonon interaction results in a continuous transition from a large to a small radius polaron state, the transition from BCS superconductivity of wide band electrons to bipolaron superconductivity (BS) is anticipated also to be continuous, Fig. 15. The maximum value T_c^* of transition temperature lies in the region of PS at $\lambda \cong 1$. To estimate T_c^* one can use the weak-coupling expression (3.17), keeping in mind that the mass of a two-site small bipolaron may be of the same order of magnitude as the small polaron mass. This estimate is valid for the "crablike" tunneling of the two-site (Heitler–London) bipolaron, Fig. 16.

One can show that in this case the weak-coupling expression (3.17) works well for all values of λ.

For the half-filled band, $\mu = 0$, $n_e = 1$:

$$T_c \approx 1{,}14(W/2)\exp(-W/2v_0). \tag{8.1}$$

To estimate T_c^* we take $v_0 = g^2\omega$, assuming the Coulomb repulsion to be small. As a result T_c^* is attained at the bare bandwidth value of

$$D^* = 2g^2\omega \exp g^2 \tag{8.2}$$

and turns out to be equal to

$$T_c^* = 1{,}14g^2\omega/e. \tag{8.3}$$

The value of D^* (or g^2) is restricted by the condition (2.10) for the existence of a small polaron so that in Eq. (8.3) one has

$$g^2 \le 0{,}5\ln(2z). \tag{8.4}$$

Substitution of Eq. (8.4) into Eq. (8.3) leads to

$$T_c^* \le 1{,}14(\omega/2e)\ln(2z), \tag{8.5}$$

which in the case of a simple cubic lattice ($z = 6$) can be written as

$$T_c^* \le 0{,}5\omega. \tag{8.6}$$

Taking into account that ω may be larger than the optical phonon frequency (Sec. 2) the values of $T_c^* \cong 500$ K may seem quite possible.

Let us now consider the case when the transition from the large-radius polaron state to the small-radius one is of a discontinuous type, Fig. 17. Two possibilities arise. If the interaction constant is not too large, $g^2 \cong 1$, i.e. the adiabatic parameter ω/D is not too small, the polaron band will be relatively wide near the transition point at $\lambda \gtrsim \lambda_c$. In this case PS is possible just above the transition, with an abrupt

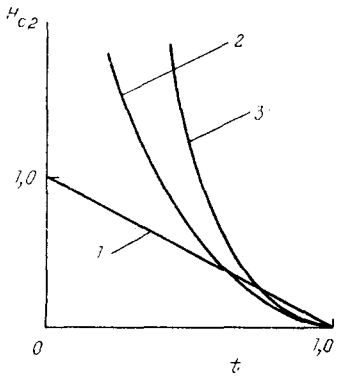

FIG. 14. Temperature dependence of the upper critical magnetic field for an ordinary BCS superconductor (*1*), for bosons with short-range interaction (*2*), and for bosons interacting with impurities (*3*).

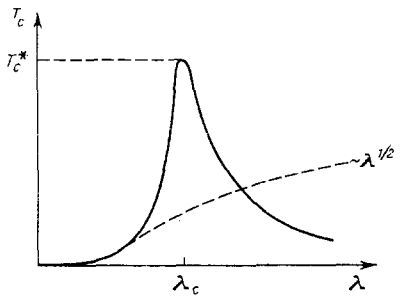

FIG. 15. Continuous variation of the critical temperature as a function of λ (intermediate values of g^2). The dashed line corresponds to the Eliashberg theory.

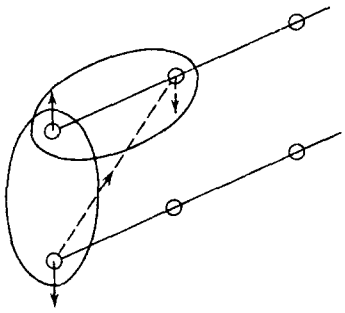

FIG. 16. "Crablike" motion of a two-site bipolaron.

change of T_c, (Fig. 17, curve *1*) under the condition that the binding energy is smaller than the polaron bandwidth:

$$\Delta_c \leq W_c. \tag{8.7}$$

With an increase in $\lambda > \lambda_c$ a smooth transition from polaron to bipolaron superconductivity takes place.

If on the other hand the adiabatic parameter is small and $g^2 \gg 1$, or the binding energy just above the transition is large:

$$\Delta_c \gg W_c, \tag{8.8}$$

a jumplike transition from BCS superconductivity directly to BS occurs with higher or lower T_c value depending on the electron concentration and the magnitude of the constant g^2, (Fig. 17 curves *2* and *3*). PS is absent in this limit.

An attempt of computer calculation of $T_c(\lambda)$ dependence has been undertaken by Nasu[80] within the framework of a combined version of variational and mean field approach to the initial Hamiltonian, Eq. (1.1). The variational parameter ρ was introduced into the Lang-Firsov transformation in the following manner (cf. Eq. (1.20)):

$$S_1 = \rho \sum_{i,q} \frac{n_i}{\omega(q)} (U(q) e^{-iqm} d_q - \text{H.c.}). \tag{8.9}$$

From the physical point of view the parameter ρ determines the "thickness" of the phonon cloud surrounding a polaron. The transformed Hamiltonian is averaged using the phonon density matrix as has been described in Sec. 1. The numerical results are in qualitative agreement with Fig. 15 for intermediate values of $D/\omega \cong 2$ and with Fig. 17 for $D/\omega \cong 10$. It should be noted however that for $\rho < 1$ the essential portion of the electron-phonon interaction remains in the transformed Hamiltonian:

$$\tilde{H}_{e-ph} = (1-\rho) \sum_{i,q} c_i^+ c_i (U(q) e^{-iqm} d_q + \text{H.c.}), \tag{8.10}$$

which being averaged over phonon variables makes no contribution to the final results.

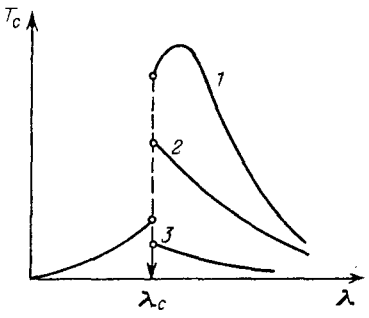

FIG. 17. Transition from BCS superconductivity to bipolaron superconductivity at large g^2 values.

9. POLARON THEORY OF SUPERCONDUCTIVITY AND THE PHYSICAL PROPERTIES OF HIGH-TEMPERATURE METALLIC OXIDES

Under the condition of $\lambda \geqslant 1$ the electron potential energy associated with the local deformation of the lattice has the same order or exceeds the value of the bare bandwidth D. Hence beginning approximately from this value of the effective coupling the usual carrier tunneling through the lattice becomes impossible and exponential mass renormalization occurs. It leads according to the preceeding sections to small polaron or bipolaron superconductivity with high T_c values.

The polaron superconductors are characterized by a strong electron-phonon interaction $\lambda \geqslant 1$, by a high effective mass value of the carriers, and by an extremely narrow energy band. In the case of a bipolaron superconductor one should add the existence in the normal phase (above T_c) of Bose-like doubly charged electron excitations.

We wish to show in the following discussion that there is available certain experimental evidence in favor of these properties in high-temperature metallic oxides.

9.1. Importance of the electron-phonon interaction

Ample experimental information is now available indicating that the electron-phonon interaction in the new superconductors is strong. Specifically one should mention the effect of softening at the transition point of certain phonon modes which was reported in Refs. 81–83 and analyzed in Ref. 84, as well as the important differences between the phonon spectra of the superconducting and nonsuperconducting samples of $YBa_2Cu_3O_{7-x}$ and $YBa_2(CuZn)O_{7-x}$ with varying oxygen content observed in Ref. 85 by neutron spectroscopy techniques. The direct observation by infrared absorption measurements of small polaron states in experiments on photogeneration of the carriers in nonsuperconducting samples which is discussed later in this section is to be also mentioned here.

Now it is already clear that in all the known high-temperature metallic oxides a measurable oxygen isotope effect does exist. There are some compounds (see Table I) demonstrating even higher isotope shift values than those predicted by the BCS theory ($\alpha = 0.5$).[86]

The dependence of α on the dopant concentration for the ceramic compound $La_{2-x}Sr_xCuO_4$ characterized by the maximum of $\alpha \approx 0.7$ at $x = 0.12$ was studied recently in Ref. 87. One of the possible explanations discussed by the authors is associated with the strong electron-phonon interaction with a soft optical phonon mode assumed to be responsible for the superconductivity. A substantial isotope effect ($\alpha \approx 0.35$) too large to be considered simply as "parasitic" and irrelevant to superconductivity was observed also in the system Ba-K-Bi-O.[88]

As far as the "1-2-3" compounds are concerned the situation is not clear yet. There are some experiments with a

TABLE I.

Compound	T_c, K	Isotope shift	BCS Shift K*)	O^{18}, %	$\alpha = -\frac{\partial \ln T_c}{\partial \ln M}$
$BaPb_{0.75}Bi_{0.25}O_3$	11	0,6	0,63	60	0,8!
$La_{1.85}Ca_{0.15}CuO_4$	20,6	1,6	1,14	75	≈ 1!
$La_{1.85}Sr_{0.15}CuO_4$	37,0	1,0	2,10	75	0,3!
$YBa_2Cu_3O_7$	91,1	0,9	5,21	67	≤ 0,1

*)BCS theory prediction for T_c shift with $\alpha = 0.5$ and 100% substitution by O^{18}.

high degree ($\approx$90%) of oxygen $O^{16} \rightarrow O^{18}$ replacement in $YBa_2Cu_3O_{7-x}$ ceramic samples[89] demonstrating an isotope shift of $\delta T_c \cong 1.5$ K comparable with the BCS value.

Small α values in the experiments with substitution of O^{16} by O^{18} may stem from the fact that O^{16} atoms do not leave those crystallographic positions the isotope state of which affects the T_c value. These conclusions have been confirmed by the first experiments with the YBCO samples synthesized from the oxides initially not containing the O^{16} isotope:[90]

$$\alpha \approx 2{,}5. \tag{9.1}$$

This value exceeding the results of the initial partial substitution measurements by almost two orders of magnitude corresponds to a T_c decrease from 92 K in the O^{16} samples to 59 K and 77 K in the identically prepared O^{18} and O^{17} samples respectively. The giant isotope effect (9.1) is by a factor of five greater than the limiting BCS value for the cases of weak and strong electron-phonon interaction.

To explain the isotope effect on the basis of polaron theory which predicts the formation of heavy small bipolarons having an effective mass m^{**} and condensing to a charged superfluid Bose liquid when the electron-phonon interaction is sufficiently strong ($\lambda \geqslant 1$) let us start with the following expression for the critical temperature:

$$T_c = f(n)/m^{**}, \tag{9.2}$$

where $f(n)$ is a function of boson concentration n (per unit volume) independent of the isotope mass. For low concentrations one has

$$f(n) \approx 3{,}31 n^{2/3}. \tag{9.3}$$

Following the paper of Alexandrov and Kabanov[10] in the simple case of interaction with the dispersionless phonon mode of frequency ω we express the bipolaron mass in the form:

$$m/m^{**} = [2J \exp(-4g^2)/\Delta] M[1,1 + (\Delta/\omega) \cdot 2g^2]: \tag{9.4}$$

Here Δ denotes the bipolaron binding energy which does not depend on the isotope mass M, and $M(\alpha,\beta,z)$ is the degenerate hypergeometric function a power series expansion of which leads to the bipolaron mass expressions obtained previously in Sec. 5. Assuming that $\omega \propto M^{-1/2}$ and $g^2 \propto M^{1/2}$ we find from Eqs. (9.2), (9.4)

$$\alpha = g^2 F(\Delta/\omega, 2g^2) \cdot \tag{9.5}$$

Here

$$F(x, y) = 1 + \left(M(1,1 + x, y) - \frac{x}{y}\frac{\partial M(1,1 + x, y)}{\partial x}\right) M^{-1}(1,2 + x, y) \tag{9.6}$$

varies from $F(0,y) = 1$ to $F(\infty,y) = 2$.

As is clear from Eq. (9.5) the bipolaron theory makes it possible to explain the isotope effect with an $\alpha > 0.5$ value if $g^2 \geqslant 1$. Eq. (9.5) also results in a monotonic increase of α with g^2 or λ. At the same time T_c decreases with λ. Therefore the stronger isotope effect is predicted by bipolaron theory for compounds with lower T_c values in agreement with the data for metallic oxides (see Table I). Near the maximum of the $T_c(\lambda)$ function the isotope effect tends to zero.

One of the most interesting manifestations of the strong electron-phonon interaction is the polaron plasmon-phonon mixing resulting in the formation of a new type of vibrational excitations ("plasphons") discussed in Sec. 4. Meanwhile the "extra" vibrational mode (extra-mode) of high frequency was observed in a neutron scattering experiment.[91] According to the authors' claim it provides evidence of a strong electron-lattice interaction. Interpreting this vibrational mode together with the other high-frequency vibrational mode as plasphon branches of excitations with the observed frequencies[91]

$$\Omega_1/2\pi = 22\,\text{THz}, \quad \Omega_2/2\pi = 14\,\text{THz} \tag{9.7}$$

and the relative weight $P_1/P_2 \approx 1$, one obtains with the aid of Eqs. (4.70) and (4.73) for the plasma frequency the value

$$\omega_p/2\pi \approx \tilde{\omega}/2\pi \approx 18\ \text{THz}. \tag{9.8}$$

Taking as an estimate the bare phonon frequency equal to the renormalized one $\omega \approx \tilde{\omega}$, we find for the effective coupling the value $\beta \approx 0.1$ which should be considered as the lower bound because in general $\omega > \tilde{\omega}$.

The extra-mode disappears in the long wavelength limit $\mathbf{q} \rightarrow 0$ (Ref. 91) this being the case for the intramolecular as well as the acoustical phonons. It is not true for the case of long-wave optical phonons for which in this limit $\beta = (\varepsilon_0 \varepsilon_d^{-1} - 1)$. It disappears also in the small wavelength limit. This fact may be related to the short-range interpolaron attraction $v(\mathbf{q}) < 0$ leading to the disappearance of the short wavelength plasmon in accordance with Eq. (4.29).

Let us give now an ordinary estimate of plasma frequency Eq. (4.30) to be compared with Eq. (9.8). Using the experimental values $\varepsilon = \varepsilon_d = 50$ (Ref. 92), $m^* = 25 m_e$ (Ref. 93), and choosing $n_e = 1$ (a half-filled band) one arrives at $\omega_p \cong 110$ THz, which turns out to be in surprising agreement with the estimate of Eq. (9.8) thus confirming the plasphon nature of the extra-mode.

At the end of this subsection we wish to note that the point contact and the tunneling spectra of superconducting oxides[94] exhibit the same phonon maxima as observed by neutron spectroscopy. This fact is indicative of strong inelastic scattering of electrons by phonons.

It should be added that the nearly temperature-inde-

pendent thermal conductivity above the transition in combination with its sharp rise below T_c also points to a strong interaction of the lattice with the carriers in high-temperature superconductors.[95]

9.2. Heavy carriers

To get $T_c \simeq 100$K from Eq. (9.2) with the hole concentration $n_p = (0.5 - 1) \times 10^{22}\,\mathrm{cm}^{-3}$ (Hall measurements for $YBa_2Cu_3O_7$) one has to take

$$m^{**}/m \leq 40 - 100. \tag{9.9}$$

For the oxygen band in the Cu–O planes with $D = 1$ eV and $z = 4$ the small polaron formation according to Eq. (2.10) needs $g^2 > 3$ if $\omega \simeq 0.1$ eV. With this value of g one has

$$m^*/m \gtrsim 20, \tag{9.10}$$

where m is the band electron mass. It has been mentioned already that the intersite small bipolarons may have an effective mass of the same order of magnitude as m^* due to processes when only one of the two small polarons forming a pair tunnels between the two sites. Bipolaron effective mass may therefore be much smaller than that corresponding to simultaneous two particle transfer described by Eq. (9.4). Moreover one should remember that in crystals with a large lattice constant a the band mass may be smaller than the free electron mass m_e even for rather narrow bands with the width $D \simeq 1$ eV:

$$m = z/2Da^2. \tag{9.11}$$

Thus the small polaron and bipolaron masses of the order of a few tens of the free electron mass m_e are quite probable and as a consequence may give rise to rather high values of T_c ($\geqslant 100$ K) even for comparatively low carrier concentrations such as $\simeq 10^{21}\,\mathrm{cm}^{-3}$. In this context we would like to stress that a great number of London penetration depth measurements both for ceramic and single crystal samples of LaSr(Ba)CuO,[96] BaBiPbO,[97] and YBaCuO[98,99] with the field oriented perpendicular to the Cu–O planes give an enormously high value of

$$\lambda_H \geq 2000\ \text{Å}, \tag{9.12}$$

that is compatible with considerable mass enhancement.

The normal state specific heat $\gamma_N = C_e/T$ estimates obtained by subtraction of the phonon contribution from the total heat capacity[100] lead to an extremely high value of

$$\gamma_N \geq 40\ \mathrm{mJ/mol \cdot K^2} \quad \text{for LaBa(Sr)CuO}, \tag{9.13}$$

exceeding the value of γ_N for A–15 compounds. For YBaCuO one can estimate γ_N using the well-known BCS relation for the heat capacity jump ΔC at $T = T_c$ which, according to Ref. 101, turns out to be very high:

$$\Delta C \geq 5\ \mathrm{J/mol \cdot K}. \tag{9.14}$$

The result is practically the same as in Eq. (9.13). Taking into account that $\gamma_N \simeq m^*$ for free fermions or using the value of γ_N for the narrow-band Bose gas on a lattice[11] one obtains

$$m^*,\ m^{**} \geq 30 m_e, \tag{9.15}$$

which also agrees well with the hypothesis of polaron mass enhancement. In this regard it would be fair to point out also that estimates based on optical measurements[102] give somewhat smaller mass values $m^* \simeq 10 m_e$.

9.3. Narrow band

The heat capacity jump, Eq. (9.14), normalized to a single carrier turns out to be surprisingly high:

$$\Delta C/n_p \approx k_B, \tag{9.16}$$

while from the BCS theory

$$\Delta C/n_p = 7k_B T_c/E_F. \tag{9.17}$$

Eqs. (9.16), (9.17) are unambigiously pointing to the nonadiabatic character of the carrier motion

$$E_F \leq 0{,}05\ \mathrm{eV} \leqslant \omega \tag{9.18}$$

thus confirming the fact that all the carriers participate in Bose-condensate formation as predicted by the polaron theory of superconductivity.

Localization effects, the almost temperature-independent thermoelectric power S, and the difference in activation energy for S and electrical resistivity of the semiconducting phase of $YBa_2Cu_3O_{7-\delta}$ ($\delta > 0.5$) are typical for narrow bands and polaron transport.

The electron photoemission spectra as well as Hall measurements show that the carriers in high-temperature La-, Y-, Bi- and Tl-based oxides are holes, moving in the oxygen band. Hence the energy band structure may be viewed as presented in Fig. 18 with the narrow "oxygen" polaron band lying inside the Coulomb gap U between two "copper" Hubbard subbands.

9.4. Charged bosons

An unambigious proof of the bipolaron nature of high-T_c oxides would be observation of charged particles with zero or unity spin in the above-T_c region. According to Ref. 103 the absence of the thermopower dependence on the magnetic field strength up to values of 30 T lends credence to models in which the carriers are of Bose type, existing as pairs with total spin equal to zero.

In the experimentally studied normal-metal to high-T_c superconductor tunneling spectra[104–110] an asymmetry in conductance as a function of bias voltage has been reported. It was noted[111] that for one sign of the bias voltage the conductance rises linearly, whereas for the other it seems to saturate at a finite value. These features were previously predicted in Ref. 112, as a consequence of different statistics of carriers on both sides of the barrier, specifically Bose-like bipolarons on the one side, and ordinary electrons on the other (cf. also Ref. 113).

The data interpretation for the tunneling conductivity

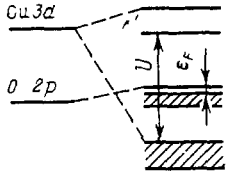

FIG. 18. Band structure of metallic oxides.

remains a rather controversial issue. The experiments[114] with a junction of $YBa_2Cu_3O_7$ (thin film)/barrier/Pb(In) type showed with high reproducibility a gap-like structure in the conductance which reflects the properties of the quasiparticle excitation spectrum of $YBa_2Cu_3O_7$. Two gaps were found (see Fig. 19). The smaller one has a value $2\Delta/T_c \leqslant 1$ and disappears at $T < T_c$. The second (and the larger) gap disappears at $T = T_c$ predominantly by weakening rather than by a shift of the peak to lower voltages as predicted by BCS-theory. One might suppose that this temperature-independent gap is related to the bipolaron binding energy Δ, while the smaller one is a gap in the superfluid Bose gas density of states, arising from the long-range Coulomb interaction between charged bosons (plasma gap). On the other hand, if the interaction between bosons is short-range due to screening effects, one can obtain using Eq. (6.34) for the superfluid state:

$$N(\varepsilon) \propto \varepsilon^2 \tag{9.19}$$

which is much smaller at low energies than the normal state $N(\varepsilon) \propto \sqrt{\varepsilon}$.

In the high resolution photoemission experiments with Bi-Sr-Ca-Cu-O compounds[115] an anomalous peak near the chemical potential was observed. It was interpreted as the gap in the spectrum with the value

$$\Delta \approx 8T_c \quad (T_c \approx 90\ \text{K},\ k_B = 1), \tag{9.20}$$

which seems to be temperature-independent for $T \leqslant 100$ K. Similar results with the same value of the gap existing possibly even above T_c and independent of the oxygen content were reported in the infrared absorption experiments for Y-Ba-Cu-O structure,[116-118] as well as in the electron energy loss high resolution spectra analysis.[119] Identifying this anomalous gap with the bipolaron binding energy as it was suggested earlier one obtains the value

$$\Delta \approx 720\ \text{K}. \tag{9.21}$$

Taking this binding energy to be equal to the value of the interpolaron attractive potential $|U_c| \cong \Delta \cong 720$ K (see Sec. 4), let us estimate the characteristic temperature T_b of bipolaron formation (4.27) for the half-filled band ($n_e = 1$):

$$T_b \approx 360\ \text{K}. \tag{9.22}$$

It falls in the range of tetra-ortho stucture phase transition

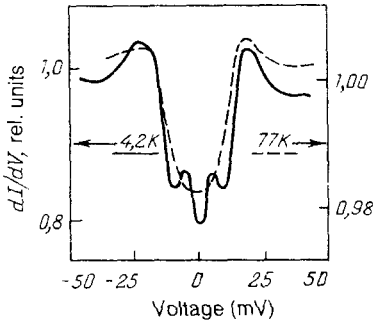

FIG. 19. Comparison of the shape of the normalized conductance traces at $T = 4.2$ K (left-hand scale) and at $T = 77$ K (right-hand scale) for a tunnel junction on thin films of Y–Ba–Cu–O.

corresponding in this approach to the intersite bipolaron formation. In the above-T_b region the carriers are small bipolarons with the characteristic activation-like temperature dependence of mobility.

Qualitative differences from the BCS-theory predictions are observed in some measurements of the $\lambda_H(T)$ temperature behavior including the low temperature range.[120]

For charged bosons with the short-range interaction the temperature dependence $\lambda_H(T)$ may be calculated by a standard approach with the help of temperature Green's functions.[121] To the first order in the gas parameter $\eta = ln^{1/3}$ (l is the scattering length for the particle scattering by each other) it is easy to obtain:

$$\left(\frac{\lambda_H(0)}{\lambda_H(T)}\right)^2 = 1 + \frac{1}{3nm^{**}}\int \frac{d^3p}{(2\pi)^3} p^2 \frac{\partial f_b}{\partial \varepsilon}, \tag{9.23}$$

where $f_b(\varepsilon) = 1/\{\exp[\varepsilon(p)/T] - 1\}$. The quasiparticle spectrum $\varepsilon(p)$ in the same approximation is defined by the well-known expression:

$$\varepsilon(p) = \left[\frac{4\pi l n_0}{(m^{**})^2}p^2 + \left(\frac{p^2}{2m^{**}}\right)^2\right]^{1/2}; \tag{9.24}$$

Here $n_0 = n(1 - t^{3/2})$ is the concentration of the particles in the condensate and $t = T/T_c$. Substituting Eq. (9.24) into Eq. (9.23) one obtains

$$\left(\frac{\lambda_H(0)}{\lambda_H(T)}\right)^2 = 1 - \frac{1}{6}\frac{t^{3/2}}{\Gamma(3/2)\zeta(3/2)}\int_0^\infty \frac{x^{3/2}dx}{\text{sh}^2(\xi/2)}, \tag{9.25}$$

where $\Gamma(x)$ is the Γ-function, $\zeta(x)$ is the Riemann ζ-function, and

$$\xi = [x(x+\delta)]^{1/2}, \quad \delta = 4[\zeta(3/2)]^{2/3}\eta(1 - t^{3/2})/t. \tag{9.26}$$

A few words about the effect of crystal anisotropy on the above results. Introducing the reciprocal effective mass tensor $(1/m^{**})_{ik}$ with the masses in the (x,y)-plane assumed to be equal and denoted by $m_\parallel^{**}$ and the mass in the z-axis direction denoted by $m_\perp^{**}$, one can use for the penetration depths $\lambda_H^\parallel$, $\lambda_H^\perp$ the result analogous to Eq. (9.23) by replacing in it m^{**} by $m_\parallel^{**}$ and $m_\perp^{**}$ respectively. Here, $\lambda_H^\parallel$ denotes the penetration depth in the (x,y)-plane, and $\lambda_H^\perp$ is the penetration depth in the z-axis direction. The temperature dependence of the $\lambda_H(0)/\lambda_H(T)$ ratio will remain the same as in Eq. (9.25).

To compare our calculations with experiment the data from Ref. 120 were taken. We used only the most reliable results obtained for samples with maximum value of grain size and maximum diamagnetic shielding. Fig. 20 presents a comparison of these data with the theory ($\eta = 0.02$) in the low-temperature range. Fig. 21 shows the same for the whole temperature interval. The power-law character of the temperature dependence at low temperatures is qualitatively different from the $[1 - (T/T_c)^4]^{-1/2}$ law interpolating the experimental data for ordinary BCS-like superconductors (dashed line) and can be satisfactorily described in terms of the charged short-range Bose-gas model.

The long-range Coulomb potential in high-T_c super-

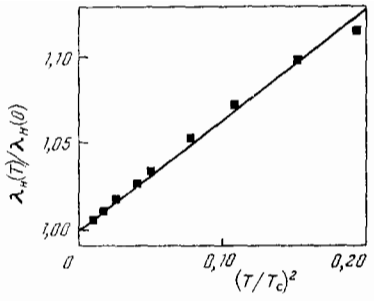

FIG. 20. Temperature dependence of the magnetic field penetration depth in the close to zero region at $\eta = 0.02$.

conductors can become suppressed by light carriers screening if there is a wide electron band in these compounds. This screening may be due to the huge value of the static permittivity of the order of $\varepsilon_0 = 10^5$, as in BaBiPbO. In this case the corresponding plasma frequency for such a heavy charged Bose-liquid will be quite low:

$$\omega_p = c/\lambda_H \varepsilon^{1/2} < 20 \text{ K}. \tag{9.27}$$

Nevertheless the existence of the plasma gap, as well as the lack of agreement between the different measurements of λ_H make the interpretation of existing results in terms of $\lambda_H(T)$ dependence rather difficult.

The λ-like behavior of the heat capacity similar to that of ^{4}He[122,123] and the positive second derivative of the upper critical field near T_c[124] anticipated in Ref. 11 should be considered as important independent arguments in favor of the bipolaron picture of high-temperature superconductivity. The nonlinear character of the H_{c2} behavior in the vicinity of the transition point was not so obvious in the initial measurements which were carried out for a number of 1-2-3 compounds because of the relative narrowness of the experimentally accessible temperature interval. In the "low-temperature" metallic oxides, such as BiKBaO and the "electron" superconductor NdCeCuO, on the other hand, the positive sign of the second derivative is observed over a wide temperature range.[125]

According to the theoretical analysis of Sec. 7 near the point of transition to normal phase

$$H_{c2} \propto (T_c - T)^{2\nu}, \quad 2\nu \approx 1{,}5. \tag{9.28}$$

The data parametrization in terms of this expression results in ν values varying from 0.65 (for magnetic field parallel to the c-axis) to 0.8 (for magnetic field perpendicular to the c-axis). It should be pointed out that the value of ν as well as the T-interval ΔT corresponding to the positive sign of the second derivative of the upper critical field considerably exceed the values ($2\nu = 4/3$, $\Delta T = 0.2$ K) predicted in the fluctuation theory.

A detailed comparison of the polaron theory results for H_{c2} with experiment was carried out in Refs. 126, 127. As illustrated by Fig. 22 from Ref. 127 the data for H_{c2} in the 1-2-3 compounds in the region close to T_c (with the field orientation along the Cu–O planes) agree well with the theoretical curve. The same comparison for the case of the lower-T_c K–Ba–Bi–O compound and also for the case of Eu–Ba–Cu–O (with field orientation perpendicular to the planes) in the wider T/T_c range is shown in Fig. 23 from Ref. 126. At low temperature and strong magnetic field the large value of the bipolaron mass may lead to the carrier localization and as a consequence to a finite value of $H_{c2}(0)$, which may be the case for Eu–Ba–Cu–O.

New data were recently reported by the Argonne National Laboratory group[128,129] for the Y–Ba–Cu–O single crystals raising doubts about the reliability of the resistive method of H_{c2} determination as compared to that based on magnetization measurements. In spite of the apparent difference in the results obtained by these two methods the abnormal behavior of H_{c2} (although to a different extent) may be seen in both cases. The future study of this problem will probably raise the question of further detalization or even modification of our estimates. In our opinion for this to be done some more experimental information is necessary.

The relation of T_c with magnetic field penetration depth[125] and plasma frequency[130] in LaSrCuO and YBaCuO has the form

$$T_c \propto \lambda_L^{-2} \propto \omega_p^2, \tag{9.29}$$

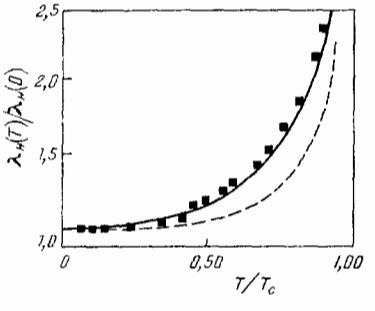

FIG. 21. Magnetic field penetration depth as a function of T in the entire temperature range.

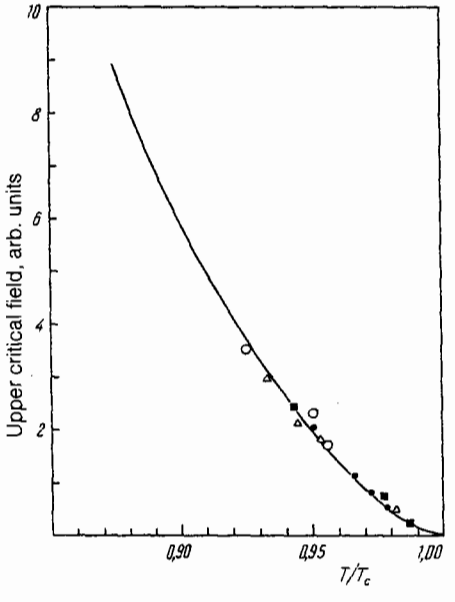

FIG. 22. Upper critical field as a function of temperature for 1–2–3 compounds in the near T_c region with the field orientation along the planes.[127] Solid line—bipolaron theory result.

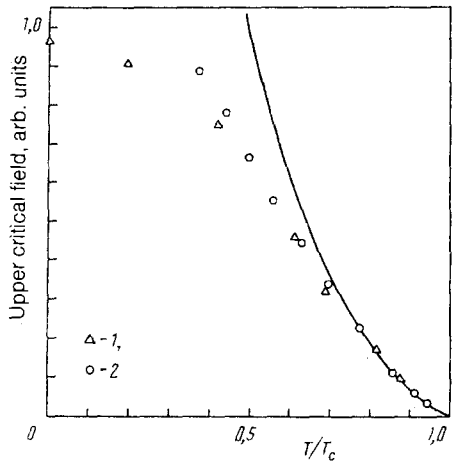

FIG. 23. Upper critical field as a function of temperature for $EuBa_2Cu_3O_{7-x}$—Δ (field parallel to c-axis) and for $Ba_{0.63}K_{0.37}BiO_3$—O.[126] Solid line—bipolaron theory result.

and is consistent with the expectation for the charged two-dimensional Bose gas

$$T_c \propto n/m^{**}. \tag{9.30}$$

As shown in Ref. 131, the anomalous pressure dependence $T_c(p)$ for the lanthanum and yttrium ceramics rules out the BCS as well as the Anderson resonating valence bond (RVB)[132] models, but can be explained within the framework of the bipolaron approach. Using Eq. (9.2) one can easily obtain a very large value of the derivative dT_c/dp for bipolaron superconductors and a much lower value for polaron ones, Eq. (3.15).

Let us turn now to a discussion of sound propagation in HTSC.[133] A stiffening of the lattice was inferred from the temperature dependence of the acoustic sound velocity.[134–136] Upon decreasing the temperature, going from the normal to superconducting state, a stepwise increase in the sound velocity derivative $ds(T)/dT$ occurs, indicating an abrupt stiffening of the lattice just below T_c. These results were obtained both for ceramic and single crystal samples. Our aim is to show that the bipolaron theory can explain these findings.

Let us consider a system of free charged bosons on a lattice which couple weakly to the long-wavelength acoustic lattice vibrations. Expressing the acoustic phonon self-energy in terms of the carrier polarization function we obtain for the renormalized phonon frequency:

$$\bar{\omega}_q \approx \omega_q\left(1 - \frac{g_{ac}^2(\omega_q)}{\varepsilon_0\omega_q}\Pi(q, \omega_q)\right), \tag{9.31}$$

where $\omega_q = sq$, $g_{ac}(\omega_q)$ denotes the coupling of the carriers with the deformation potential, and ε_0 is the static permittivity.

$$\Pi(q, \omega) = \sum_k \frac{f_b(\varepsilon_k) - f_b(\varepsilon_{k-q})}{\omega + \varepsilon(k-q) - \varepsilon(k)} \tag{9.32}$$

represents the irreducible polarizability of the charged carriers in the simplest RPA. Using an isotropic effective mass approximation, $\varepsilon(k) = k^2/2m^{**}$, we evaluate the relative change in the sound velocity $\Delta s(T)/s$ and the sound wave damping $\Gamma(\omega_q)$

$$\frac{\Delta s(T)}{s} = -(g_{ac}^2(\omega_q)/\omega_q\varepsilon_0)\mathrm{Re}\,\Pi(q, \omega_q),$$
$$\Gamma(\omega_q) = (g_{ac}^2(\omega_q)/\varepsilon_0)\mathrm{Im}\,\Pi(q, \omega_q). \tag{9.33}$$

Let us first calculate the sound velocity renormalization $\Delta s = s(T) - s$. In the case of free bosons and $0 < T \leqslant T_c$ the chemical potential $\mu \equiv 0$. For $T > T_c$ μ is determined by the relation:

$$n = \left(\frac{m^{**}T}{2\pi}\right)^{3/2}\sum_{j=1}^{\infty}\frac{\varphi^j}{j^{3/2}}, \tag{9.34}$$

where $\varphi = \exp(\beta\mu)$, and $\beta = 1/T$. In the vicinity of the transition point $(T - T_c)/T_c \equiv (t-1) \ll 1$ one has $\beta\mu \cong 0.5429(t^{3/2} - 1)^2$.

Separating out in the sum over k, of Eq. (9.32) the condensate state ($k = 0, k - q = 0$) contribution and replacing the sum by an integral over k for the thermally excited bosons we obtain:

$$\frac{\Delta s(T)}{s} = \frac{g_{ac}^2(\omega_q)}{\omega_q\varepsilon_0}\left[\frac{n(1 - t^{3/2})}{m^{**}s^2}\theta(1-t) - \sum_k \frac{\partial f_b(\varepsilon_k)}{\partial\varepsilon_k}\frac{(qk)^2}{(m^{**}\omega_q)^2 - (qk)^2}\right]$$
$$= \gamma\left[(1 - t^{3/2})\theta(1-t) + \frac{2t^{1/2}}{\sqrt{\pi}\zeta(3/2)}\frac{T^*}{T_c}\int_0^{\infty}\frac{x^{1/2}dx}{(\varphi e^x - 1)(T^*/T - x)}\right]. \tag{9.35}$$

In this expression θ denotes the step function, $T^* = m^{**}s^2/2$, and $\gamma = g_{ac}^2(\omega_q)n/\omega_q\varepsilon_0 m^{**}s^2$ represents a frequency-independent factor since $g_{ac}^2(\omega_q)$ is proportional to ω_q. For the typical sound velocity values $s = 5\times 10^5$ sm/s one can easily estimate $T^* = 0.8\, m^{**}/m_e$ K.

In the superconducting state, $(T < T_c)$, $\Delta s(T)$ first increases with increasing T and then begins to decrease. At $T = T_c$ there is a kink in $\Delta s(T)$ arising from the contribution of the condensed bosons which disappears at the transition point. Upon a further increase of T the temperature dependence of the second term in Eq. (9.35) is essentially determined by the chemical potential behavior. The presence of a discontinuity in the second derivative of μ with respect to T leads to a rapid drop of $\Delta s(T)$ with temperature, which becomes negative, then passes through a minimum and finally tends to zero as $\Delta s/\gamma s \simeq -2T^*/T$ for $T \gg T^*$.

The temperature behavior of the sound velocity renormalization is thus rather different for charged bosons compared to fermions (electrons). For the case of bosons Δs increases with a decrease in T showing a discontinuous rise of derivative upon passing from the normal to the superconducting phase. For fermions one can write

$$\Delta s/\gamma s \approx (3/2)(T^*/T_F)[1 - (\pi^2/12)(T/T_F)^2] \tag{9.36}$$

(T_F—is the Fermi temperature). At $T = T_c^{BCS}$ the sound velocity slope also changes its value but now it is lower in the superconducting state and higher in the normal one. The sound velocity renormalization appears to be larger for bo-

sons than for fermions by a factor of $(T_c/T_F)^3$ provided that g_{ac} is approximately the same for both cases. Moreover the temperature variation of Δs for fermions being very small, of the relative magnitude of the order of $(T/T_F)^2$, is practically inaccessible for experimental investigation. On the contrary for the case of bosons $\Delta s(T)$ should be easily measurable. Its behavior for different T^*/T_c values is demonstrated in Fig. 24. To observe the jump in the sound velocity slope Fig. 25 shows the same quantity in the very narrow temperature interval near T_c. For $T^*/T_c = 1$ the change of the slope is quite visible. A qualitatively similar behavior is observed for $T^*/T_c = 0.5$ and 0.1, but it is more difficult to distinguish on the scale of Fig. 25.

Let us now briefly discuss the sound wave damping $\Gamma(\omega_q)$, Eq. (9.33), given by

$$\frac{\Gamma(\omega_q)}{\bar{\gamma}} = \left(\exp\frac{T^* - \mu}{T} - 1\right)^{-1}, \tag{9.37}$$

with

$$\bar{\gamma} = \frac{g_{ac}^2(\omega_q) x V (m^{**})^2}{4\pi\varepsilon_0}. \tag{9.38}$$

At low temperature $T \ll T^*$ one obtains an exponentially small value for $\Gamma(\omega_q) \propto \exp(-T^*/T)$ which shows a linear behavior

$$\Gamma(\omega_q)/\bar{\gamma} = T/T^* \tag{9.39}$$

with increasing T. It goes through a maximum just above T_c and then tends to zero as $\Gamma(\omega_q)/\bar{\gamma} \propto t^{-3/2}\zeta(3/2)$ as T is further increased (see Fig. 24). This decrease in $\Gamma(\omega_q)$ is due to the fact that in the non-degenerate Bose gas phonon emission and absorption processes have equal probabilities as $T \to \infty$. The function $\Gamma(\omega_q)$ depends linearly on the frequency and has no singularities at T_c, because only normal processes contribute to the damping.

Let us summarize our findings.

1) Charged bosons on a lattice lead to a temperature dependent sound velocity with a negative temperature gradient and a jump of the first derivative of $s(T)$ at $T = T_c$ indicating a stiffening of the lattice in the superconducting phase. This is opposite to what is expected for fermions.
2) The damping (ultrasound wave attenuation) is linear in practically the entire superconducting temperature regime and goes through a maximum above T_c before decreasing as T is increased further.
3) The experimental results on sound propagation in high-T_c oxides seem to favor the picture of charge carriers which are bosons (bipolarons). For these materials we expect $0.1 < T^*/T_c < 1$ according to the value of m^{**} and the carrier concentration n_p. Choosing $T^*/T_c = 1$ we find upon fitting our curves (Fig. 25) for $T < T_c$ to the experimental results[133] $\gamma s \approx 10^{-2}$ cm/s. Once we have fixed these parameters our theory then predicts

$$\left.\frac{d\Delta s(T)}{dT}\right|_{T=T_c} \approx -0{,}8 \cdot 10^{-4} \text{ cm/s·K}, \tag{9.40}$$

which is in good agreement with experiment $(-0.6, -0.8)^* 10^{-4}$ cm/sK. Decreasing T^*/T_c would decrease the magnitude of the jump in the slope of $\Delta s(T)$ at the transition point.

The gross features of the temperature dependence of the sound velocity and its damping are independent of the precise form of the dispersion $\varepsilon(\mathbf{p})$ for $T < T_c$. Only for $T \gg T_c$ the finite bandwidth of the carriers may noticeably change the temperature dependence.

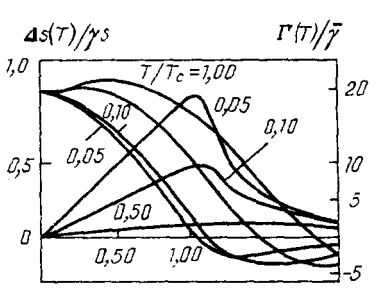

FIG. 24. Temperature dependence of renormalization of the sound velocity and the sound wave attenuation in a system of charged bosons on a lattice for different values of T^*/T_c (0.05;0.1;0.5;1.0).

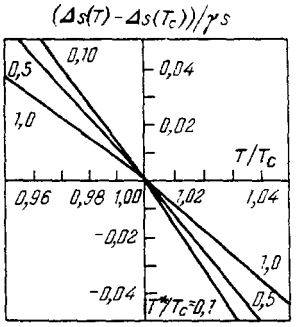

FIG. 25. Temperature dependence of renormalization of the sound velocity in the near T_c region for different values of T^*/T_c (0.1;0.5;1.0).

9.5. Direct evidence of polarons (bipolarons) in high-T_c oxides

Studies of photoinduced carriers in the semiconducting "parent" compounds of the high-temperature superconducting oxides have provided an insight into the nature of charged carriers and their interaction with the crystal lattice. Photoinduced infrared (IR) absorption measurements on the three high-temperature oxides, La_2CuO_4, $YBa_2Cu_3O_{7-\delta}$ ($\delta = 0.75$) and $Tl_2Ba_2Ca_{(1-x)}Gd_xCu_2O_8$ ($x = 0.02$) (Refs. 93, 137 and 138) have demonstrated the formation of self-localized polaron (or bipolaron) states (see also Refs. 139 and 140).

In the experiment of Ref. 93 the sample was pumped by a laser beam with the optical quanta energies ≈ 2.5 eV. For the infrared absorption measurements an interferometer was used covering the spectral range of 120–8000 cm^{-1} (0.015-1 eV) with resolution of 2–4 cm^{-1}. The net change in the absorption coefficient was determined from the photoinduced change in transmission. For the three systems studied photoinduced IRAV modes and photoinduced phonon flashes have been reported, indicating the formation of a localized structural distortion around the photogenerated charge carrier. In addition, a broad peak of photoinduced

absorption by electrons at low energy was observed in all three systems, indicating the formation of localized electron states deep inside the semiconducting energy gap. The identification of the gap state with the localized structural distortion was implied by the common temperature and intensity dependence of the corresponding photoinduced spectral features. These two aspects of the data confirm the formation of self-localized polarons; after photoexcitation, a localized distortion is formed around the carrier and associated with this distortion is a localized electron state in the energy gap. This unambiguous observation of polaron formation provides direct evidence of the importance of the electron-phonon interaction in these systems.

The dynamic polaron mass (M_d) has been determined for all three systems. It was proved to be correlated with the critical temperature of the corresponding superconducting phase: T_c rises linearly with $1/M_d$.[93] The strong correlation of T_c with M_d suggests a relationship between polaron formation and high-temperature superconductivity.

The existence of a peak in absorption by electrons at low energy (≈ 0.095 eV in the case of the Tl system) implies in the opinion of the authors of Ref. 3 an unusually large low-frequency polarizability of the formed self-localized polaron state. As a result, a singlet bipolaron might be stabilized by the Van der Waals attractive interaction arising from this large electron polarizability as a possible mechanism for pairing in real space.

At the end of this section we wish to discuss briefly two questions concerning the polaron theory and the possibility of its application to high-temperature superconductivity.

The first one is related to the well-known objection of B. K. Chakraverty[141] who argued that high T_c values can not be obtained in bipolaron theory for the reason of the required high value of the effective constant $\lambda > 3$ (and a high value of the bipolaron mass as a consequence). We have already replied to this objection.[142] The range of values of λ in which the polaron and bipolaron picture proves to be valid remains one of the most important and also difficult issues of the theory. Our point of view being based on the analysis of numerous studies of polaron properties by different authors was thoroughly argued both in this section and in Sec. 2 previously. According to the above mentioned studies and to our own estimates the polaron approach may be applied already at $\lambda \approx 1$. As we have pointed out in Sec. 8, the mass of a small bipolaron may turn out to be of the same order as that of an unpaired polaron thus leading for moderate λ to reasonable T_c values agreeing with experiment.

The second question is associated with experimental observations of the Fermi surface and their interpretation within the framework of the polaron theory. Generally speaking small polarons have the same Fermi surface as electrons but with a much lower value of the Fermi energy. Nevertheless this does not mean that there is no problem here at all. In the recent study of A. S. Alexandrov and J. Ranninger now in press the photoemission spectra of polarons excited by photons from the polaron band were calculated and shown to have a rather similar shape to that of x-ray angle-resolved photoemission spectroscopy data for the Bi–Sr–Ca–Cu–O system. Although this circumstance seems to be rather promising the question remains concerning the overall self-contained description of these and all the rest of the experimental results within the framework of the polaron

TABLE II.

	Physical properties	Ground state: Fermi-liquid	Ground state: Bose-liquid
NORMAL PHASE:	Magnetic susceptibility χ	$\chi = \text{const} > 0$	$\chi < 0$
	Heat capacity C_e	$C_e = \gamma_e T$	$C_e = \gamma_B T$ (2-dim.)
	Resistivity R	depends on H	independent of H (singlet bipolar)
	Thermopower S	$S \propto T$, depends on H	independent of H (singlet bipolar)
	Photoemission spectra	Fermi-edge	Shift near μ $\approx \Delta \leqslant 0.1$ eV
	Relaxation rate of nuclear spin T_1^{-1}	$T_1^{-1} \propto T$	Nonlinear temperature dependence
SUPERCONDUCTING PHASE:	Energy gap Δ	$3.5 \leqslant 2\Delta_{BCS}/T_c \leqslant 6$	Two gaps: $2\Delta_{min}/T_c \leqslant 1$ $2\Delta_{max}/T_c \gg 1$
	Coherence length ξ	$\xi \gg n^{-1/3}$	$\xi \approx n^{-1/3}$
	Heat capacity jump ΔC	$\Delta C/nk_B \ll 1$	$\Delta C/nk_B \approx 1$ (λ-like)
	T_1^{-1}	$\propto \exp(-\Delta_{BCS}/T)$, $T \to 0$	$\propto \exp(-\Delta/T)$
	H_{c2}	$\propto (T_c - T)$ near T_c	$\propto (T_c - T)^{3/2}$
	Sound velocity s and attenuation Γ	$\Delta s(T) < 0$ $\Gamma \propto \exp(-\Delta_{BCS}/T)$	$\Delta s(T) > 0$ $\Gamma \propto T$

approach. It is worthwhile to note that similar difficulties are met by almost all the presently developed theoretical models of high-temperature superconductivity.

10. FERMI OR BOSE LIQUID?

The nature of the ground state of carriers in high-temperature oxides is one of the most challenging questions. The classical theory of the normal and superconducting state of metals, based on the assumption that the Fermi energy is much higher than any correlation energy, leads to well-known predictions. Some of them as well as the predictions of bipolaron theory are listed in Table II.

The classical manifestations of the Fermi-liquid behavior are the temperature-independent Pauli susceptibility, and the linear heat capacity, along with the field-dependent quantum oscillations of susceptibility, resistivity, and thermopower in strong magnetic fields (Table II).

On the other hand, the charged Bose-gas exhibits diamagnetic behavior in the normal phase, field-independent resistivity and thermopower up to enormously high magnetic field values $\mu_B H^* \approx \Delta$, destroying bipolarons. The heat capacity of the two-dimensional Bose-gas has a linear temperature dependence.

The photoemission spectra are similar for both the Fermi and Bose liquids for the electron energies $|E-\mu| \geqslant \Delta$. A shift to low energy of the order of Δ in photoemission from a Bose-liquid near the chemical potential μ is anticipated.

Nuclear spin relaxation in a singlet Bose-liquid may occur as the result of the interaction of the nuclear spin with thermally activated single polarons or triplet bipolarons. Their bands are expected to lie above the singlet bipolaron band and the numbers of both are expected to rise exponentially with temperature. That is why the Korringa law is violated in this system.

The main difference of bipolaron superconductivity from that of the BCS-type is expressed by the fact that the total number of electrons, rather than a small fraction of them of the order of T_c/E_F, participates in the formation of the superfluid condensate. As a result significant fluctuations in the entire region of $\delta T \approx T_c$ are anticipated.

A crucial confirmation of the bipolaron nature of high-temperature oxides would be the observation of electron (hole) excitations with double ($2e$) charge and zero (or unity) spin at temperatures above T_c. In this regard attention should be drawn once more to the results of thermo-emf measurement[103] which had revealed its independence of the magnetic field for values up to $H \approx 30$ T, as well as to the absence in numerous experiments of an EPR signal above T_c.

An analysis of many other experiments, presented in the detailed review articles of Refs. 24 and 28, is also indicative in favor of the polaron theory of the discovered superconducting metallic oxides.

[1] J. G. Bednorz and K. A. Muller, Z. Phys. Kl. B. **64**, 189 (1986).
[2] A. B. Migdal, Zh. Eksp. Teor. Fiz. **34**, 1438 (1958). [Sov. Phys. JETP **7**, 996 (1958)].
[3] G. M. Eliashberg, Zh. Eksp. Teor. Fiz. **38**, 966 (1960); **39**, 1437 (1960) [Sov. Phys. JETP (1960) **11**, 696 (1960); **12**, 1000 (1961)].
[4] D. J. Scalapino, Superconductivity, Academic N.Y. **1**, 449 (1969).
[5] A. S. Alexandrov, V. N. Grebenev, and E. A. Mazur, Pis'ma Zh. Eksp. Teor. Fiz. **45**, 357 (1987) [JETP. Lett. **45**, 455 (1987)].
[6] A. A. Abrikosov, L. P. Gor'kov, and I. E. Dzyaloshinskii, *Methods of Quantum Field Theory in Statistical Physics*, Prentice-Hall, N.J. (1963) [Russ. original, Fizmatgiz., M. (1962)].
[7] A. Alexandrov and J. Ranninger, Phys. Rev. B **23**, 1796 (1981).
[8] A. Alexandrov and J. Ranninger, Phys. Rev. B. **24**, 1164 (1981).
[9] A. S. Alexandrov, Zh. Fiz. Khim. **57**, 273 (1983). [Russ. J. Phys. Chem. **57**, 167 (1983)].
[10] A. S. Alexandrov and V. V. Kabanov, Fiz. Tverd. Tela. **28**, 1129 (1986) [Sov. Phys. Solid State, **28**, 631 (1986)].
[11] A. Alexandrov, J. Ranninger, and S. Robaszkiewicz, Phys. Rev. Lett. **56**, 949 (1986); Phys. Rev. B **33**, 4526 (1986).
[12] A. S. Alexandrov, Pis'ma Zh. Eksp. Teor. Fiz. (Prilozh), **46**, 128 (1987) [JETP Lett. Suppl. **46**, 107 (1987)].
[13] A. S. Alexandrov, D. A. Samarchenko, and S. V. Traven', Zh. Eksp. Teor. Fiz. **93**, 1007 (1987) [Sov. Phys. JETP **66**, 567 (1987)].
[14] A. S. Alexandrov, Phys. Rev. B **38**, 925 (1988).
[15] A. S. Alexandrov, Physica C **158**, 337 (1989); *Studies of High Temperature Superconductors*, (Ed.) A. V. Narlikar, New Delhi, **6**, 195 (1990).
[16] A. S. Alexandrov, and E. A. Mazur, Zh. Eksp. Teor. Fiz. **96**, 1773 (1989) [Sov. Phys. JETP **69**, 1001 (1989)].
[17] A. S. Alexandrov and A. B. Krebs, Pis'ma Zh. Eksp. Teor. Fiz. **50**, 280 (1989) [JETP Lett. **50**, 311 (1989)].
[18] L. D. Landau, Phys. Z. Sowjetunion **3**, 664 (1933).
[19] S. I. Pekar, *Research in Electron Theory of Crystals*, US AEC Report AEC-tr-5575, 1963 [Russ. original, Gostekhizdat, M., 1951].
[20] Polarons, (Ed.) Yu. A. Firsov, (In Russian) Nauka, M., 1975.
[21] Polarons and Excitons, (Ed.) C. G. Whitfield, Oliver and Boyd, Edinburgh, 1963.
[22] *Polarons in Ionic Crystals and Polar Semiconductors*, (Ed.) J. T. Devreese. North-Holland, Amsterdam, 1972.
[23] N. Mott, Nature, **327**, 185 (1987).
[24] L. J. de Jongh, Physica, C. **152**, 171 (1988).
[25] P. Prelovsek, T. M. Rice, F. C. Zhang, J. Phys. C. **20**, L229 (1987).
[26] D. K. Ray, Philos. Mag. Lett. **55**, 271 (1987).
[27] H. Kamimura, Jpn. J. Appl. Phys. **26**, L627 (1987).
[28] R. Micnas, J. Ranninger, and S. Robaszkiewicz, Rev. Mod. Phys. **62**, 113 (1990).
[29] R. P. Feynman, Phys. Rev. **97**, 660 (1955).
[30] E. I. Rashba, Excitons, (Eds.) E. I. Rashba and M. D. Sturge, North-Holland, Amsterdam, 1982 [Russ. original, Nauka, M., p. 385, 1985].
[31] D. Emin and T. Holstein, Phys. Rev. Lett. **36**, 323 (1976).
[32] A. S. Alexandrov and A. B. Krebs, Preprint (In Russian) MIFI 018-88, Moscow, 1988.
[33] D. E. Farrel and B. S. Chandrasekhar, Phys. Rev. Lett. **38**, 788 (1977).
[34] A. Birnboim and H. Gutfreund, Phys. Rev. **B9**, 139 (1974).
[35] A. G. Pedan, Fiz. Nizk. Temp. **12**, 709 (1986) [Sov. J. Low Temp. Phys. **12**, 402 (1986)].
[36] J. Hubbard, Proc. R. Soc. London **A276**, 238 (1963).
[37] A. S. Alexandrov and V. F. Elesin, Fiz. Tverd. Tela. **25**, 456 (1983) [Sov. Phys. Solid State **25**, 257 (1983)].
[38] V. N. Bogomolov, E. K. Kudinov, and Yu. A. Firsov, Fiz. Tverd. Tela. **9**, 3175 (1967) [Sov. Phys. Solid State **9**, 2502 (1967)].
[39] A. J. Bosman and H. J. van Daal, Adv. Phys. **19**, No. 77, 1 (1970).
[40] D. M. Eagles, Phys. Rev. **181**, 1278 (1969).
[41] P. W. Anderson, Phys. Rev. Lett. **34**, 953 (1975).
[42] S. Lakkis, C. Schlenker, B. K. Chakraverty, and R. Buder, Phys. Rev. B **14**, 1429 (1976).
[43] C. Schlenker, S. Ahmed, R. Buder, and M. Gourmala, J. Phys. C. **12**, 3503 (1979).
[44] B. K. Chakraverty, M. J. Sienko, J. Bonnerot, Phys. Rev. B **17**, 3781 (1978).
[45] O. F. Schirmer and E. Salje, J. Phys. C **13**, L1067 (1980).
[46] I. A. Chernik, S. N. Likov, and N. I. Grechko, Fiz. Tverd. Tela **24**, 2991 (1982) [Sov. Phys. Solid State **24**, 1661 (1982)].
[47] A. S. Alexandrov, V. F. Elesin, and V. V. Kabanov, Zh. Eksp. Teor. Fiz. **86**, 1937 (1984) [Sov. Phys. JETP **59**, 1125 (1984)].
[48] A. S. Alexandrov and V. F. Elesin, Izv. Akad. Nauk SSSR, Ser. Fiz. **49**, 326 (1985) [Bull. Acad. Sci. USSR Phys. Ser. **49**(2), 105 (1985)].
[49] T. M. Rice and L. Sneddon, Phys. Rev. Lett. **47**, 689 (1981).
[50] J. G. Bednorz and K. A. Muller, Rev. Mod. Phys. **60**, 585 (1988) [Russ. Transl., Usp. Fiz. Nauk. **156**, 323 (1988)].
[51] T. M. Rice, *Superconductivity in Magnetic and Exotic Materials* (Eds.) T. Matsubara and A. Kotani, Springer Verlag, Berlin, 178 (1984).
[52] T. Holstein, Ann. Phys. (N.V.) **8**, 325, 343 (1989).
[53] A. A. Gogolin, Phys. Status Solidi B **109**, 95 (1982).
[54] D. M. Eagles, Phys. Rev. **145**, 645 (1966).
[55] D. Emin, Adv. Phys. **22**, 57 (1973).
[56] H. de Raedt and A. Lagendijk Phys. Rev. B. **27**, 6097 (1983); **30**, 1671 (1984).
[57] H. de Raedt and A. Lagendijk, Phys. Rep. C **127**, 233 (1985).
[58] K. Miyake *et al.* Prog. Theor. Phys. **72**, 1063 (1984).

[59] A. M. Clogston and V. Jaccarino, Phys. Rev. **121**, 1357 (1961).
[60] J. Kanamori, Prog. Theor. Phys. **30**, 275 (1963).
[61] A. Alexandrov and H. Capellmann, Phys. Rev. B **43**, 2042 (1991).
[62] I. G. Lang and Yu. A. Firsov, Zh. Eksp. Teor. Fiz. **43**, 1843 (1962) [Sov. Phys. JETP **16**, 1301 (1963)].
[63] A. S. Alexandrov, Physica C **191**, 115 (1992).
[64] T. Matsubara and A. Matsuda, Prog. Theor. Phys. **16**, 569 (1956).
[65] K. Kubo and S. Takada, J. Phys. Soc. Jpn. **52**, 2108 (1983).
[66] S. Robaszkiewicz, R. Micnas, and K. A. Chao, Phys. Rev. B **23**, 1447 (1981); **24**, 1579 (1981).
[67] E. F. Makarov, I. I. Amelin, and S. P. Ionov, Phys. Status Solidi **71**, 135 (1975).
[68] S. P. Ionov *et al.* Phys. Status Solidi B **72**, 515 (1975).
[69] I. O. Kulik and A. G. Pedan, Zh. Eksp. Teor. Fiz. **79**, 1469 (1980) [Sov. Phys. JETP **52**, 742 (1980)].
[70] I. O. Kulik and A. G. Pedan, Fiz. Nizk. Temp. **9**, 256 (1983) [Sov. J. Low Temp. Phys. **9**, 127 (1983)].
[71] S. B. Haley and P. Erdos, Phys. Rev. B. **5**, 1106 (1972).
[72] S. B. Haley, Phys. Rev. B. **17**, 337 (1978).
[73] S. V. Tyablikov, *Methods in The Quantum Theory of Magnetism*, Plenum, N.Y., 1967 [Russ. original, Nauka, M., 1965 and 1975].
[74] T. Oguchi, J. Phys. Soc. Jpn. **30**, 988 (1971).
[75] V. M. Agranovich, *Theory of Excitons*, (In Russian) Nauka, M. (1968).
[76] E. M. Lifshitz and L. P. Pitaevskiĭ *Statistical Physics*, Pergamon, [Russ. original, Nauka, M. (1978)].
[77] M. R. Schafroth, Phys. Rev. **100**, 463 (1955).
[78] R. Kubo, S. J. Miyake, and N. Hashitsume, Solid State Phys. **17**, 169 (1965).
[79] A. S. Alexandrov and V. F. Elesin, Fiz. Tekh. Poluprovodn. **8**, 111 (1974). [Sov. Phys. Semicond. **8**, 69 (1974)].
[80] K. Nasu, Phys. Rev. B **35**, 1748 (1987); **37**, 5075 (1988).
[81] S. L. Cooper *et al.* Phys. Rev. B **37**, 5920 (1988).
[82] C. Thomsen *et al.* Phys. Rev. B **37**, 9860 (1988).
[83] M. Krantz *et al.* Phys. Rev. B **38**, 4992 (1988).
[84] R. Zeyher and G. Zwicknagl, Z. Phys. B **78**, 175 (1990).
[85] W. Reichardt *et al.*, *Proc. of Int. Conf. on Neutron Scatt.*, Grenoble, 1988.
[86] H.-C. Loye *et al.* Science **238**, 1558 (1987).
[87] M. K. Crawford *et al.* Phys. Rev. B **41**, 282 (1990).
[88] S. Kondoh *et al.* Physica C. **157**, 469 (1989).
[89] J. P. Franck *et al.* Physica C **162–164**, 753 (1989).
[90] K. Otts, Superconductivity News **1**, 7 (1988).
[91] H. Rietshel, L. Pintschovious and W. Reichardt, Physica C **162–164**, 1705 (1989).
[92] C. Y. Chen *et al.* Physica C **162–164**, 1031 (1989).
[93] C. M. Foster *et al.* Solid State Commun. **71**, 945 (1989).
[94] I. K. Janson *et al.* Fiz. Nizk. Temp. **13**, 557 (1987) [Sov. J. Low Temp. Phys. **13**, 315 (1987)].
[95] D. T. Morelli, J. Heremans, and D. E. Swets, Phys. Rev. B **36**, 3917 (1987).
[96] G. Aeppli *et al.* Phys. Rev. B **35**, 7129 (1987).
[97] B. Batlogg, Physica B + C **126**, 275 (1984).
[98] P. Monod, B. Dubois, and P. Odier Physica C **153–155**, 1489 (1988).
[99] J. R. Cooper *et al.* Physica C **153–155**, 1491 (1988).
[100] M. E. Reeves, T. A. Friedman, and D. M. Ginsberg, Phys. Rev. B **35**, 7207 (1987).
[101] M. V. Nevitt, G. W. Grabtree, and T. E. Klippert, Phys. Rev. B **36**, 2398 (1987).
[102] G. A. Thomas *et al.*, Phys. Rev. Lett. **61**, 1313 (1988).
[103] R. C. Yu *et al.*, Phys. Rev. B **37**, 7963 (1988).
[104] S. Pan *et al.*, Phys. Rev. B **35**, 7220 (1987).
[105] J. R. Kirtley *et al.*, Jpn. J. Appl. Phys. **26**, 997 (1987).
[106] M. E. Hawley *et al.*, Phys. Rev. B **35**, 7224 (1987).
[107] M. D. Kirk *et al.* Phys. Rev. B **35**, 8850 (1987).
[108] J. R. Kirtley *et al.* Phys. Rev. B **35**, 7216 (1987).
[109] M. F. Grommie *et al.* Phys. Rev. B **35**, 8853 (1987).
[110] M. Naito *et al.* Phys. Rev. B **35**, 7228 (1987).
[111] K. Flensberg, P. Hedegard, and M. Brix, Phys. Rev. B **38**, 841 (1988).
[112] A. S. Alexandrov and M. P. Kazeko, *Problems of High-Temperature Superconductivity*, (In Russian) Published by Ural Branch, Acad. Sci. USSR, Sverdlovsk, 153 (1987).
[113] A. S. Alexandrov, M. P. Kazeko, and S. G. Rubin, Zh. Eksp. Teor. Fiz. **98**, 1656 (1990) [Sov. Phys. JETP **71**, 928 (1990)].
[114] J. Geerk, X. X. Xi, and G. Linker, Z. Phys. B **73**, 329 (1989).
[115] J. M. Imer *et al.* Phys. Rev. Lett. **62**, 336 (1989).
[116] R. T. Collins *et al.* Phys. Rev. Lett. **65**, 801 (1990).
[117] J. Orenstein *et al.* Phys. Rev. B **42**, 6342 (1990).
[118] D. van der Marel *et al.* Phys. Rev. B **43**, 8606 (1991).
[119] J. E. Demuth *et al.* Phys. Rev. Lett. **64**, 603 (1990).
[120] J. R. Cooper *et al.* Phys. Rev. B **37**, 638 (1988).
[121] A. S. Alexandrov and S. V. Traven', Pis'ma Zh. Eksp. Teor. Fiz. **48**, 426 (1988) [JETP Lett. **48**, 468 (1988)].
[122] S. E. Inderhees *et al.* Phys. Rev. Lett. **60**, 1170 (1988).
[123] M. B. Salamon *et al.* Phys. Rev. B **38**, 885 (1988).
[124] T. K. Worthington *et al.* Physica C **153–155**, 33 (1988).
[125] Y. J. Uemura *et al.* Phys. Rev. B **38**, 909 (1988); C. L. Seaman, *et al.* Physica C **159**, 391 (1989).
[126] A. S. Alexandrov and D. A. Samartchenko, Physica B **165–166**, 1041 (1990).
[127] A. S. Alexandrov and D. A. Samarchenko, Zh. Eksp. Teor. Fiz. **99**, 574 (1991) [Sov. Phys. JETP. **72**, 321 (1991)].
[128] U. Welp *et al.* Phys. Rev. Lett. **62**, 1908 (1989).
[129] W. K. Kwok *et al.* Phys. Rev. Lett. **67**, 390 (1991).
[130] S. Uchida, Bull. Am. Phys. Soc. **33**, 507 (1988).
[131] R. J. Wijngaarden and R. Griessen, *Studies of High Temperature Superconductors* (Ed.) A. V. Narlikar, New Delhi, 1990, V. 2.
[132] P. W. Anderson, Science **235**, 1196 (1987).
[133] A. Alexandrov and J. Ranninger, Physica C **159**, 367 (1989).
[134] D. J. Bishop *et al.* Phys. Rev. B **35**, 8788 (1987); **36**, 2408 (1987).
[135] S. Bhattacharya *et al.* Phys. Rev. B **37**, 5901 (1988).
[136] A. Migliori *et al.*, Solid State Commun. **63**, 827 (1987).
[137] Y. H. Kim *et al.* Phys. Rev. B **36**, 7252 (1987).
[138] Y. H. Kim *et al.* Phys. Rev. B **38**, 6478 (1988).
[139] J. M. Ginder *et al.* Phys. Rev. B **37**, 7506 (1988).
[140] C. Taliani *et al.* Solid State Commun. **66**, 487 (1988).
[141] B. K. Chakraverty, M. Avingnon, and D. Feinberg, J. Less-Common Met. **150**, 11 (1989).
[142] A. S. Alexandrov and D. K. Ray, Philos. Mag. Lett. **63**, 295 (1991).

English text (differing in minor respects from the Russian text in Usp. Fiz. Nauk) was supplied by the authors.